INFORMATION TO USERS

This manuscript has been reproduced from the microfilm master. UMI films the text directly from the original or copy submitted. Thus, some thesis and dissertation copies are in typewriter face, while others may be from any type of computer printer.

The quality of this reproduction is dependent upon the quality of the copy submitted. Broken or indistinct print, colored or poor quality illustrations and photographs, print bleedthrough, substandard margins, and improper alignment can adversely affect reproduction.

In the unlikely event that the author did not send UMI a complete manuscript and there are missing pages, these will be noted. Also, if unauthorized copyright material had to be removed, a note will indicate the deletion.

Oversize materials (e.g., maps, drawings, charts) are reproduced by sectioning the original, beginning at the upper left-hand corner and continuing from left to right in equal sections with small overlaps.

Photographs included in the original manuscript have been reproduced xerographically in this copy. Higher quality 6" x 9" black and white photographic prints are available for any photographs or illustrations appearing in this copy for an additional charge. Contact UMI directly to order.

ProQuest Information and Learning
300 North Zeeb Road, Ann Arbor, MI 48106-1346 USA
800-521-0600

UMI®

A

Infrared Microspectroscopic Studies of Processes in Cell Biology

By:

Anthony Pacifico

A dissertation submitted to the Graduate Faculty in Biochemistry in partial fulfillment of the requirements for the Doctor of Philosophy, The City University of New York

2002

This manuscript has been read and accepted for the Graduate Faculty in Biochemistry in satisfaction of the dissertation requirement for the degree of Doctor of Philosophy.

12-6-2001
Date

Chair of Examining Committee

12-6-2001
Date

Executive Officer

Supervisory Committee

The City University of New York

Acknowledgements: I would like to thank my parents Pat Pacifico and Pauline Christiano. I would also like to thank my friends Greg Habeeb, Bernard "Sonny" Curry, George Vamvoukakis, Andrea Trondle, John Foster, Paul Castadonis and Maria Raha as well as the rest of my family, especially Vito Christiano and my wife Erin.

Special thanks to Dr. Max Diem, Dr. Alex Pevsner Dr. Peter Lasch and Dr. Luis Chiriboga for helping me with my endeavors at Hunter. I also owe a debt of gratitude to Dr. Glenn Vogel and Dr. Jon Kirchhoff.

Table of Contents

List of Tables

List of Figures

I. Introduction:

A. Aim and Scope of Thesis Research: Over the past decade, several research groups have been developing infrared (**IR**) spectroscopy and infrared microspectroscopy (**IR-MSP**, also referred to as infrared microscopy) as a diagnostic technique for use in biology and medicine. This technique offers fast data acquisition and can be non-destructive of any sample studied. This work has opened possibilities for measurements of physiological or pathological changes within cells and tissues to be performed in vitro and potentially in vivo.

The principle behind **IR** spectroscopy is that it is capable of monitoring changes in chemical composition or conformation of any given sample. This is accomplished by measuring how many **IR** photons are absorbed by the sample at any wavelength. This data reveals information about the conformation and presence of various biomolecules located within cells as they absorb **IR** photons. This simple premise allows it to be applicable towards studying cells and tissues as well.

Early publications aimed at establishing **IR-MSP** as a diagnostic tool to detect cancerous cells and tissue **(Wong, et al., 1991; Rigas and Wong, 1992)** reported overly optimistic interpretations of the **IR-MSP** results. More recent studies have that revealed subtle changes between normal and cancerous cells and tissues exist **(Chiriboga, et al., 2000a; Chiriboga, et al., 2000b; Lasch & Naumann, 1998)**. These studies also

revealed that many confounding effects existed. More basic studies still need to be carried out to understand the observed spectral changes.

Some of the spectral results, caused by disease or other factors, are quite large and obvious. For example, the depletion of glycogen in cervical cells may accompany the transition from normal to abnormal states of health. This has been well studied and characterized using **IR-MSP**. On the other hand, some spectral changes are exceedingly small, and are not detectable by a visual inspection of the observed spectral patterns.

Thus, the understanding of infrared spectra of individual cells becomes of paramount importance for the interpretation of spectra of tissue samples. In early work, we found early that the spectra of individual (exfoliated) cervical cells can vary widely, depending on the stage of a cell's life and division cycle, on its maturation and differentiation, and its state of health.

The spectroscopic results obtained from cells are difficult to interpret. There are differences between cell types including morphology, metabolism and the presence or absence of various organelles, which may cause spectral variation. Some of these parameters should vary even within a homogenous population of cells.

This was found to be true for the cultured cells that we have used herein. The sensitivity of this technique does allow for these very small changes to be detected and analyzed. We are in the process of

investigating these changes using the spectra obtained from our samples. These studies may ultimately serve as basic models for subsequent applications of **IR-MSP** to study the inhibition of cell growth by certain drugs, or contrarily, the very early onset of uncontrolled cell proliferation.

In 1998 the first ever cell division cycle dependent infrared microspectra of myeloid leukemia cells **(Boydston-White, et al, 1999)** was reported. These previous studies were carried out using cells that were fractionated according to their phase in the cell cycle by centrifugal elutriation. In this thesis, it will be demonstrated that enormous, and not completely understood, spectral changes accompany the replication of deoxyribonucleic acid **(DNA)** in the **S phase** of the cell division cycle.

Unfortunately, elutriation is a slow, expensive and impractical step for routine analysis of cell proliferation. Elutriation also adds an additional level of complexity to the analysis of cultured cells. We decided to investigate the effects of cell proliferation on averaged ensembles of eukaryotic cells. The desirable spectral changes for **IR-MSP** would be from whole populations of cultured cells, as the changes observed would be averaged over many cells. The spectral features associated with a particular treatment would therefore be averaged over many cells to give an accurate representation of a large sample.

The interpretation of infrared spectral features of eukaryotic cells is still in its infancy, but follows an approach similar to that chosen by Naumann and coworkers **(Helm, et al., 1991)** for the identification and

characterization of prokaryotes by infrared spectroscopy. Small changes between strains of bacteria were detected using second derivative IR analysis of the spectra obtained and correlated against microbiological classification of the strains. This was accomplished through the use of hierarchical cluster analysis. In these efforts, libraries of prokaryotic cell spectra were established that by now contain well over 1000 spectra of different bacterial strains. These studies established that IR spectroscopy can distinguish drug resistant from sensitive strains, gram positive from gram negative cells, and mutations of organisms. Overall, identifications could be carried out faster and use less cells than other biological methods.

In the study described herein, we wish to expand upon the principles outlined for prokaryotic cells to the study of eukaryotes. We have chosen a two- fold approach for the interpretation of the spectral features from cultured cells. We have been able to chemically treat the cells to remove biomolecules such as phospholipids and ribonucleic acid (RNA) using ethanol and ribonuclease A (RNase), respectively. These molecules complicate the interpretation of spectral data as information related to proliferation of mammalian cells is in DNA spectral features. The data after these stages of treatment reveal changes within the samples at the level of DNA.

In the other direction, changes due to variations in cells within a sample depending on the cell cycle are addressed. Thus, we concentrated

our efforts on one aspect: the distinction between exponentially growing and growth arrested cell cultures. This has been done using external factors that may influence cell growth by two different methods. One method involved comparing spectra of exponentially growing cells, and cells that have reached confluence. It has been shown that as the level of confluence increases, cells decrease in their proliferative activities and leave the cell cycle **(Baba, et al., 2001)**. The other method involves removal of the growth factors necessary for cellular proliferation. Without these factors the cells should also exit the cell cycle.

II. Background: The aim of this thesis is to establish **IR** spectroscopic methods to monitor cell biology. In this thesis the spectroscopic background is kept intentionally short. For a review of spectroscopy, see **Diem** (1993).

A. Phenomenological Description of Infrared (IR) Spectroscopy:

Spectroscopy is the study of the interaction of electromagnetic radiation with atoms and molecules. Electromagnetic radiation has two major properties that describe its behavior. The first is the ability to propagate as waves. All waves have three primary characteristics: wavelength (λ), frequency (ν) and velocity. All electromagnetic radiation travels at the speed of light (**c**) so the relationship in **equation 1.1** may be used.

$$\lambda \nu = c \quad (c = 3.00 \bullet 10^{8}\ m\ s^{-1}) \qquad (1.1)$$

Electromagnetic radiation contains fixed amounts of energy (**E**) that is proportional to its frequency as in **equation 1.2**. This equation demonstrated that matter gained or emitted energy in whole number quantities of $h \nu$, where **h** is a constant that was determined by experiment and **n** is an integer. The second is that electromagnetic radiation can also be viewed as a stream of particles or photons with a mass (**m**) as shown in **equation 1.3**.

$$E = n\ h \nu \ (h = 6.626 \bullet 10^{-34}\ J\ s) \qquad (1.2)$$

$$m\ c = \hbar / \lambda \qquad (1.3)$$

Electromagnetic radiation is composed of an electric and a magnetic field that are perpendicular to each other. An atom or molecule can interact with the electric field of a photon if $\Delta E = E_f - E_i = h\nu$. The frequencies used in mid – Infrared spectroscopy are between 100 – 4000 cm^{-1}. This corresponds to wavelengths between 0.1 mm to approximately 2.5 μm **(Diem, 1993, pg. 29)**.

In spectroscopy, absorption and emission of photons is measured versus wavelength or frequency. The resulting data is referred to as a spectrum. To simplify the discussion here, we will deal only the absorption process. Lambert – Beer's law states that the absorbance (**A**) of photons is dependent upon three parameters, the sample thickness **d**, the concentration of the absorbing species **c** and the wavelength dependent extinction coefficient ε, as shown in **equations 1.4** and **1.5**.

$$A(\lambda) = \varepsilon(\lambda)\, c\, d \qquad (1.4)$$

Or in terms of Frequency:

$$A(\nu) = \varepsilon(\nu)\, c\, d,\ \nu = 1/\lambda \qquad (1.5)$$

In **IR** spectroscopy a molecule is exposed polychromatic **IR** radiation from 2.5 –100 μm wavelengths. When the energy of a photon matches the vibrational frequency of a functional group on a molecule, the

photon is absorbed. The energy absorbed is subsequently released as a photon, or is lost due to collisional quenching.

Characteristic group frequencies of biomolecules are shown in **Table 1**. Each group is attributed to particular functional groups within a biomolecule. The structures of many biomolecules are characterized in terms of the functional groups they contain. Absorbance of photons characteristic of certain functional groups therefore leads to an interpretation of the presence or absence of a particular biomolecule within a sample.

The data provided in **Table 3** give group frequency ranges. The discrete wavenumber values depend on external factors and environment of the groups. For proteins, the principal absorption bands of the amide linkage in proteins are dependent upon protein conformation. These bands are the amide A (⇐N-H⇒), the Amide I (⇐C-O⇒) and the Amide II (C-N-H deformation mode). The vibrations of all these groups are vibrationally coupled. This is referred to as exciton splitting. This leads to a potential splitting of each band into a series of several bands. The intensities will vary with the strength of the resulting dipole that is determined by these interactions. Spectral features of these molecules will be discussed in section **I.D**.

Wavenumber (cm-1)	Assignment
1737	>C=O (ester) stretch
1690 –1620	amide I
1570 – 1530	amide II
1340 - 1240	amide III
1237	PO_2^- - antisymmetric stretch
1160, 1120	Ribose C-O stretch of RNA
1150	C-O stretch, C-O-H bend (carbohydrates, mucin)
1015	Ribose C-O stretch of RNA and DNA
1083	PO_2^- - symmetric stretch
1063	-CO-O-C symmetric stretch
1050	C-O stretch, (carbohydrates, mucin)
968	C-O phosphodiester residue (DNA)

Table 1: Characteristic group frequencies associated with functional groups within biomolecules.

B. Instrumentation of IR Spectroscopy: Dispersive instruments used gratings or prisms to produce rays of monochromatic light to irradiate the sample. In order to record a spectrum, $A(\lambda)/A_0(\lambda)$ is measured. Such instruments could not be used to achieve the sensitivity needed to observe single cells. They dissipate much of the energy from the light source of the instrument and thus lower the signal to noise ratio. Also, these instruments could only scan through wavelengths sequentially, which made them very slow.

The enhancement in sensitivity needed to observe single cell spectra was partially obtained with the introduction of the Michelson interferometer. This instrumental design allows for the simultaneous detection of many wavelengths of IR radiation. The optics used in the interferometer eliminate the low signal levels of dispersive instruments thereby boosting the signal to noise ratio.

In interferometery, collimated polychromatic radiation falls upon a beam splitter, which transmits half the light. This transmitted light is reflected by a fixed mirror back to the beam splitter and is focused to the detector. The reflected light falls upon a movable mirror and is reflected back through the beam splitter. The laser – tracked, mobile mirror changes the phase of the light focused by it. Thus, the light can recombine with the initially transmitted light to produce constructive or destructive interference. This depends on the path difference created by the displacement of the mobile mirror and yields what is commonly called a

fringe pattern or interferogram. The desired absorption spectrum **A (ν)**, can be subsequently constructed by Fourier transform of the interferogram according to as shown in **equation 1.6**. **N** represents a normalization constant and $i = \sqrt{-1}$. The function converts the interferogram **S (x)** from mirror displacement to the frequency domain.

For the study of cells, the spectrophotometer must at least have the spatial resolution to observe a single cell. Therefore a microscope capable of measurements in the **IR** conforms to the basic principals of a light microscope. The optics used in the **IR** microscopes are capable of both resolving single cells and the ability to focus and detect **IR** radiation transmitted by single cells. The spatial resolution of an **IR** microscope is not as high as that of a visible microscope due to the optics needed to focus the **IR** beam upon the sample.

After the light is transmitted through the sample, it is detected by a Mercury Cadmium Telluride **(HgCdTe)** cryogenic detector. The stage upon which the **IR** transparent slides (ZnSe or BaF_2) are mounted is computer controlled and is capable of moving with high precision over small areas (1μm precision).

$$S(\nu) = 1/N \int_{-\infty}^{\infty} J(x)\, e^{-2\pi i \nu x}\, dx \qquad (1.6)$$

C. Properties of Biomolecules:

1. Nucleotides: Eukaryotic Cells contain a mixture of biomolecules. These molecules are mostly proteins, lipids and nucleotides such as **DNA** and **RNA** and carbohydrates. In order to facilitate a better understanding of the bonding within these molecules and their biological properties, a cursory introduction to these major classes of biomolecules is provided here.

DNA is used to store the biological information of the cell. The structure of **DNA** is well characterized and consists of deoxyribonucleotides within a double helix motif . The helix is held together by hydrogen boding interactions between adjacent base pairs. The nucleotides, deoxy – adenine, thymine, guanine and cytosine compose the helix as shown schematically in **Figure 1**. The hydrogen bonding between the bases is always discrete with the base adenine, **A** interacting with thymine, **T**. The base guanine, **G** also intreracts exclusively with cytosine, **C**.

RNA serves a diverse set of functions. These molecules function as intermediates between **DNA** and proteins and also have the ability to carry out catalytic functions like proteins. It has been well established that the ribosomes of cells, which carry out protein biosynthesis, are composed of nearly 2/3 **RNA**.

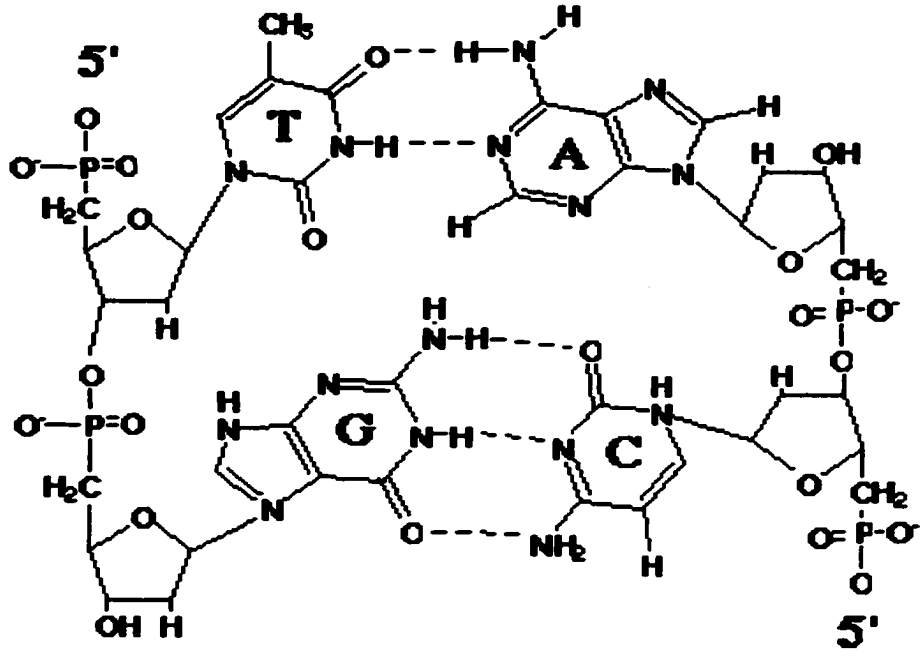

Figure 1: Structure of DNA showing the hydrogen bonding between the nucleotides. Shown are the deoxyriobnucleotides with the bases thymidine (T), adenine (A), guanosine (G) and cytosine (C).

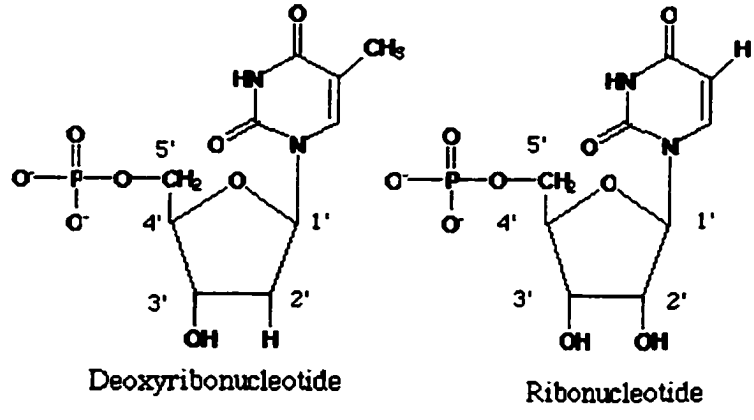

Figure 2: Structures of Deoxy and Ribonucleotides. The bases shown are Thymine and Uracil, respectively.

RNA and **DNA** are nearly identical. The small differences in structure do however give rise to biomolecules with quite different roles within the cell. **RNA** contains an extra hydroxyl group at the 2' position versus **DNA** as shown in **Figure 2**. **RNA** also does not contain the nucleotide base Thymine which is replaced Uracil. The difference is a lack of a methyl group at the 5' position on Uracil.

2. Lipids: Lipids serve three purposes within a cell. First, they are a fuel source. Second, they are involved in signal transduction processes. The lipids also provide a semi- permeable bilayer membrane by which the cell can sequester biomolecules within itself or organelles. These lipids most often are diacylglycerides and are members of a larger class called phospholipids. These molecules contain a glycerol backbone with a polar phosphate headgroup. Additional organic moieties are often esterfied to the phosphate headgroup as shown in **Table 2**. Two fatty acid residues are esterfied to the remaining free hydroxyl groups as in **Table 3**. Plasmologens and cardiolipins are also members of this class but are quite similar structurally to the diacylglycerides.

Sphingolipids are another class of lipid. These molecules are much less abundant than the phospholipids discussed previously. These molecules are derivatives of sphingosine. The major subgroups of sphingolipids are sphingomyelins, cerebrosides and ceramides.

Ceramides are generated by the acylation of various fatty acids to the amine group and have been shown to be involved in apoptosis **(Dbaibo et al., 2001)**. Sphingomyelins feature either a choline or ethanolamine headgroup esterfied to 1 position hydroxyl group. Sphingomyelins are quite different from phospholipids in structure, however, they are quite similar in charge, size and conformation and are quite often found in membranes. Cerebrosides are sphingoglycolipids. These molecules have headgroups composed of single or multiple sugar

residues. The sugars are directly bound to the sphingosine/ dihyrdosphingosine backbone and therefore lack phosphate groups. These molecules are also bioactive and are synthesized in cells undergoing programmed cell death or apoptosis.

It is important to mention the steroids here. Cholesterol is a member of the steroid class of biomolecules and is the precursor for all other steroids. This molecule is synthesized from the same basic building block as lipids, Acetyl-CoA. But its synthesis diverges considerably from there.

The overall biosynthesis of these molecules is quite different from that of fatty acids and shall not be reviewed here. These molecules also are involved in signal transduction processes within cells and control sexual development. Due to their non-polar nature, steroids freely diffuse through lipid membranes and act at the nuclear level **(Quack et al., 1998).**

Cholesterol is also necessary to maintain the fluidity of these membranes. A plasma membrane can contain up to 50% cholesterol by weight. The permeability of these membranes is also increased due to presence of cholesterol. Membranes can approach the order of liquid crystals due to the packing forces present. The rigidity of lipid membranes is thus greatly decreased by the presence of cholesterol.

HEAD GROUPS

Common name	Structure	Letter Symbol
Phosphatidic acid	PO4	PA
Phosphatidylcholine(lecithin)	PO4-CH2-CH2-N(CH3)3	PC
Phosphatidylserine	PO4-CH2-CH2-(NH3,CO2)	PS
Phosphatidylethanolamine	PO4-CH2-CH2-NH3	PE
Phosphatidylinositol	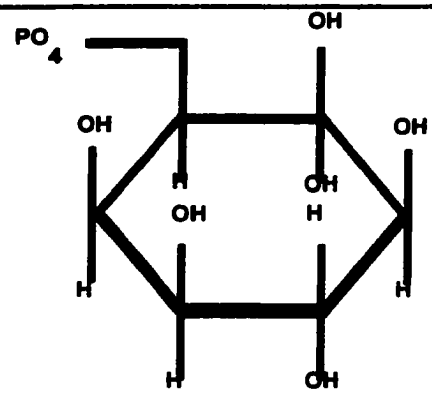	PI

Table 2: Structures of the most common types of headgroups associated with lipids. These groups attach directly to the glycerol backbone through a phosphate linkage.

FATTY ACIDS

Common name	Systematic name	Symbol	Structure
Saturated			
Capric	n-decanoic	10:0	CH3(CH2)8-COOH
lauric	n-dodecanoic	12:0	CH3(CH2)10-COOH
myristic	n-tetradecanoic	14:0	CH3(CH2)12-COOH
palmitic	n-hexadecanoic	16:0	CH3(CH2)14-COOH
stearic	n-octadecanoic	18:0	CH3(CH2)16-COOH
archidic	n-eicosanoic	20:0	CH3(CH2)18-COOH
behenic	n-docosanoic	22:0	CH3(CH2)20-COOH
Lignoceric	n-tetracosanoic	24:0	CH3(CH2)22-COOH
Unsaturated			
palmitoleic	cis-9-hexadecanoic	16:1	CH3(CH2)5CH=CH(CH2)7-COOH
oleic	cis-9-octadecanoic	18:1	CH3(CH2)7CH=CH(CH2)7-COOH
linoleic	cis,cis-9,12-octadecadienoic	18:2	CH3(CH2)7CH=CHCH2CH=CH(CH2)7-COOH
linolenic	all cis-9,12,15-octadecatrienoic	18:3	CH3CH2CH=CHCH2CH=CHCH2CH=CH(CH2)7-COOH
arachidonic	all cis-5,8,11,14-eiscotetraenoic	20:4	CH3(CH2)4(CH=CHCH2)3CH

Table 3 : The most common fatty acids associated with lipids. Unsaturated species feature alkene bonds, which are indicated in the symbol column.

3. Proteins: Proteins are the cornerstone molecules of any cell. These molecules function as enzymes, catalyzing reactions essential to the everyday activities of cells. Indeed, proteins also regulate these activities as well. Cell signaling is widely controlled by these molecules as protein messengers known as hormones that regulate physiological processes. Proteins also act to transport other important molecules such as Oxygen and Iron. In addition, proteins perform mechanical duties as well. They form muscle fibers necessary for the motility of eukaryotes and facilitate the separation of chromosomes during cell division. Lastly, they provide bones, tendons and ligaments with their tensile strength through the formation of collagen networks.

Despite the diversity of roles that proteins carry out, the structure of all proteins are based primarily on the 20 essential amino acids. Amino acids are polymerized together in a head to tail fashion through the formation of amide bonds. This is referred to as the primary structure of a protein.

The secondary structure depends on the network of amide bonds and gives rise to structural motifs. The most common structural motifs composing all proteins are known as α - **helix** and β – **sheet**. These two motifs clearly have different structural properties although these molecules are composed of relatively similar arrangements of atoms. The difference in topology between these two structures is exclusively due to the backbone conformation. The torsional angles of the amino acid backbone

in helical structures are quite different from those of the extended sheets. The tortional angles are dictated by a number of properties but primarily steric interactions.

The tertiary structure describes how these motifs are arranged to yield a three dimensional structure of the protein. The motifs interact with each other through electrostatic and hydrophobic interactions to form the native structure of the protein. The mechanisms behind protein folding at this level are far from completely understood.

Lastly, there are quaternary interactions. Proteins often form dimers, heterodimers and the like. Protein folding at this level considers these interactions. For example, hemoglobin is composed of four non – covalently bound protein subunits, referred to as $\alpha_2\beta_2$ arrangement. Other proteins such as collagen form covalent cross-links between adjacent strands for tensile strength.

4. Carbohydrates: Carbohydrates are essential biomolecules for all organisms. These molecules have the general structure of $(CH_20)_n$,where n is greater or equal to 3. They serve as structural materials, fuel and are involved in signal transduction processes as well. Carbohydrates are therefore an extremely structurally diverse group of molecules. Many carbohydrates form covalent complexes with other biomolecules.

Due to the necessity of these biomolecules for all organisms, there are a variety of pathways to create them including gluconeogenesis and photosynthesis. The monomers of sugars are used to make polysaccharide polymers. This makes the sugars easier to store as either starch in plants or glycogen in animals. Both of these molecules are formed from glucose monomers but differ in the bonding between the monomers linking them together. A comprehensive review of these molecules can be found in "Biochemistry" **(Voet et al. 1995, pages 251 – 276)**.

D. IR Spectroscopic Properties of Biomolecules: The **IR** spectra of cells and tissues are dominated by proteins. The average cell is composed of 60% protein by weight. The secondary, tertiary and quaternary levels of protein dictate the ultimate spectral properties of each protein. Shown in **Figure 3** are the spectrum from human serum albumin **(HSA)** and chymotrypsin. The structure of **HSA** is mostly α helical whereas chymotrypsin is mostly β sheet. Collagen is quite unique, in the fact that it has unique tertiary interactions that make it differ from other cellular proteins. The amide I, II and III differ somewhat spectroscopically in these proteins from one and other.

The infrared absorption spectra of **DNA** and **RNA** are also shown in **Figure 4** The most prominent features are due to the asymmetric and symmetric phosphate stretching vibrations at ca. 1235 and 1086 cm^{-1} respectively. In the region below 1140 cm^{-1} there are additional vibrations due to ribose ring vibrations as well. Nucleotides contain carbonyl groups in their aromatic bases. This leads to the spectral characteristics between 1550 cm^{-1} to 1650 cm^{-1}.

Phospholipids show considerable contributions to the **IR** spectrum of cells as shown in **Figure 5**. The spectrum of phospholipid is similar to that of **DNA** and **RNA**. The asymmetric and symmetric phosphate vibrations at 1235 and 1086 cm^{-1} are present, respectively. The carbonyl stretch of these molecules, at 1730 cm^{-1}, is distinct from proteins and nucleic acids.

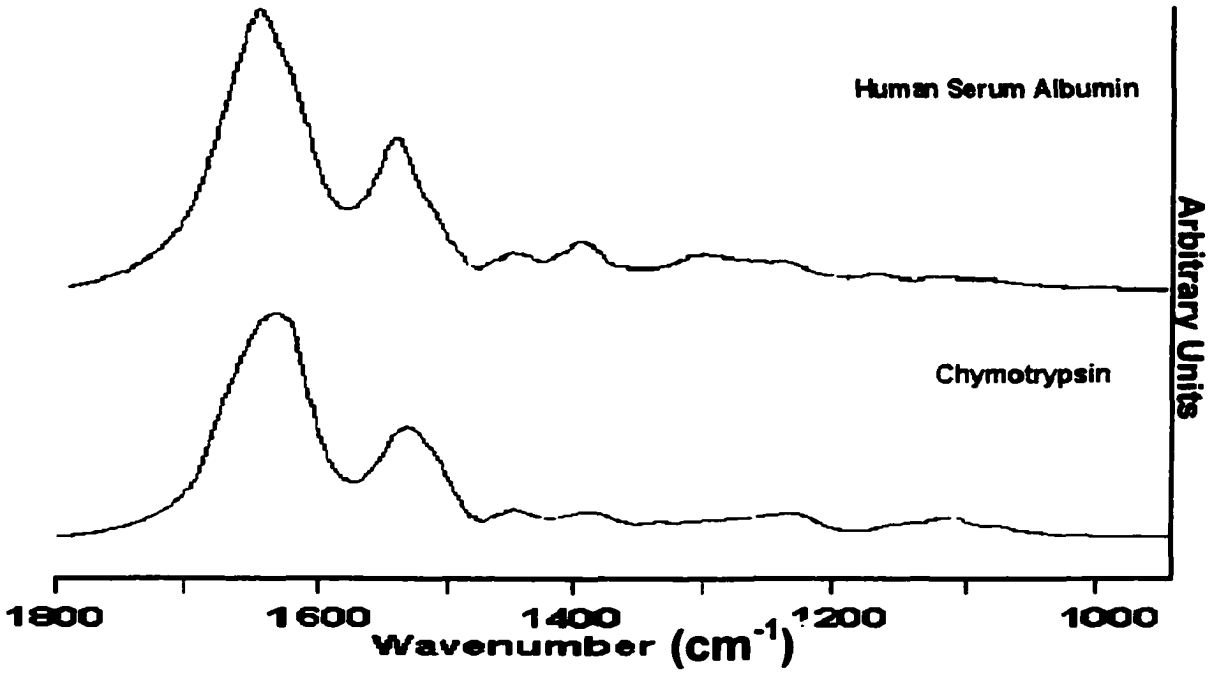

Figure 3: IR spectra of human serum albumin (HSA) and chymotrypsin.

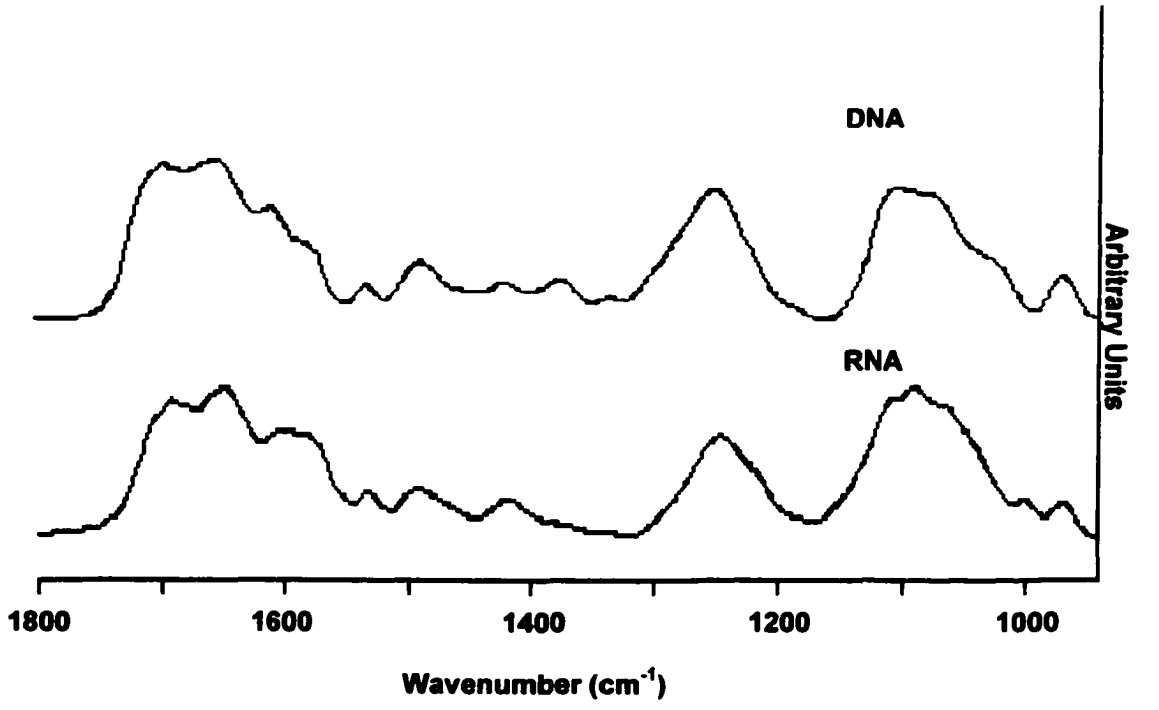

Figure 4: IR spectra deoxyribonucleic (DNA) and ribonucleic (RNA) acids.

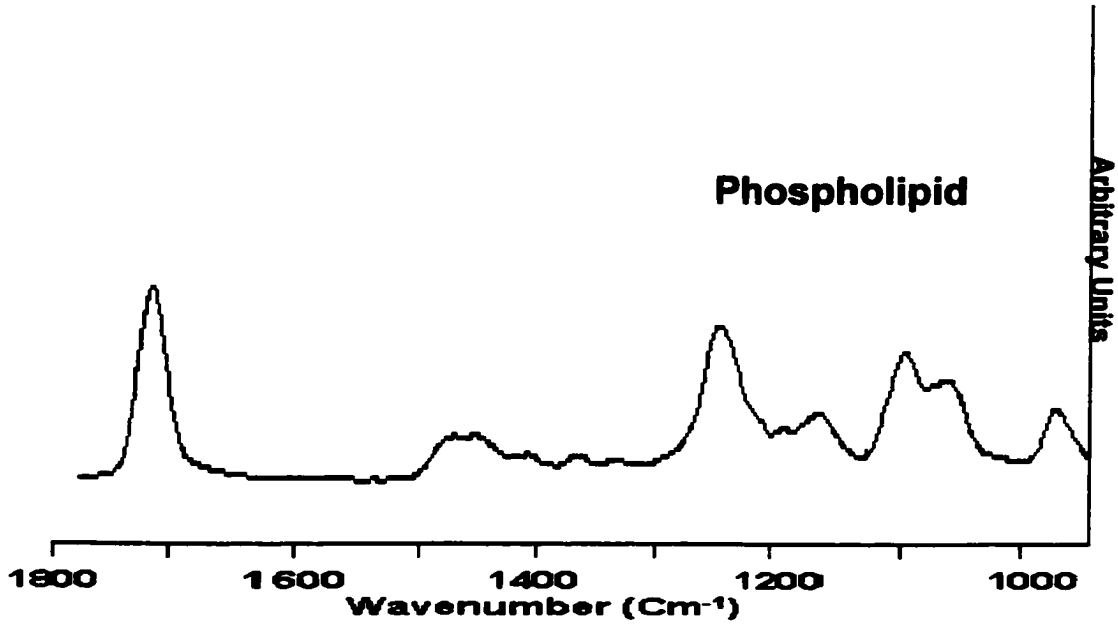

Figure 5: IR spectrum of phospholipid.

E. Cell Biology: The work considered here is heavily based on the processes of modern cell biology. Cells respond to external stimuli and that signal is transduced to the appropriate organelles within the cell. These signals are supplied as biochemical messengers to accomplish certain tasks for the good of an organism such as repair, growth or the maintenance of homeostasis. As organisms have become more complicated, the role that proper communication between cells plays an increasingly more important one.

1. Stages of the Cell Cycle: The principles of regulation processes involved in cells are crucial for the following work. As has been alluded to in the previous text, the rates of growth and repair within an organism are closely mediated by elaborate series of signaling mechanisms. These signal cascades are carefully coordinated events that allow for the faithful replication of a given cell. The coordination is regulated and modulated to ensure the cell divides with the proper genetic information. The cell cycle control system is conserved throughout evolution and is a common thread shared by organisms. Many of the systems employed in mammalian cells are nearly identical to those of yeast cells. The first elements of the cell cycle control system appeared over a billion years ago.

The cell cycle, at a fundamental level, is composed of two stages, interphase and mitosis **(M phase)**. Interphase represents a growth stage where the cell synthesizes all of the necessary materials prior to division. Interphase is broken up into several phases. The several phases of the cell cycle that compose Interphase are each important to successfully coordinated cell growth as in **Figure 6**.

The **G1** phase is responsible for providing the time for growth before replication of **DNA** can occur. This includes synthesis of proteins and **RNA** necessary for the length of **S** phase. **DNA** replication occurs during synthesis or **S phase**. **G2** phase allows the cell a period of time in which to prepare itself for mitosis.

Both of the **G1** and **G2** phases are very important as they provide checkpoints for growth control. The **G1** phase of cell growth allows the cell to monitor its environment as discussed earlier and also its size. When the proper conditions are satisfied, the commitment to **DNA** synthesis and entrance into **S phase** will occur. The **G2** phase is redundant and provides a safety gap to ensure that **DNA** replication has completed.

The **G1** phase is unique. This phase of the cell cycle can vary in length of time to complete from 12 hours to an indefinite period of time. The longer periods of **G1** are due to a lack of commitment to the replication of **DNA** by a given eukaryotic cell. Cells that remain in **G1** longer than 12 hours may not have received a mitogenic signal for cell cycle progression. A poor growth environment as well as damage or alterations to the genome (senescent cells, differentiation, **DNA** damage) of a given cell may also be responsible. Any of these conditions will force the cells to remain in **G1**. These cells can also enter a special resting state within **G1** referred to as **G0**. Any newly divided cell less than 3.5 hours old has the option, as it proceeds through **G1**, to enter **G0**.

During **G0**, protein synthesis in this period may fall to 20% of the level found in a cycling cell. Cells that choose enter **G0** must stay in this resting phase for at least 8 hours **(Alberts et al., 1994)** and may stay for an indefinite period of time. Commitment to **G0** requires that the cell spend at least 8 hours in this phase. This period of time is required for the disassembly and reassembly of the cell cycle control system.

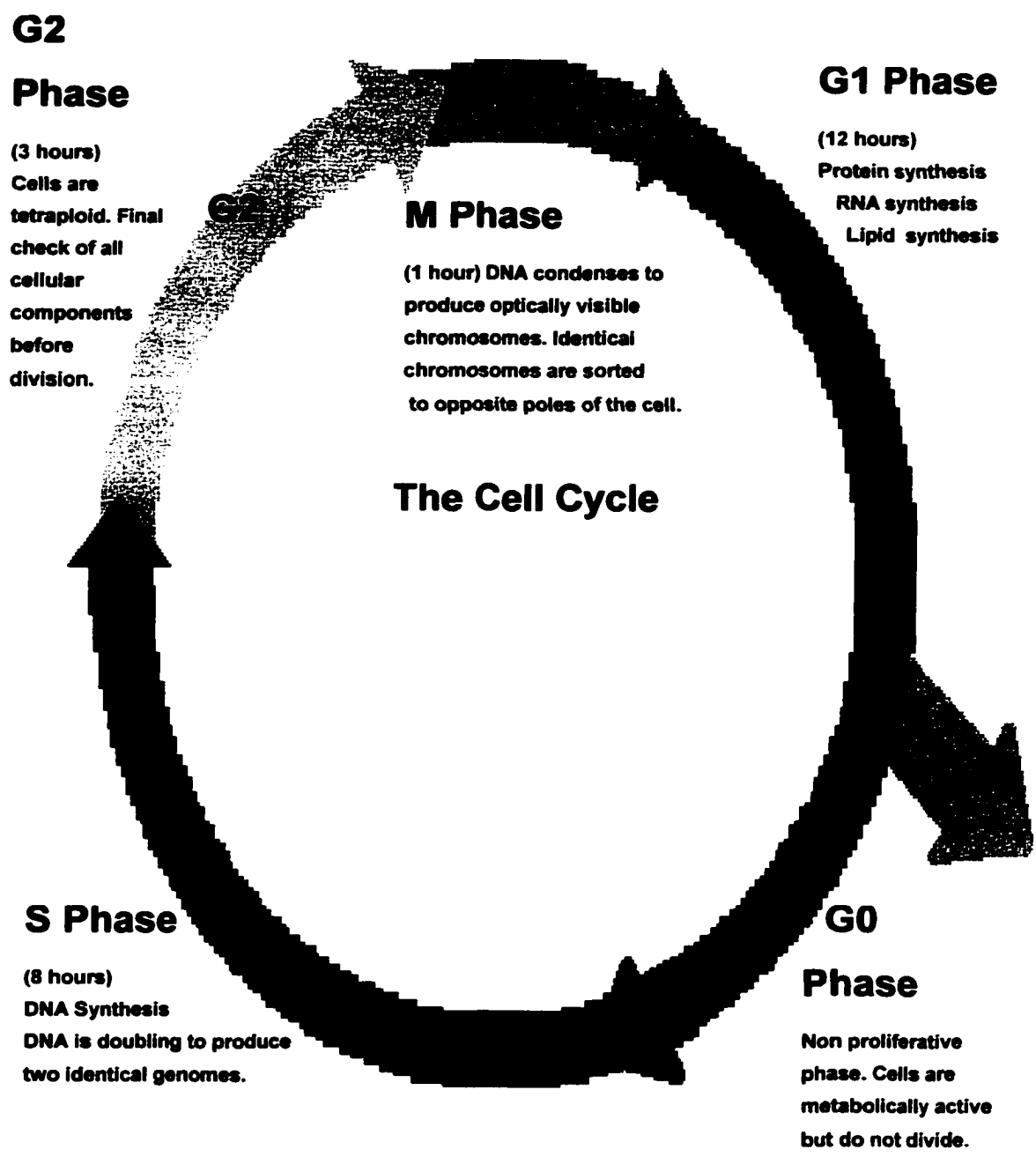

Figure 6: Stages of the cell cycle.

Mitosis is the process concerning the actual division of the contents of the parental cell into two identical daughter cells. This stage is well characterized, as the events are easily observable under the light microscope. The stage begins with the breakdown of the nuclear envelope, which is followed by the condensation of **DNA** into visible chromosomes. The cellular cytoskeleton rearranges to form the mitotic spindle. This tubulin-based network is critical for the separation of identical chromosomes, which permits for the proper **DNA** content of the resulting daughter cells. In the later stages of this process, the two identical sets of chromosomes are sorted to opposite poles of the cell and decondense. Nuclear membranes quickly form around the two sets of chromosomes and cytokinesis begins. Cytokinesis is the process by which the parental cell physically divides to yield two identical daughter cells and is mediated by a cytoskeletal network of actin filaments that forms a ring within the center of the parental cell. **ATP** dependent myosin filaments provide the pinching action of this ring **(Mc Intosh et al. 1989, Sawin et al. 1991).**

The cell-cycle control system is ultimately regulated by the interactions between two families of proteins. The first of which are the cyclin - dependent protein kinases **(CDKs)**. These proteins can phosphorylate specific target proteins on serine and threonine residues. As implied by the name, **CDKs** require a family of proteins known as cyclins for enzymatic activity. The synthesis of cyclins and the

assembly/disassembly of cyclin-CDK complexes play a pivotal role in progression through the cell cycle.

As implied by the name of these molecules, the expression and degradation of cyclins depends on the progress through the cell cycle (Evans et al., 1983). These molecules come in two subfamilies. There are the mitotic cyclins and the G1 cyclins. The mitotic cyclins bind to CDKs during G2 and allow passage into M phase. The G1 cyclins bind CDKs during G1 and allow passage into S phase. The degradation of the cyclin moieties permits the exit from M and S phase, respectively. In addition to the requirement for assembly, the activity of these complexes are regulated at the level of phosphorylation / dephosphorylation.

The protein machinery that controls progression through the cell cycle has enzymatic activity. The most common activity of which is the ability to carry out the phosphorylation of gene regulatory proteins. This results in the expression of special proteins needed only at certain stage of the cell cycle. Another important use of this type of activity is the phosphorylation of histones. These proteins are used to decondense the DNA into a compact structure. Phosphorylation of histones is therefore key to the replication and proper sorting of genetic information as the chromosomes need to condense during mitosis. One can now see how the mitogenic signal received at the membrane may be transduced and amplified to the nucleus by a cascade of phosphorylation.

2. General aspects of cell signaling: Eukaryotic cells use three primary types of pathways to deliver a message. There is the passive mechanism in which small molecules such as nitric oxide **(Anggard, 1994)**, or non- polar molecules such as steroids, function as messengers. These molecules are free to diffuse through the cell membrane due to their size or ability to traverse a cell membrane due to their non- polar attributes. The small molecules often act at short distances because they are rapidly scavenged. The non- polar molecules are capable of acting over long distances but require proteins such as human serum albumin **(HSA)** to boost their solubility in the aqueous environment of the bloodstream **(Broderson, 1977)**.

Another important signaling pathway involves the secretion of some large hydrophilic factors such as a protein using the secretory machinery of the cell. The factors that are secreted are referred to as ligands. These ligands are highly specific for receptors on the surface of the target cell. Since this pathway involves the synthesis and secretion of proteins, this process is referred to as active signaling.

Serum contains many peptides that are involved in active signaling at the cell membrane. The growth-stimulating factor, epidermal growth factor **(EGF)** serves as an excellent example. This peptide is secreted by the submaxillary glands and acts on the membranes of cells at a distance from where it is created. **(Cohen, 1960)**. Upon binding to a target cell, a ligand receptor complex is formed. This triggers a conformational change

in the receptor. As the enzymatic activities of receptors are activated upon ligand binding, a signaling cascade begins. This occurs through phosphorylation cascades that have been initiated quite often by either the receptor kinases such as **EGF**.

Other mitogenic receptors lack autophosphorylation capabilities and couple their activation to the recruitment and subsequent activation of G proteins. This pathway controls processes such as glycogen breakdown. Upon activation of the receptor, a G protein is recruited by the receptor. This causes the release of GDP as well as a G protein specific inhibitory peptide. Upon GTP binding, the G protein undergoes a conformational change allowing it to activate adenyl cyclase, which produces cyclic adenosine monophosphate **(cAMP)**. The cAMP often goes on to activate A – Kinase to phosphorylate other proteins.

The release of various intracellular ligands inside the target cell often accompanies either of these cascades. Calcium **(Ca^{+2})**, inositol triphosphate **(IP3)**, diacylglycerol **(DG)** and also cyclic adenosine monophosphate **(cAMP)** represent some of these intracellular signaling molecules. These molecules may be released from organelles or the cell membrane. The signal that was received at the cell surface are amplified or fine tuned by these biomolecules, therefore these cascades are carefully regulated at each step.

Many eukaryotic cells require stimulus from the immediate surroundings in order to grow or survive. One such process by which cells

have been shown to respond to the environment involves contact dependent growth inhibition. Proteins such as the integrins are secreted onto the membrane of an eukaryotic cell and these proteins are capable of relaying information about the environment back to the nucleus. Another protein involved in tumor suppression called VHL is induced at high cell density and mediates contact inhibition of cell growth **(Baba et al., 2001)**.

Contact inhibition provides a critical control towards the proliferation of cells. Normal cells that have lost their proper attachment to their substrates can no longer grow and therefore die. This process fails in tumerogenesis. Tumor cells lose their requirement for attachment and therefore become capable of spreading throughout an organism.

III. A Review of Previous Literature in the Spectroscopy of Cells: Research towards detecting pathological changes associated with the onset of cancer using **IRMSP** in cells has been aggressively undertaken starting in the early 1980's. Work on tissues using IR-MSP has closely paralleled the cell research as well **(Wong et al., 1991, Chiriboga et al. 1998, 2000a, 2000b).**

Benedetti was among the first to investigate the spectral differences between normal and leukemic lymphocytes obtained from peripheral blood **(Benedetti et al. 1985)**. The differences between the normal and leukemic cells were attributed to changes associated with the phosphate vibrations of **DNA**.

Recent work by Benedetti has studied megakaryocyte cells **(MK)** **(Benedetti et al., 1998)**. **MK** cells undergo alterations leading to abnormal proliferation of these cells. This is referred to as primary thrombocytemia **(PT)**. **MK** cells isolated from patients with and without **PT** were studied. The large size of these cells with **PT** allowed for measurements to be made either from the nucleus and the cytosol of each cell.

The authors showed large differences between the spectra of **PT** cells from the nucleus and cytosol. In addition, the normal whole **MK** cells obtained yielded similar spectra compared to the cytosol of the **PT** cells. The differences were attributed in the **PT** cells to nuclear components that were not spectrally observable within the normal cells.

Changes within the cytosol were correlated to those within the nucleus using the following method. The integrated areas between 1590 – 1480 cm^{-1} and 1152-940 cm^{-1} were calculated for normal **MK** cells and **MK** cells with **PT**. This corresponds to the amide II vibration envelope and a region rich with spectral features that were associated with nucleic acids, respectively. The **MK** cells with **PT** had nearly double the contributions associated with region between 1152-940 cm^{-1} relative to the amide II vibration as compared to the normal **MK** cells.

This was thought to be useful as marker for differentiating normal **MK** cells from those with **PT**. The authors concluded that the nucleus is heavily involved with the transformation from normal **MK** cells to those with **PT**.

The effects of the anticancer treatments, Chlorambucil **(CLB)** and 2-Chlorodeoxyadenosine **(CdA)** have also been investigated on Chronic Lymphocytic Leukemia **(CLL)** cells **(Mantsch et al., 1997, 1998)**. **CLL** cells are sensitive to both of these treatments and they may be used in conjunction with other treatments.

The cells treated with **CLB** or **CdA** were obtained from patients after four weeks of chemotherapy. The data collected from these samples was correlated with the results from a cytotoxicity assay using a tetrazolium dye to measure the viability of the cells after different treatments.

Cells resistant to these treatments were compared to ones that were sensitive. The spectra of **CLB** resistant cells were mathematically subtracted from those of the **CLB** sensitive cells to yield difference spectra. This was performed for the **CdA** treated cells as well. Also, the spectroscopic data were analyzed using the first derivatives of the spectra obtained.

The difference spectra obtained between the treated and untreated cells revealed gross changes in the content of nucleotides, proteins and lipids. Both treatments induced similar changes. The **CdA** and **CLB** resistant cells both had increased spectral features associated with protein moieties. In contrast, spectral features associated with lipid and **DNA** moieties were less prevalent in the resistant cells.

The first derivative spectra also revealed small differences between **CdA** sensitive and resistant cells. This was also true in the case of **CLB**. In fact all four categories of spectra showed unique signatures. This may suggest two different mechanisms of drug resistance.

Following the work done by Mantsch et al., single ML-1 cells were studied in terms of cell cycle progression versus spectral changes **(Boydston-White, et al., 1999)**. In conjunction with **IR-MSP** and **IR** macroscopic analysis, Fluorescence-activated cell sorting **(FACS)** was used to correlate the spectra collected to the stages of the cell cycle. **FACS** analysis allows for the detection of **DNA** content within a given cell. The key to this technique is that a fluorescent dye such as ethidium

bromide (EtBr) will bind DNA non-specifically. The DNA content of a given is indirectly measured as a function of fluorescent signal. Cells can be measured arbitrarily as a function of population versus relative DNA content. Cells with the highest amount of DNA are generally cells that have passed through S phase. Cells of intermediate DNA content are the cells of S phase. The cells with relatively the lowest DNA content are either of G0 or G1 phases.

Myeloid Leukemia (ML-1) cells were obtained from an asynchronous, exponentially growing culture, and were centrifugally elutriated. Elutriation allows for a separation of cells via size and density. Fractions (17) obtained from elutriation were first subjected to FACS analysis. The first seven fractions were reported to contain 95% + cells in G1 phase. **Figure 7, trace A** shows a representative spectrum obtained from fraction 4 of these cells taken as a macroscopic measurement. In the nucleic acid region of the spectrum, a qualitative analysis reveals that RNA heavily contributes to the spectral features of this region.

Fraction 11 of the elutriated sample was found to representative of cells found in S phase. This fraction was reported to contain approximately 90 % S phase cells. The spectrum shown in **Figure 7, trace B** reveals a heavy contribution of DNA spectral characteristics. Synthetic DNA / RNA films for IR analysis have been prepared **(Benedetti et al. 1997)**. High DNA/RNA ratios in these films leads to a similar loss of sharp spectral characteristics in nucleotide absorbing regions. **Figure 7, trace C**

represents late **S** phase cells. The spectral characteristics in low frequency region around 1080 cm^{-1} are also broad as in **trace B**.

Lastly, an assessment of the final three fractions of **ML - 1** cells was performed. These fractions contained cells that were representative of **G2** phase. It was reported that **G2** phase cells composed approximately 70 % of these fractions. **Figure 7, trace D**, illustrates the type of spectra obtained from these fractions. The low frequency region of this trace resembles that of the **G1** spectrum with most of the features attributable to **RNA**.

The main conclusion of this work is that in **G1** and **G2** phase spectra, the contribution of **DNA** spectral characteristics to the low frequency region is extremely low. The **S phase** spectrum however, shows large contributions of **DNA** spectral characteristics. One however, would expect spectra of the **G2** phase to more closely resemble those of **S phase** rather than those of **G1** phase. This is because cells of the **G2** phase have already replicated their genome and now have twice the amount of **DNA** as the **G1** cells.

The work herein illustrated that the spectra of cells in **S phase** were remarkably different from the spectra of cells in either **G1** or the **G2** phases of the cell cycle. The spectra of the **S phase** cells featured intense nucleotide vibrations relative to the **G1** and **G2** spectra. This is suprising considering the fact that the nucleotide content of **G2** cells is twice that of **G1** cells.

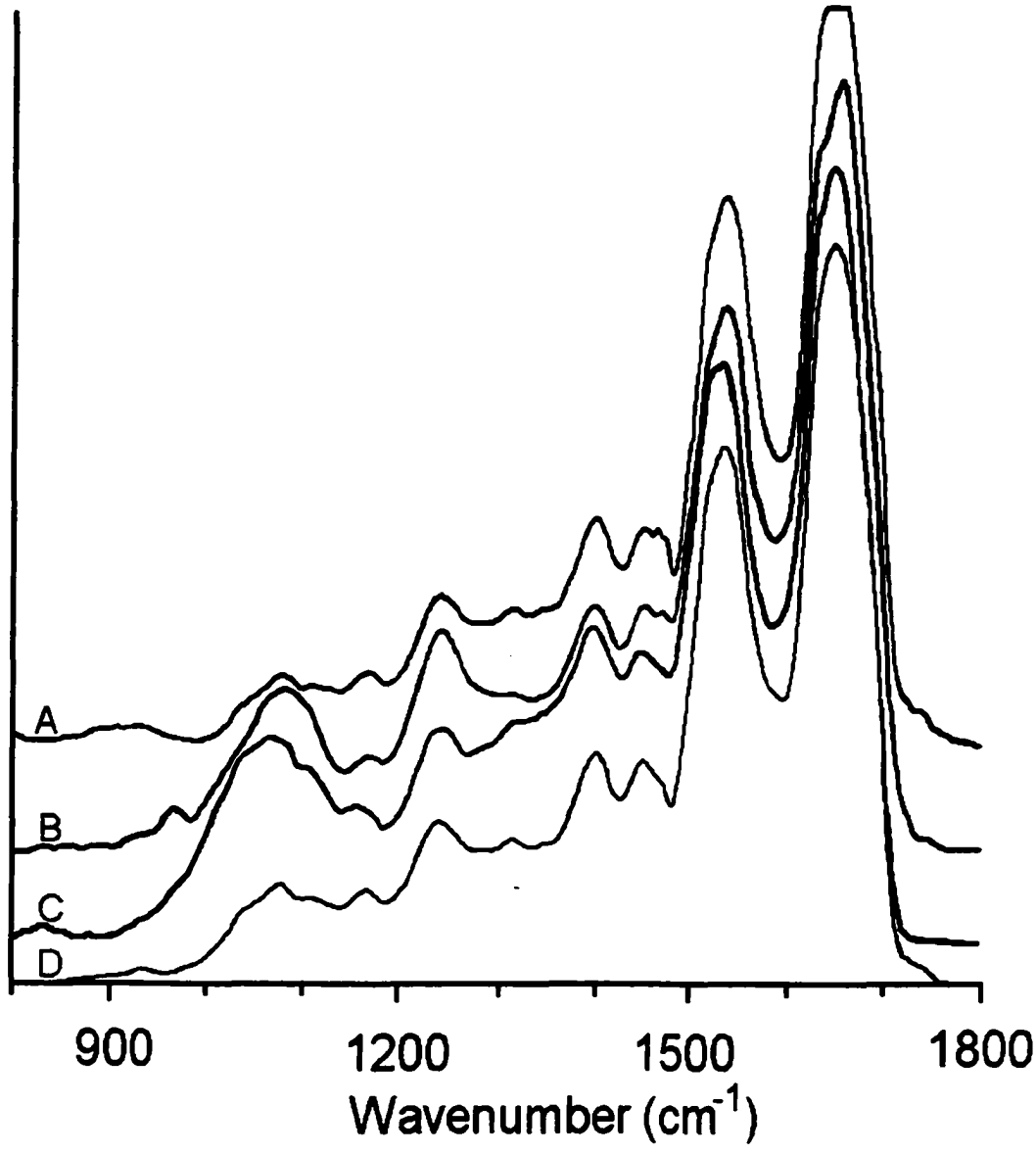

Figure 7: Spectra of the various stages of the cell cycle obtained by IR microspectroscopy. Trace A represents ML- 1 cells from G1 phase. Traces B and C represent S phase spectra and trace D represents spectral characteristics of G2 cells (Boydston-White, et al., 1999).

The molecular dynamics of lymphocyte activation have been studied (**Wood et al., 2000**). Lymphocyte cells respond quite rapidly to mitogens such as phytohaemagglutinin – L (**PHA**). The changes within spectra obtained were analyzed using 2nd derivative analysis of the acquired spectra.

Spectroscopically, the changes that were observed were quite intense. Both the characteristic symmetric and antisymmetric phosphate vibrational modes increase in intensity after only 15 minutes of exposure to **PHA**. Further changes usually associated with phosphate vibrations of nucleic acids are observable at 1050 and 966 cm^{-1}. This may be due to a number of possibilities including changes in **DNA** conformation, structure or simply increased **RNA** synthesis. The intensity of these bands continued to increase through the 30 and 60-minute intervals. After 60 minutes of stimulation, two bands unique to lymphocyte activation appeared at 1160 cm^{-1} and 1120 cm^{-1}. Both bands had been associated with **RNA** ribose stretching (**Benedetti et al., 1997**) with some contributions from proteins and carbohydrates.

The spectra at the 24 and 48-hour time points both contain all of the spectral features listed above and slightly more intense as compared to the earlier time points. These spectra lack the large changes associated with the **ML-1** cells. It is quite possible that the changes in the **ML-1** cells are cell type specific. They may depend on low sample heterogeneity in

terms of the cells present. The lymphocyte cell samples had other cells present as well.

An alternative explanation may revolve around the kinetics of entry into **S phase (Okuda et al., 1983)**. In fibroblasts, it has been shown that entry into **S phase** is a slow and gradual process taking up to eight hours for complete radio labeling of cellular **DNA** in a population of cells. This would result in a relatively low number of cells proceeding through **S phase** at any time. Many **IR** spectroscopic details associated with the **S phase** spectra of cells could be obscured by the lower numbers of **S phase** cells normally obtained in culture.

Furthermore, the individual **IR** spectroscopic contributions of subcellular organelles has recently been compiled using bovine hepatocytes **(Lasch et al., 2001)**. These measurements were of enriched organelles specially purified by sucrose density gradient centrifugation. The spectra of subcellular organelles had been published **(Jamin et al., 1998)**. However, there were no published **IR** data with a sufficient signal to noise ratio to allow an interpretation in the mid **IR** region (3000 cm^{-1} to 900 cm^{-1}).

The high quality spectra obtained from these **IR** measurements allowed for an interpretation of the contributions of these organelles to single, whole cells. It is important to note that one drawback to the sucrose density gradient centrifugation method of organelle extraction is that no sample of any organelle is completely free of contamination from other

organelles as this technique is sensitive only to the buoyancy of the particles within the gradient. One of the most important discoveries to be yielded from this work correlates quite nicely with the data from the elutriated **ML-1** cells. The differences in intensity between the four subcellular fractions assayed (nuclear pellet, microsomes , heavy and light mitochondria pellets) in terms of the symmetric phosphate stretch of nucleotides at 1083 cm^{-1} were rather small. Another surprise was the enormous contribution of phospholipid never observed before. The nuclear fraction increased only by 15% relative to either the heavy mitochondrial or microsomal pellets.

This result is slightly complicated by the fact that mitochondria contain their own genome. We calculated in our group that the contribution from mitochondrial **DNA** is rather small as it represents less than 2% of the total **DNA** content of the cell. It is conceivable that contributions from mitochondrial **DNA** as well as phospholipids and other phosphorous ester containing molecules may obscure the true magnitude of the increase in intensity at 1083 cm^{-1}.

Single cell mapping studies of Oral Mucosa Cells provide an important connection between the work on **ML-1** cells and the subcellular fractionation results. These cells are non-proliferative, terminally differentiated and metabolically inactive and are therefore primarily in the **G0** phase of the cell cycle. Measurements were carefully taken using the precisely controlled stage of the **IR** microscope within our lab. These

results also showed the same small consistent changes in comparing nucleus to the cytosol as shown in the liver hepatocyte fractions. This is an important proof as it shows that the intensity changes are not due to the structural integrity of the cell. The same spectral changes are seen in the organelles whether the cell is whole or fractionated. Again these results are slightly obscured as the presence of mucin, a glycoprotein is present on the cell surface is present. It features strong absorbencies at 1150 and 1050 cm^{-1} and therefore makes the symmetric phosphate vibration at 1083 cm^{-1} difficult to interpret.

These results do point to the architecture in which nuclear **DNA** is packed and protected within nucleosomes. It may be important and at the heart of explaining these experimental results. In both the **G1** and **G2** phases the **DNA** in the nucleus may be so condensed that it resembles an opaque body within the cell which renders the **DNA** unobservable to the **IR** beam. In the case of the **S** phase spectrum, contributions of **DNA** spectral characteristics to the low frequency region may be due to the unwinding of nuclear **DNA**. This unwound **DNA** may no longer be opaque to the **IR** beam and therefore may absorb **IR** photons. The subcellular organelle studies bolster this concept as the small changes between the various pellets is relatively small. It is known that the majority of hepatocytes rest in the **G0** phase. The length of the average hepatocyte cell life cycle is 150 days **(Leonhardt, 1981)**. The results from the **ML-1** cells and the liver hepatocytes fit quite nicely as they predict small

changes for cells in the nucleotide region of the mid- IR spectrum of cells unless there is a large presence of S phase cells.

Spatially resolved infrared studies for single cells have also been reported (Diem et al., 2001). The data obtained at high spatial resolution of skin fibroblasts and giant sarcoma cells, both exhibited high levels of metabolic and divisional activity. It was expected that DNA is partly uncoiled during replication and, hence, detectable. In order to be able to differentiate between the phosphate signals from lipids (phospholipids), RNA and DNA, all experiments were carried out on cell samples treated with alcohol, RNase, and DNase. Indeed, we find that small DNA signals are detected in the nuclei after removal of other sources of phosphate groups.

Furthermore, we report for the first time large signals of phospholipid in the cytoplasm, and large cytoplasmic RNA signals. Both these components appear to be observed only in physiologically active cells.

The data of this study support the hypothesis that IR-MSP of tissues monitors the level of cell activity rather than signatures specific to cancer. Furthermore, it appears that the higher the cell's divisional and metabolic activity, the more pronounced the $-PO_2^-$- bands of DNA, RNA and phospholipids will be. The experimental data of the present study also support the hypothesis that condensed DNA of inactive (pyknotic) nuclei is invisible to IR transmission spectroscopy.

There are several shortcomings in the interpretation of data from early results. It is important to consider these in later efforts as interpretation of the spectral results with the biological properties of cells is the ultimate goal of this technique.

Benedetti et al. showed gross changes between normal **MK** cells and those with **PT**. It is however uncertain whether the spectral differences are directly attributable to changes within the structure or content of **DNA** in the **PT** cells. Possible other explanations are changes within the phospholipid, **RNA** or glycogen content of these cells. All of these molecules have spectral characteristics in the region of the spectrum associated with **DNA**.

In addition, the amide II band does contain some of the spectral characteristics associated with **DNA** and **RNA**. This makes comparing the ratio of integrated area of the amide II to that of the nucleotide envelope between 1152-940 cm^{-1} very difficult and misleading. The reasoning behind this is that as the spectral features of the nucleotide envelope change, the amide II will change as well. This prevents any real conclusion about changes between the nucleus and cytosol very difficult.

The work done by Mantsch et al. illustrates the differences due to different drugs in the same **CLL** cell line. It is however uncertain what the underlying mechanisms behind the drug resistance are. More importantly, it is unknown how these mechanisms interact within a cell to change the spectral characteristics of the biomolecules previously mentioned.

IV. Experimental:

A. Preparation of 3Y1 Cells for Cell Density and Growth Factor Dependent Measurements:

Wild type rat liver fibroblast cells (**3Y1** cell line) were thawed and deposited into 150 mm tissue culture plates containing Dulbecco' s Modified Eagle Medium (**DMEM**) (GIBCO, Grand Island, NY) that had been supplemented with bovine calf serum (HYCLONE Laboratories, Logan, UT, 10%, v/v: lot number : AKA11378). After a brief incubation period, the serum-enriched medium was replaced to remove dimethylsulfoxide (Sigma, St. Louis, Mi.,10%, v/v) (**DMSO**) used in the freezing process. The cells were then allowed to grow to 97 % confluence (*ca.* 3 days). Cells were then removed from the plates with trypsin (GIBCO, Grand Island, NY) that had been dissolved in Dulbecco' s phosphate buffered saline (GIBCO, Grand Island, NY). The cells were then pelleted and the supernatant was removed. The cells were then re-suspended in medium containing bovine calf serum (10%, v/v), and added to fresh 100 mm tissue culture plates at a concentration $6 * 10^5$ cells / plate. The cells were then allowed to grow for between 15 and 24 hours before additional treatment.

For experiments demonstrating the effects of confluence, the serum-containing medium was then rinsed away and replaced with low serum medium (0.5%, v/v) for 36 hours. Subsequently, the low serum medium was replaced with high serum containing medium (10%, v/v), and

cells were allowed to grow between 24 and 72 hours. Samples for microscopy and FLOW cytometry were prepared every 12 hours. This serum deprivation procedure ensures that the cells were at similar stages of the cell cycle before exponential growth phase was initiated. Data reported here concentrate mostly on the 24- and 72- hour samples although the samples from time points in-between clearly demonstrate the trends shown by the extreme time values.

For experiments involving the removal of growth factors, cells were seeded at a concentration of $3 * 10^5$ cells/ plate. The cells were allowed to grow for up to 24 hours in high serum containing **DMEM**. The high serum containing medium was removed and substituted low serum containing medium for 36 hours where upon it was rinsed and replaced for another 24 hours. The cells were collected after this stage.

B. Sample Preparation:

1. Preparation of 3Y1 Cells for IR Spectroscopy: Samples were prepared for IR microscopy by rinsing each 100mm cell culture plate three times thoroughly with 5 mL of saline (0.9% v/v). The cells were then removed from the plates with trypsin (GIBCO, Grand Island, NY) and a cell pellet was collected by centrifugation. The supernatant was carefully decanted and each pellet was resuspended and centrifuged three times in 5 mL saline (0.9% v/v). This procedure was repeated for rinses with doubly distilled H_2O. The final pellet was re-suspended in doubly distilled H_2O and resuspended to an appropriate concentration of cells.

For each sample an aliquot (100 μL) of each sample, containing approximately $7 \cdot 10^4$ cells were applied to a Zinc Selenide **(ZnSe)** sample substrate (Bruker Optics, Inc). This was repeated once more for each sample. After application, the samples were dried under vacuum for approximately 45 minutes. The dried cells attach to the **ZnSe** so tightly that any remaining salt residue could be removed from the substrate by rinsing the samples on the window with copious amounts of doubly distilled H_2O. Furthermore, cells can be treated with subsequent various chemical agents to remove certain cellular components. The remaining volume of cells was stored for cytological and flow cytometry analysis.

2. Preparation of Ethanol Treated, RNase and DNase Digested 3Y1 Cells for IR Spectroscopy: After the cells were prepared on the ZnSe substrate, spectra were collected. The phospholipid content of these cells was then extracted by a series of three wash cycles with copious amounts of absolute ethanol (AAPER). The remaining ethanol residue was quickly removed under vacuum. Spectra were thencollected for all data sets.

Subsequently, cells were treated Ribonuclease A **(RNase)** (SIGMA). **RNase** was dissolved in distilled H_2O at a concentration of 1 mg/mL. This solution was then boiled for some time (15 minutes) so as to denature any **DNA** degrading enzymes present in the preparation. Cells on the ZnSe substrate were completely covered with 100 μl of solution. The cells were then incubated at 37°C for 15 minutes, and rinsed with 25 mL doubly distilled H_2O. The procedure was repeated twice more. The cells were finally rinsed with copious amounts of water and dried under vacuum. Spectral data were acquired afterwards.

DNA was enzymatically removed using Deoxyribonulease I (**DNase**). **DNase** was dissolved in H_20 (2mg/ml) and added to the samples for two hours at 37°C. The cells were then rinsed with H_2O.

3. Preparation of 3Y1 Cells for FLOW Cytometry: Propidium iodide (PI) staining for DNA content was performed as follows [Spector, et al., 1998]. Cells in saline (0.9% v/v) were directly fixed in absolute alcohol. These cells were not rinsed with doubly distilled H_2O. After fixation in ethanol, the cells were stored at 4°C for 1 to 4 days. The stored cells (approximately $5 * 10^5$ cells per measurement) were centrifuged at 1000g and re-suspended in 2 mL of saline (0.9% v/v). The procedure was repeated twice. The supernatant was then carefully removed using a Beral pipette, and 250 μL of saline was added to re-suspend the pellet. This was followed by the addition of 250 μL RNase A (SIGMA Chemicals, St.Louis, MO, 5 mg/mL) and 500 μL propidium iodide (SIGMA Chemicals, 100 μg/mL) and 30-minute incubation in the dark at room temperature. The samples were analyzed using a FACSCalibur flow cytometer (Becton Dickinson Immunocytometry Systems San Jose, California) with an argon laser (PI excitation at 488 nm, emission 610-620 nm). Samples were gated to exclude debris. Data is presented as the PI intensity (FL-2 area) plotted against the number of events with the use of CellQuest™ software (Becton Dickinson Immunocytometry Systems).

4. Spectroscopic Measurement Parameters: Microscopic (IR-MSP) measurements were carried out using the Bruker IRScope II infrared microscope coupled to a Bruker Vector 22 FT-IR spectrometer (Bruker Optic, Billerica, MA). The IRScope II is equipped with a **HgCdTe** detector and a computer controlled microscope stage. The sample compartment of the **IR** microscope is enclosed in a purged Plexiglas housing to control atmospheric water vapor. The spectrometer, as well as the microscope, is controlled by a personal computer operating under OS2™ and running Bruker' s proprietary software, OPUS™ (Version 3.0). Coordinates of selected regions on the sample window are marked *via* a calibrated computer controlled stage. On average, about 36 cells were found in an aperture of 100 x 100 microns.

Typically, spectra from between 50 and 65 positions were collected. The best 50 were averaged using OPUS™ software. Spectral data were collected at 6 cm^{-1} resolution and 256 interferograms were co-added before fourier transform. The spectra selected for averaging had nearly straight baselines. Spectra with abnormally high or low intensities about the Amide I and II were rejected.

The resulting spectra were baseline corrected, normalized and averaged in the OPUS™ software. The spectra were normalized using the using the max – min normalization feature. The second derivatives for the averaged spectra were acquired using 25 smoothing points for all spectra.

V. Results: As pointed out before, the aim of the overall research program is to establish spectral differences between exponentially growing cultured cells on one hand, and confluent and serum deprived cells on the other. Thus, the emphasis is on identifying the spectral patterns accompanying these conditions, and not to optimize the stress conditions *per se*. In this thesis, we wish to report the IR results of serum deprivation, and confluence of cultured fibroblasts.

Each of the following sections addressed samples in terms of length of serum exposure. This matched quite nicely with the level of confluence and henceforth, the level of proliferation. Both averaged and randomly selected individual spectra will be displayed, as well as their second derivative spectra. It is important to demonstrate here that the averaged spectra presented both here and in the literature represent an average with some deviation.

In the following figures, the standard deviation trace is shown. It represents the deviation between the individual spectra obtained for each sample and is indicative of the variation in cells across each sample.

A. Serum Stimulated 3Y1 Cells After 24 hours: The spectra for this sample have been derived from cells that have been serum stimulated for 24 hours. These cells serve as a reference for all other samples both for serum deprivation and confluence studies. This sample contained the highest percentage of **S** and **G2** cells reported here at 43.6%. The spectral changes between samples should parallel the changes observed in the level of proliferation. The level of proliferation per sample is assayed in terms of percentages of **S** and **G2** cells per sample through FLOW cytometry.

1. Spectra Generated From Dried 3Y1 Cells After 24 Hours of Serum Stimulation: The spectrum shown in **Figure 8** represents serum stimulated cells that have been dried and fixed upon ZnSe. This spectrum contains the dominant spectral features due to proteins (amide I and II vibrations, 1655 and 1550 cm^{-1}, respectively) seen previously. The shoulder at ca. 1740 cm^{-1} is due to the phosphate ester linkage of lipids, and the broad peaks at 1070 and 1235 cm^{-1} are due to the symmetric and antisymmetric stretching vibrations, respectively, of the $-PO_2^-$ – linkage.

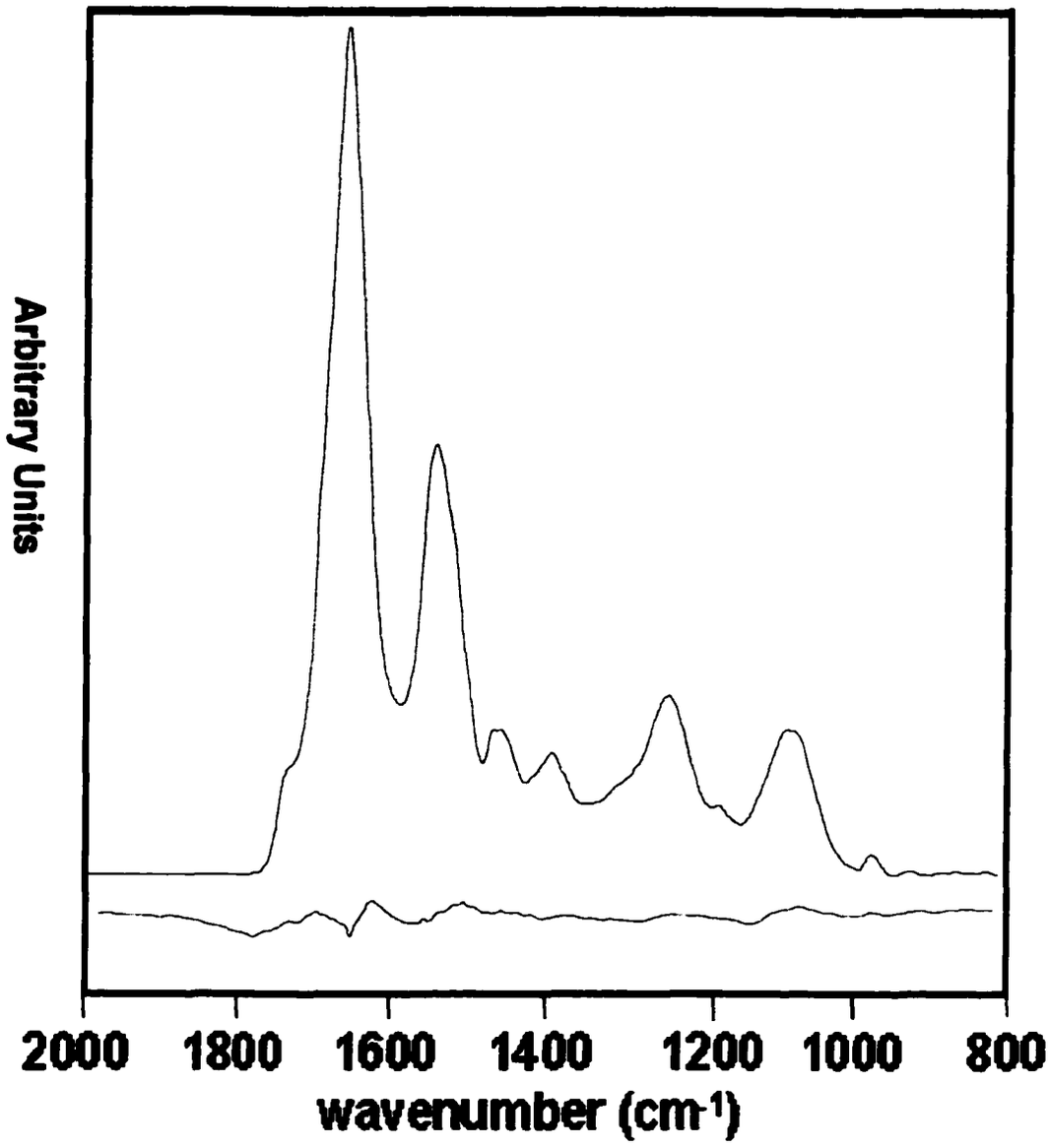

Figure 8: Averaged spectrum of dried 3Y1 cells after 24 hours of serum stimulation. Standard deviation was calculated and shown below.

2. Second Derivative Analysis of Dried Cells That Have Been Serum Stimulated for 24 hours[1]: It is thought that the changes associated with cell cycle progression will most certainly produce changes in spectral intensity in the low frequency region (between 900 –1275 cm^{-1}) of the MID IR spectrum. This region is free of vibrations associated water vapor which may potentially interfere with measurements in the mid IR between 2500 –1275 cm^{-1}.

Shown in **Figure 9** is the averaged second derivative spectrum for the serum stimulated, dried cells. Second derivative spectra are sensitive to band shape rather changes in intensity. We see a number of bands composing the nucleic acid region studied here.

The nucleotide region contains four peaks in the second derivative. The symmetric phosphate stretch occurs between 1100 -1074 cm^{-1}. There is another peak between 1135 – 1116 cm^{-1} at higher wavenumber values. At slightly lower wavenumber values, there is another peak between 1074 – 1043 cm^{-1}. The peaks between 1135 – 1116 cm^{-1} and 1074 – 1043 cm^{-1} are associated with deoxy / ribose ring C-O vibrations.

A peak between 1116 –1101 cm^{-1} is also present. This peak undergoes major changes in bandshape upon higher levels of confluence. It is also sensitive to both ethanol treatments and **RNase** digestions.

1 All second derivative spectra were multiplied by (-1) to allow a comparison with the original spectra.

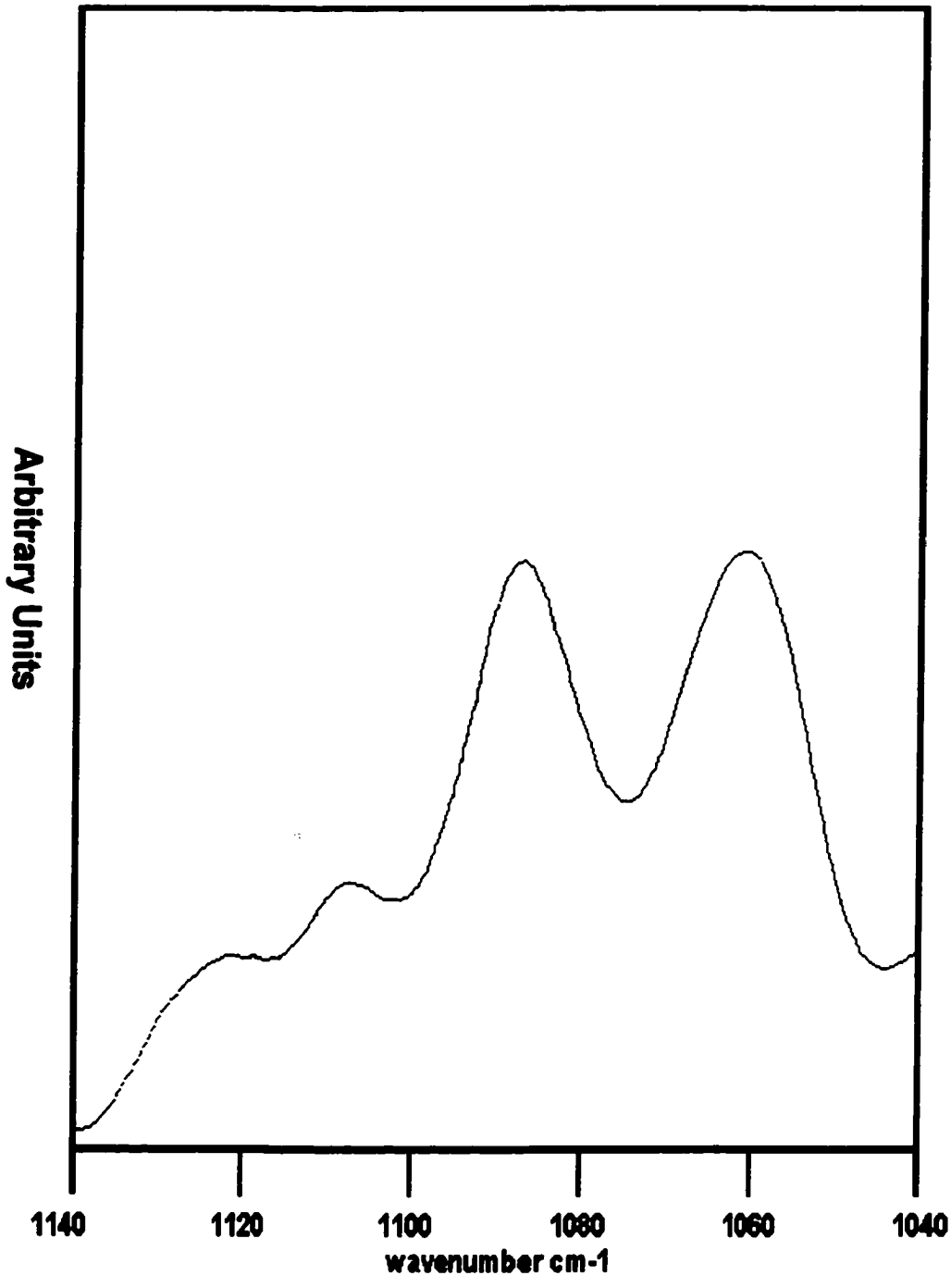

Figure 9: Averaged second derivative spectrum from dried 3Y1 cells that have been serum stimulated for 24 hours.

3. Effect of Ethanol on the Spectra Generated from 3Y1 Cells After 24 Hours of Serum Stimulation: Upon washing with 100% ethanol, the intensity of the symmetric and antisymmetric phosphate stretching vibrations at ca. 1080 and 1235 cm^{-1} respectively, decreases. The phosphoester vibration at 1740 $cm^{-1}$is nearly completely removed as in **Figure 10**. There is a loss in intensity in the nucleotide peak due to the removal of extraneous phosphorous containing compounds that are soluble in ethanol. The nucleotide peak is now enriched in terms of ribo and deoxyribonucleotides.

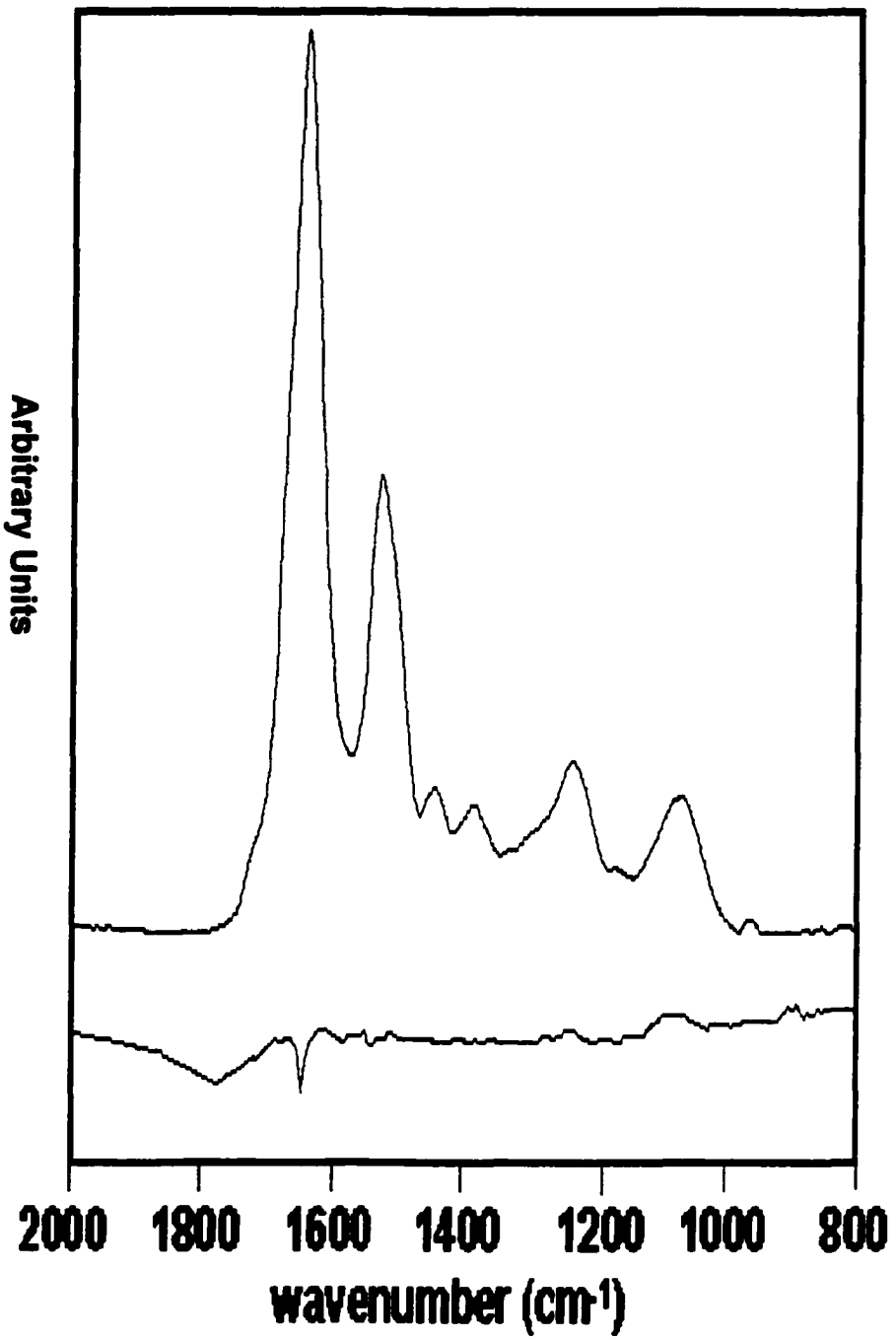

Figure 10: Spectra of ethanol treated 3Y1 cells that have been serum stimulated for 24 hours. Standard deviation was calculated and shown below.

4. Second Derivative Analysis of the Spectra From Ethanol Treated 3Y1 Cells After 24 Hours of Serum Stimulation: Despite the decrease in intensity to the nucelotide region as seen in the spectra, the bandshapes of most of the bands did not change much as in **Figure 11**. The deoxy / ribose ring vibrations between 1138 – 1108 cm^{-1} and 1076 – 1049 cm^{-1} maintain their overall widths and differed little from the dried cells in the second derivative. The symmetric phosphate peak in the dried cells between 1100 – 1074 cm^{-1} broadens slightly to between 1104 – 1074 cm^{-1} after ethanol treatment. The peak between 1116 – 1101 cm^{-1} in the dried cells was absent.

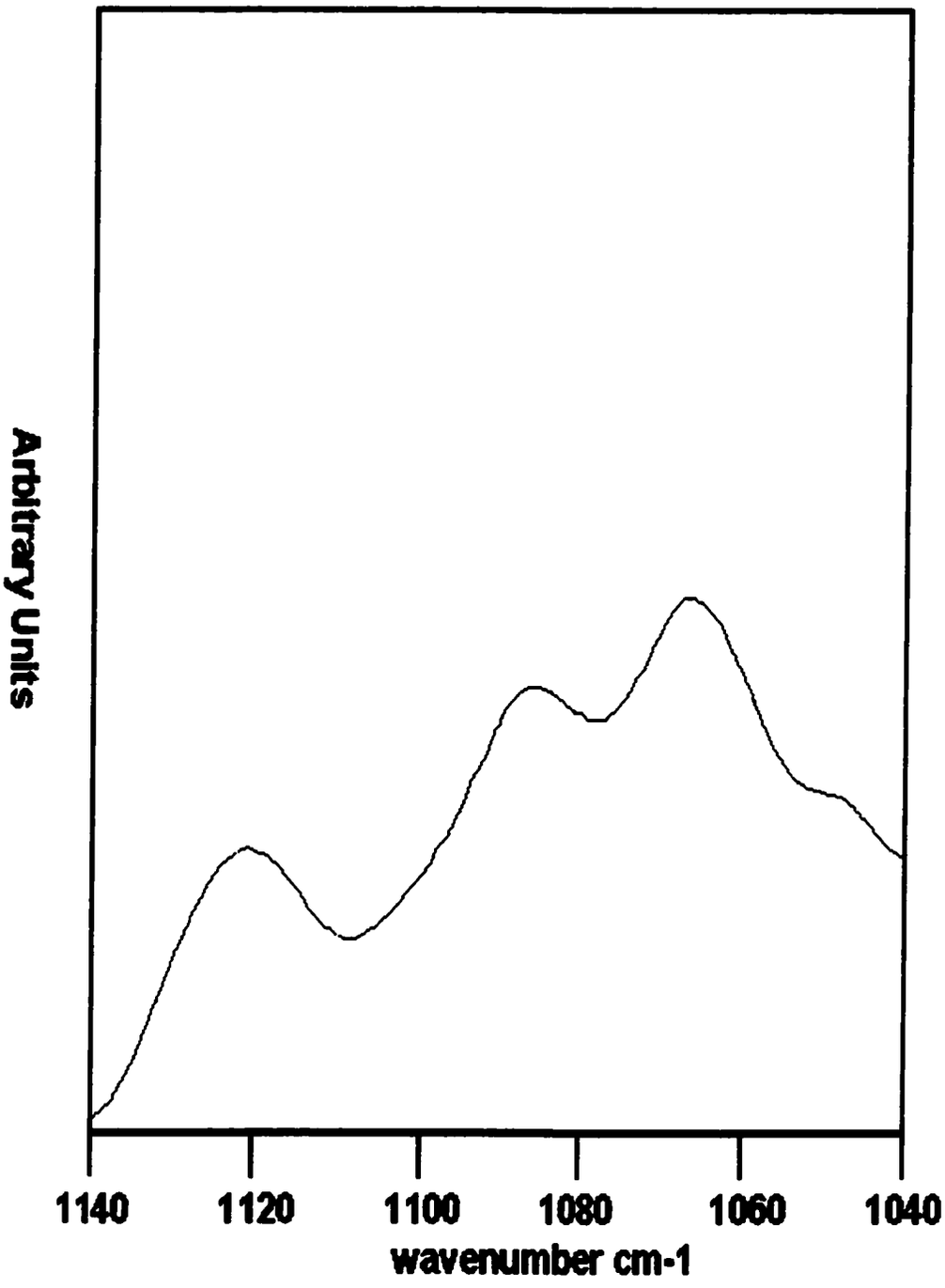

Figure 11: Second derivative analysis of the averaged spectrum generated from ethanol treated 3Y1 cells after 24 hours of serum stimulation.

5. Effect of RNase Digestion on the Spectra Generated From 3Y1 Cells After 24 Hours of Serum Stimulation: **Figure 12** shows the spectra of cells after treatment with **RNase** to remove cytoplasmic and some of the nuclear **RNA**. The ethanol treatment, followed by the **RNase** digestion, has reduced the spectrum to that of protein and **DNA**. There is a residue of phosphoester containing biomolecules as confirmed by the band at 1740 cm-1. The nucleotide peak has lost more intensity since the **Rnase** treatment as characterized by a further decrease in the symmetric and antisymmetric phosphate vibrations. The symmetric phosphate peak at ca. 1086cm^{-1} is absent.

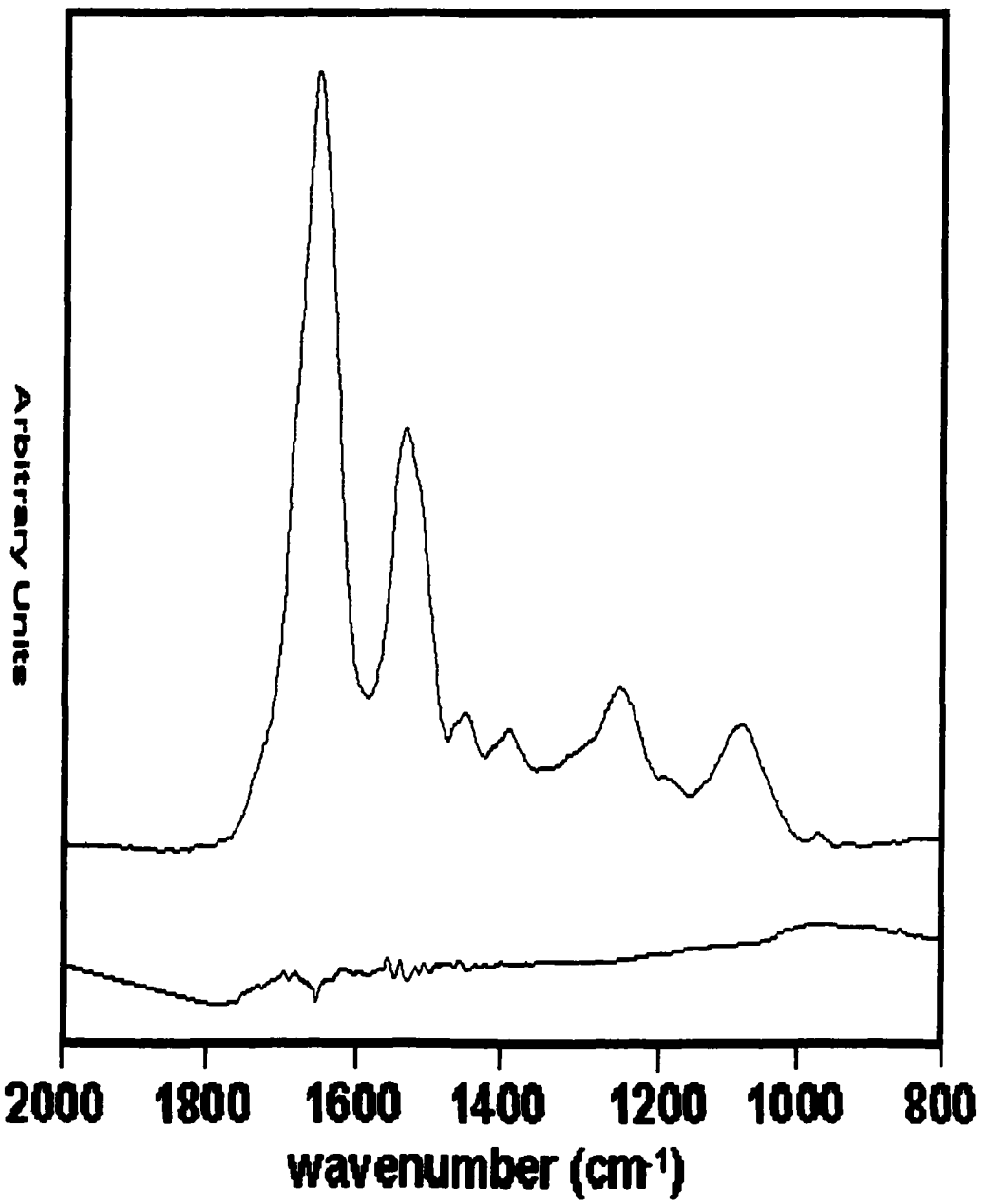

Figure 12: Spectra of RNase digested 3Y1 cells that have been serum stimulated for 24 hours. Standard deviation was calculated and shown below.

6. Second Derivative Analysis of the Spectra From RNase Digested 3Y1 Cells After 24 Hours of Serum Stimulation: The bandshapes of the symmetric phosphate stretch, the high and low wavenumber ribose ring vibrations maintain their overall widths. They differ little from the dried or ethanol treated cells in the second derivative as in **Figure 13**. These peaks are between 1108- 1075 cm^{-1}, 1137 – 1008 cm^{-1} and 1075 – 1045 cm^{-1}, respectively. The peak between 1115 – 1094 cm^{-1} remained absent as compared to the ethanol treated cells.

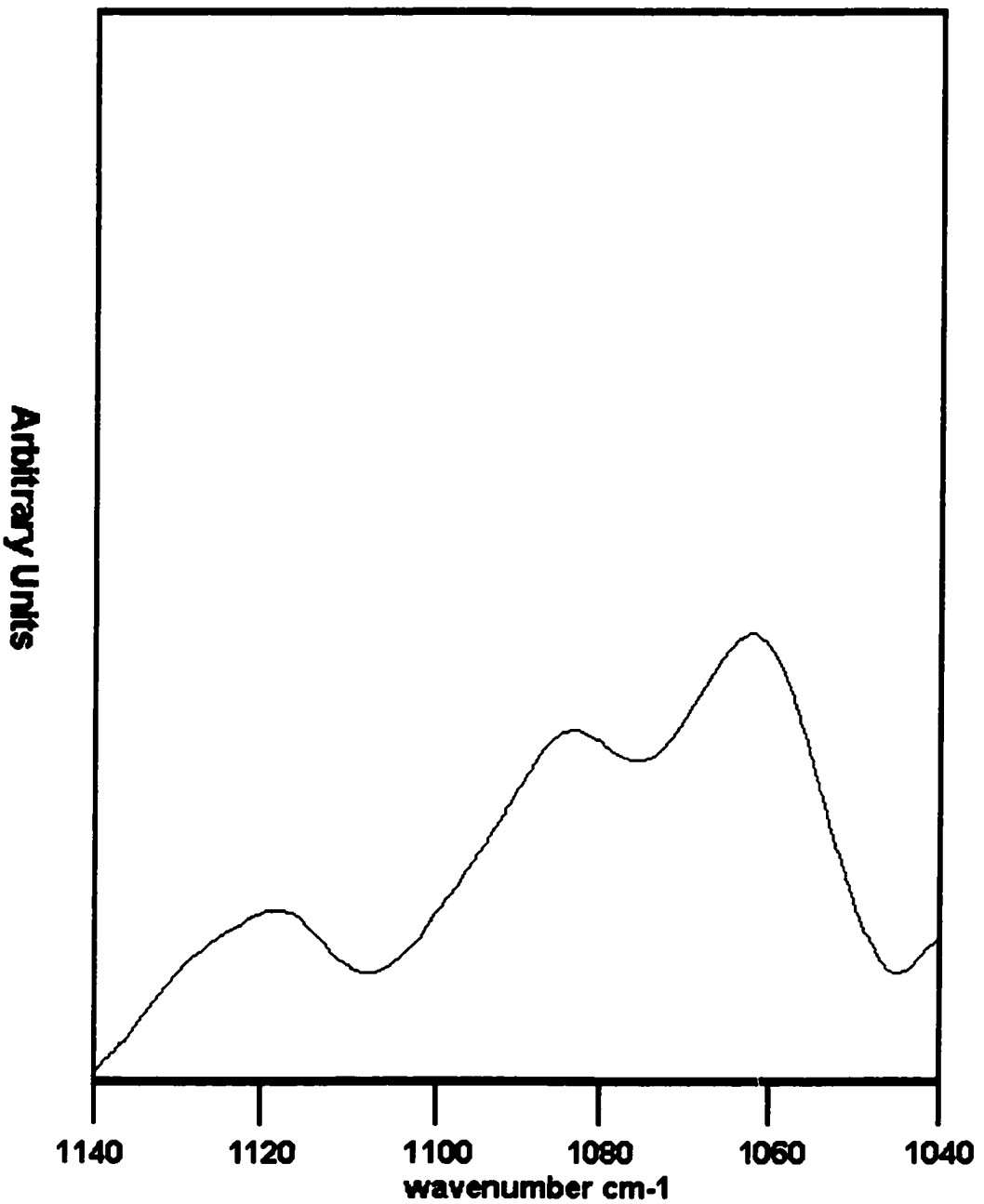

Figure 14: Second derivative analysis of the averaged spectrum generated from RNase digested 3Y1 cells after 24 hours of serum stimulation.

B. Serum Stimulated 3Y1 Cells After 36 Hours: The spectra for this sample represent the second time course point of the confluence data set. These cells have been serum stimulated for a total of 36 hours. There was a slightly lower percentage of **S Phase** and **G2** cells (32.5%) in this sample as compared to the 24 hour time point. This sample begins to manifest some differences from the 24 hour time point. This is evident as a new peak was observed in the second derivative after ethanol treatment. This peak was completely removed after **RNase** digestion.

1. Spectra Generated From Dried 3Y1 Cells After 36 Hours of Serum Stimulation: The spectrum in **Figure 14** represents serum stimulated cells that have been dried and prepared as previously described. This spectrum is in many ways almost identical to that of the serum deprived and 24 hour stimulated cells.

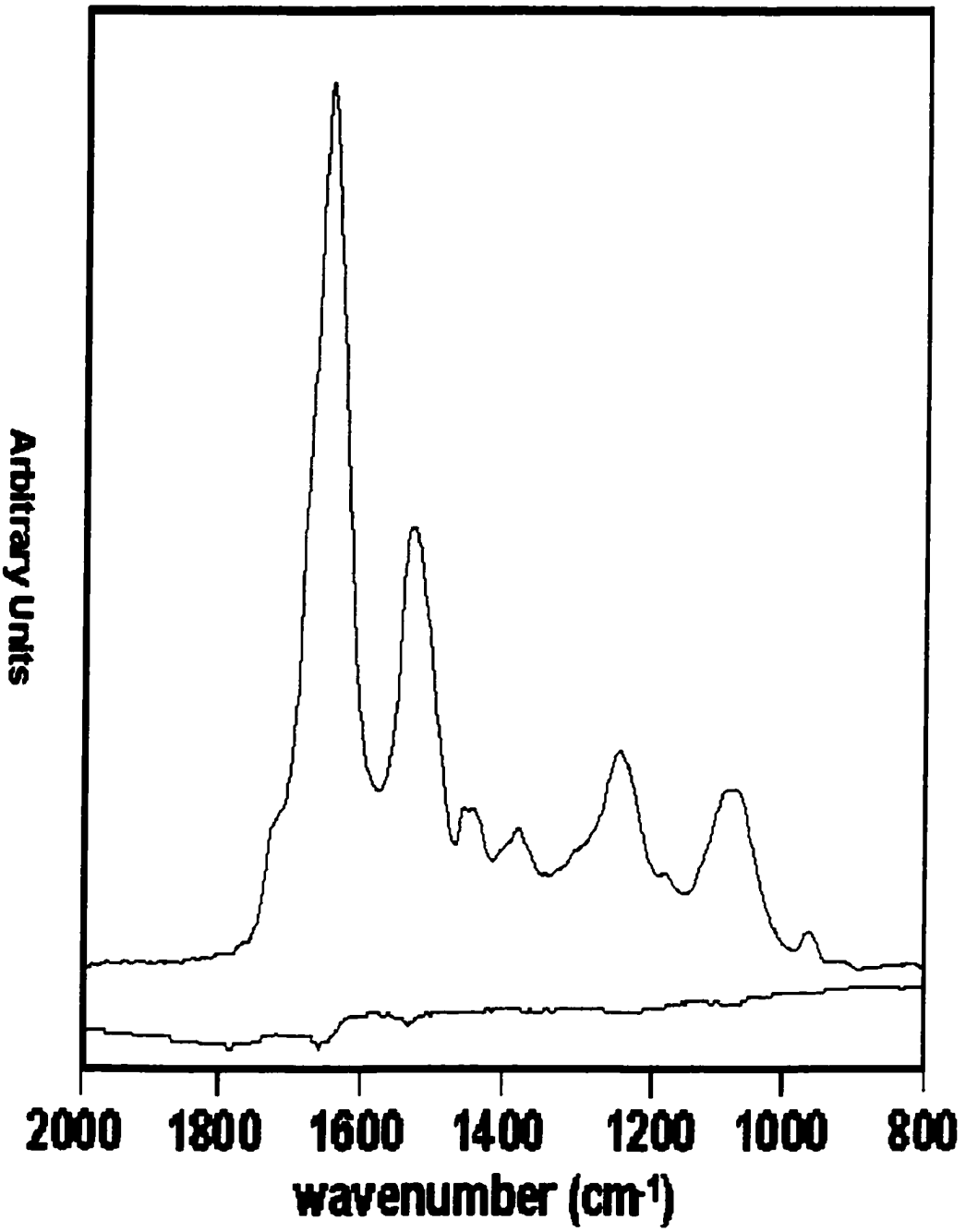

Figure 14: Averaged spectrum of dried 3Y1 cells after 36 hours of serum stimulation. Standard deviation was calculated and shown below.

2.Second Derivative Analysis of Dried Cells That Have Been Serum Stimulated for 36 hours: **Figure 15** contains the averaged second derivative spectrum for the dried cells that have been serum stimulated for 36 hours. The same peaks observed in the 24 hour timepoint are present in the nucleotide region of the averaged spectrum.

The nucleotide region contains four peaks in the second derivative. The symmetric phosphate stretch peak does not change in bandshape or width relative to the 24 hour timepoint. It is observed between 1100 -1075 cm^{-1}in this sample. The high and low wavenumber ribose ring peaks between 1137 – 1113 cm^{-1} and 1075 – 1045 cm^{-1} remain similar in bandshape and width compared to the 24 hour time point. The peak between 1116 –1101 cm^{-1} is weakly present and became narrower than in the data from 24 hours of serum stimulation. The peak is between 1110-1100 cm^{-1}after 36 hours of serum stimulation.

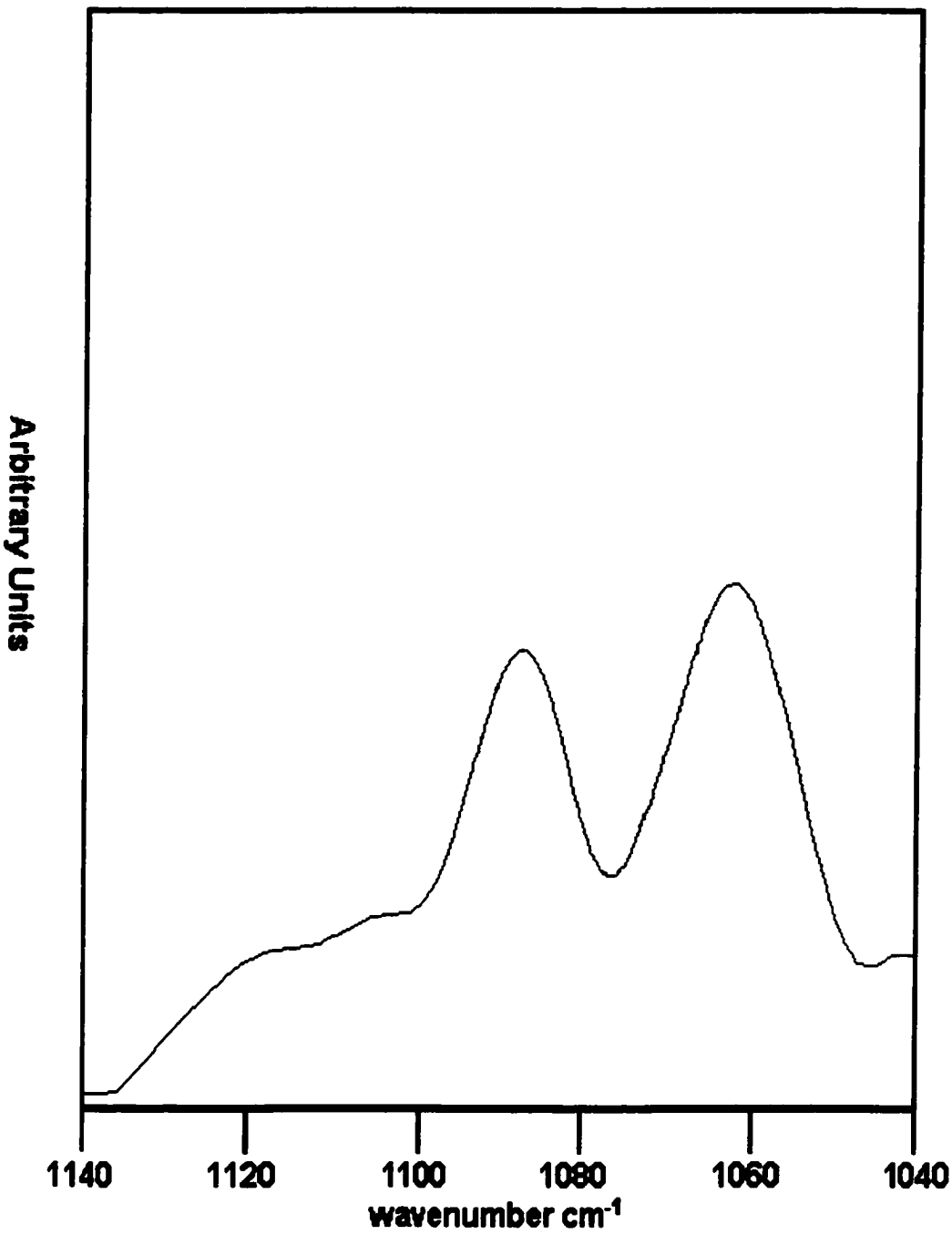

Figure 15: Averaged second derivative spectrum from dried 3Y1 cells that have been serum stimulated for 36 hours.

3. Effect of Ethanol on the Spectra Generated From 3Y1 Cells After 36 Hours of Serum Stimulation: The averaged spectrum in **Figure 16** represents serum stimulated cells that have been dried and prepared as previously described. This spectrum is in many ways almost identical to that of the serum deprived and 24 hour stimulated cells. The symmetric phosphate band at ca. 1086 cm^{-1} is absent.

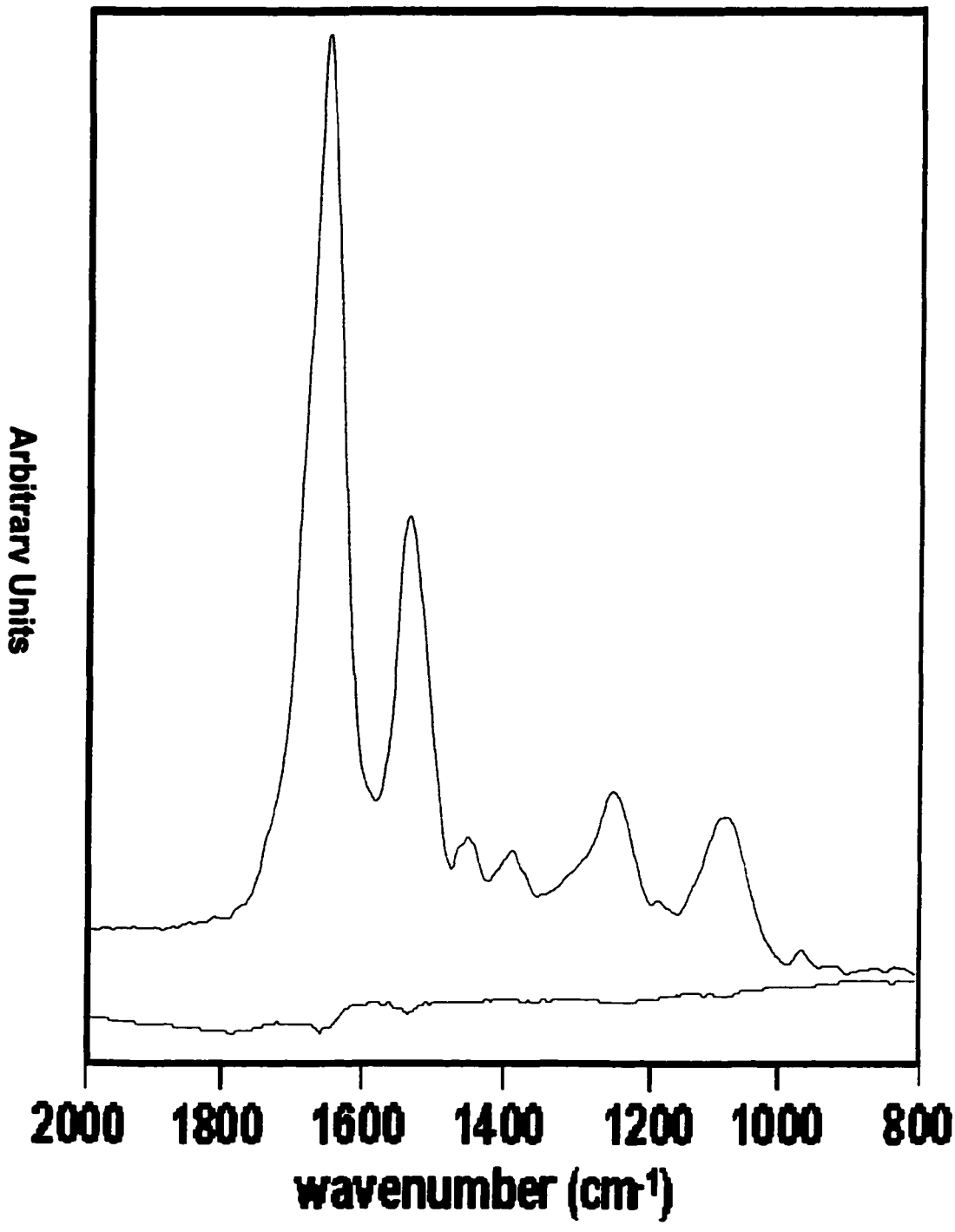

Figure 16: Spectra of ethanol treated 3Y1cells that have been serum stimulated for 36 hours. Standard deviation was calculated and shown below.

4.Second Derivative Analysis of the Spectra of Ethanol Treated 3Y1 Cells After 36 Hours of Serum Stimulation: The averaged second derivative spectrum of ethanol treated **3Y1** cells after 36 hours of serum stimulation is shown in **Figure 17**. The high wavenumber ribose ring vibration peak between 1137 – 1111 cm^{-1} maintains its overall width and shape and differs little from the 24 hour time point sample in the second derivative. The low wavenumber ribose ring vibration peak between 1076 – 1049 cm^{-1} after 24 hours broadens to between 1074 – 1035 cm^{-1}. The symmetric phosphate narrowed from between 1104 – 1074 cm^{-1} at 24 hours to 1094 – 1074 cm^{-1} in this sample. There is a presence of a new band after ethanol treatment between 1111 - 1094 cm^{-1}. This band was not observed in the ethanol treated cells that had been serum stimulated for only 24 hours.

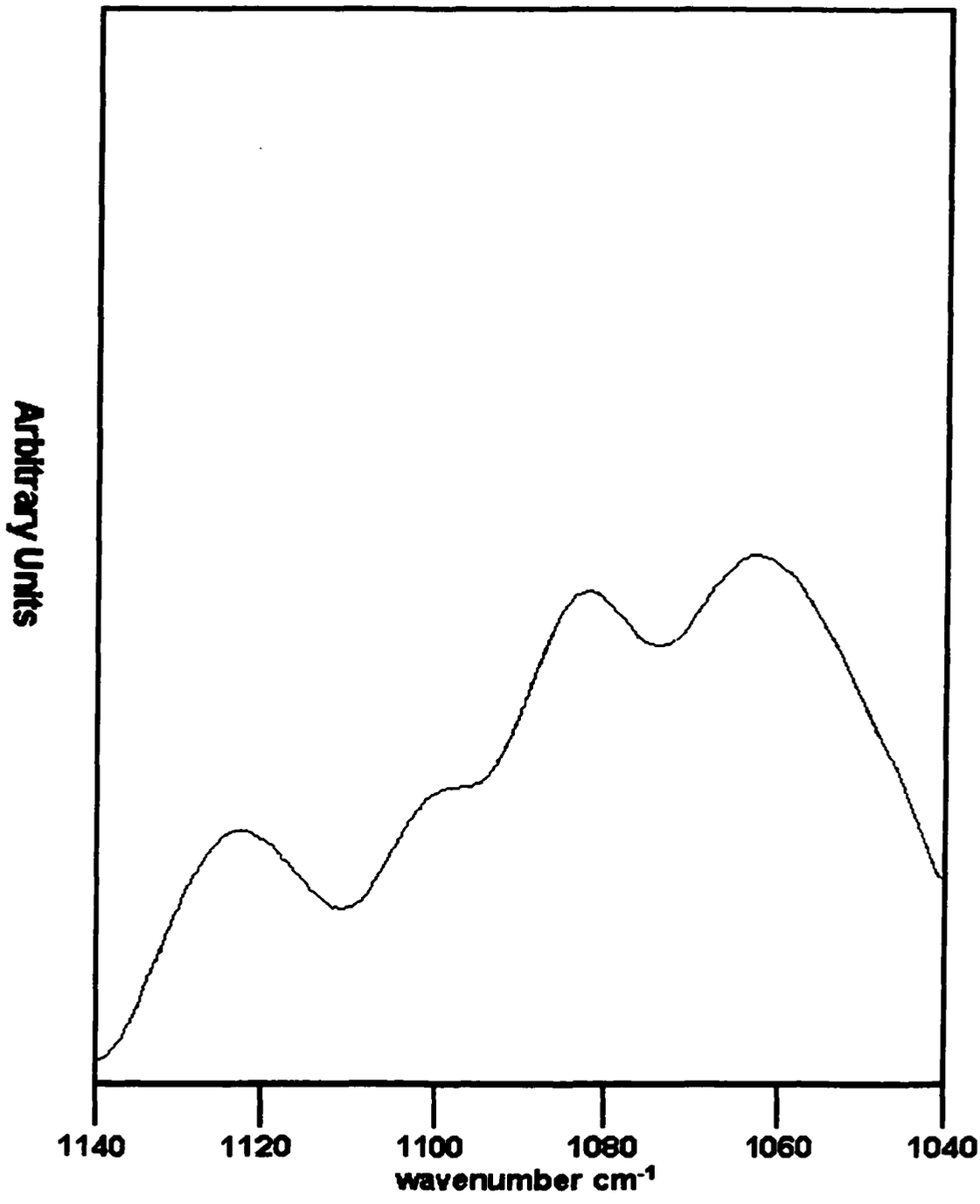

Figure 17: Averaged second derivative spectrum from ethanol treated 3Y1 cells that have been serum stimulated for 36 hours.

5. Effect of RNase Digestion on the Spectra Generated from 3Y1 Cells After 36 Hours of Serum Stimulation: The nucleotide peak has lost more intensity since the Ethanol treatment as characterized by a further decrease in the symmetric and antisymmetric phosphate vibrations as in **Figure 18**.

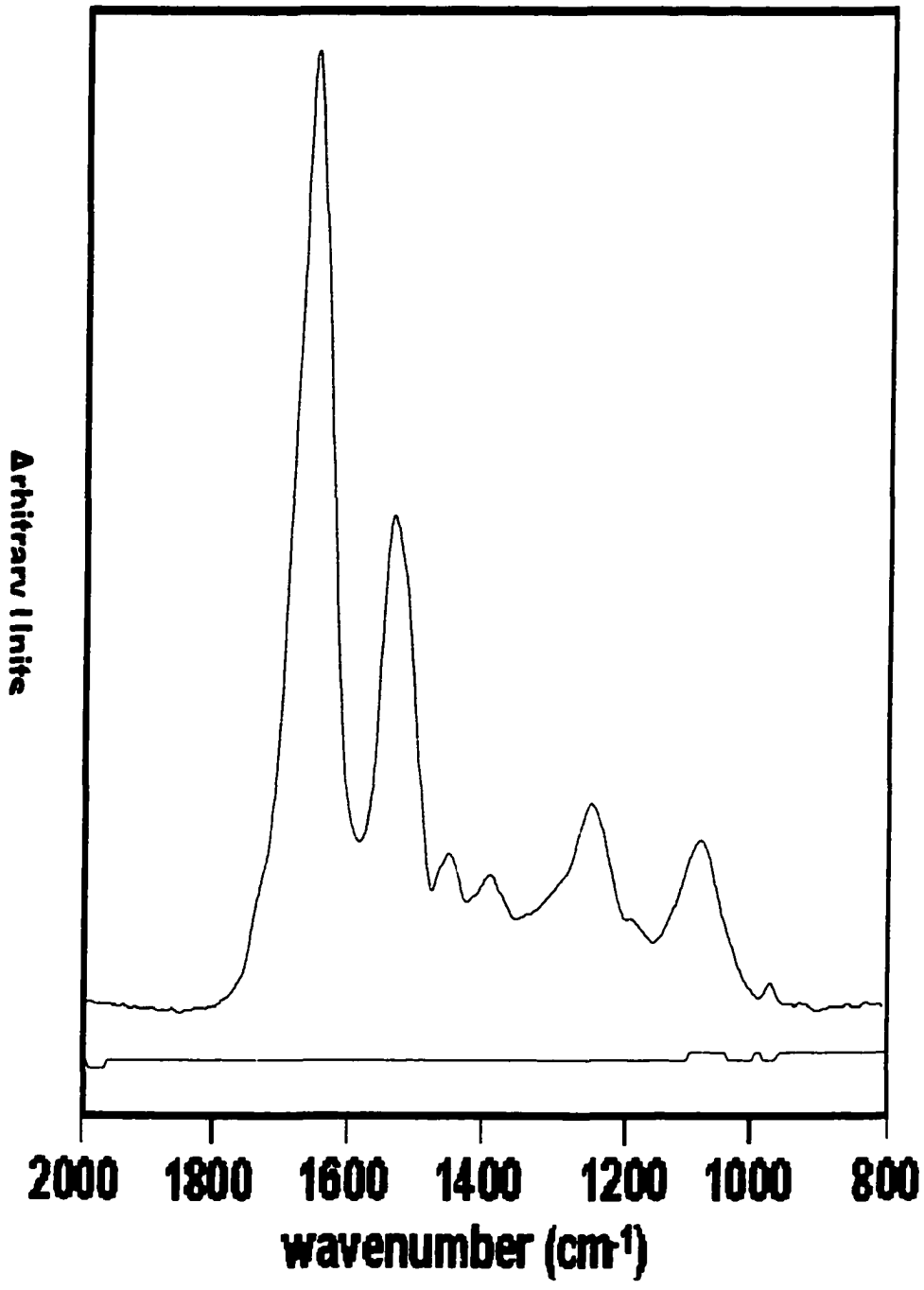

Figure 18: Spectra of RNase digested 3Y1 cells that have been serum stimulated for 36 hours. Standard deviation was calculated and shown below.

6. Second Derivative Analysis of the Spectra From RNase Digested 3Y1 Cells After 36 Hours of Serum Stimulation: The ribose ring vibration peaks between 1137 – 1109 cm^{-1}, 1079 –1042 cm^{-1} and the symmetric phosphate between 1105 – 1079 cm^{-1} have not changed as compared to the 24 hour serum stimulated cells that had been **RNase** digested. The peak observed in the ethanol treated cells between 1111 - 1094 cm^{-1}has been removed. This is due to the enzymatic digestion of **RNA** as in **Figure 19**.

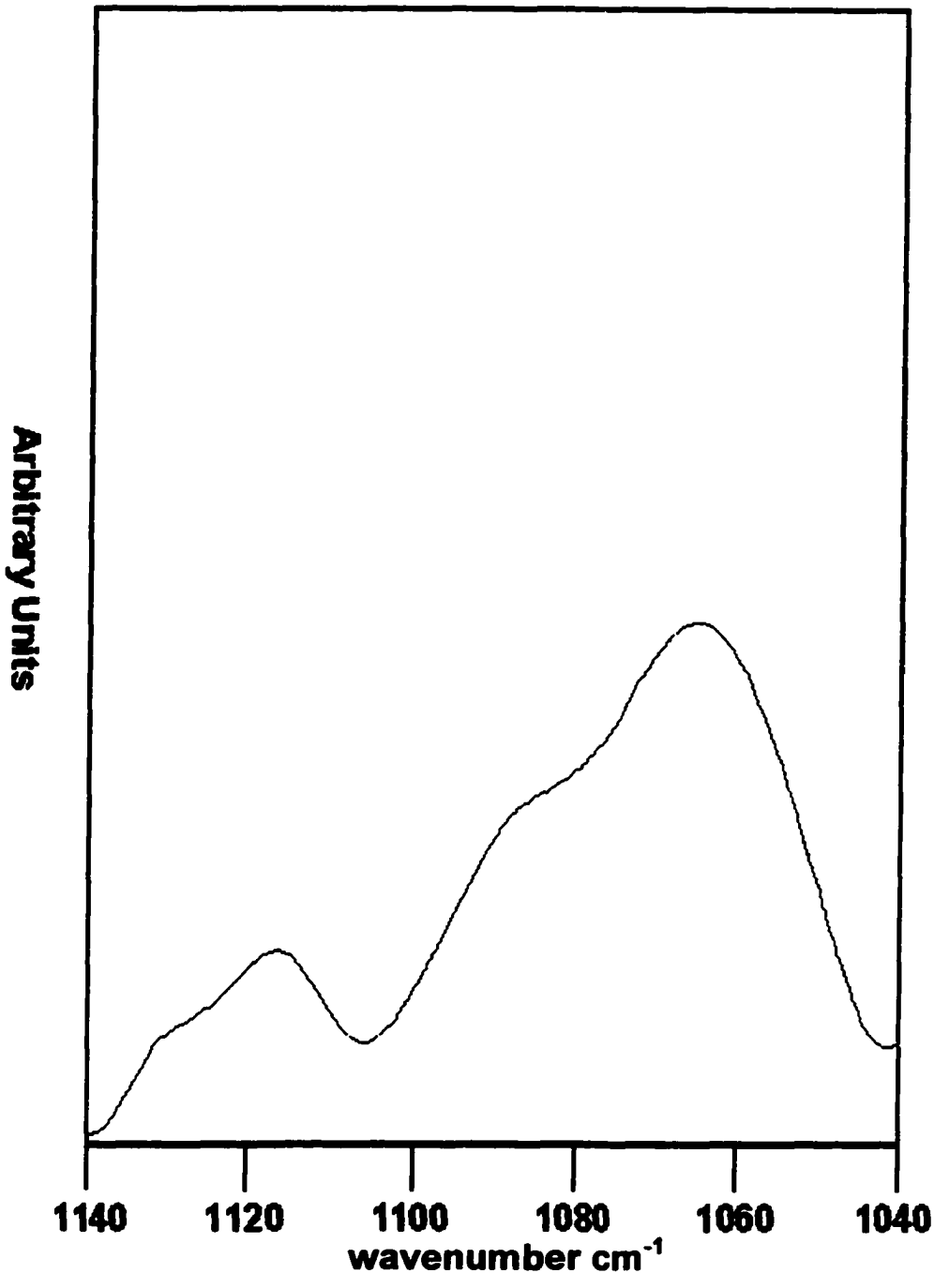

Figure 19: Averaged second derivative spectrum from RNase digested 3Y1cells that have been serum stimulated for 36 hours.

C. Serum Stimulated 3Y1 Cells After 48 hours: The spectra for this sample were derived from the third time course point of the confluence data set. These cells have been serum stimulated for a total of 48 hours. There is a continued decrease of **S phase** and **G2** cells in this sample as compared to the 24 time point to 35.1%. The data herein show the first signs of resembling the serum-starved cells. The **RNase** digestion did not remove the envelope between 1107 –1097 cm^{-1}.

1. Spectra Generated From Dried 3Y1 Cells After 48 Hours of Serum Stimulation: The spectrum shown in **Figure 20** represents serum stimulated cells that have been dried and prepared as previously mentioned. This spectrum is in many ways almost identical to that of the serum deprived and 24 hour stimulated cells.

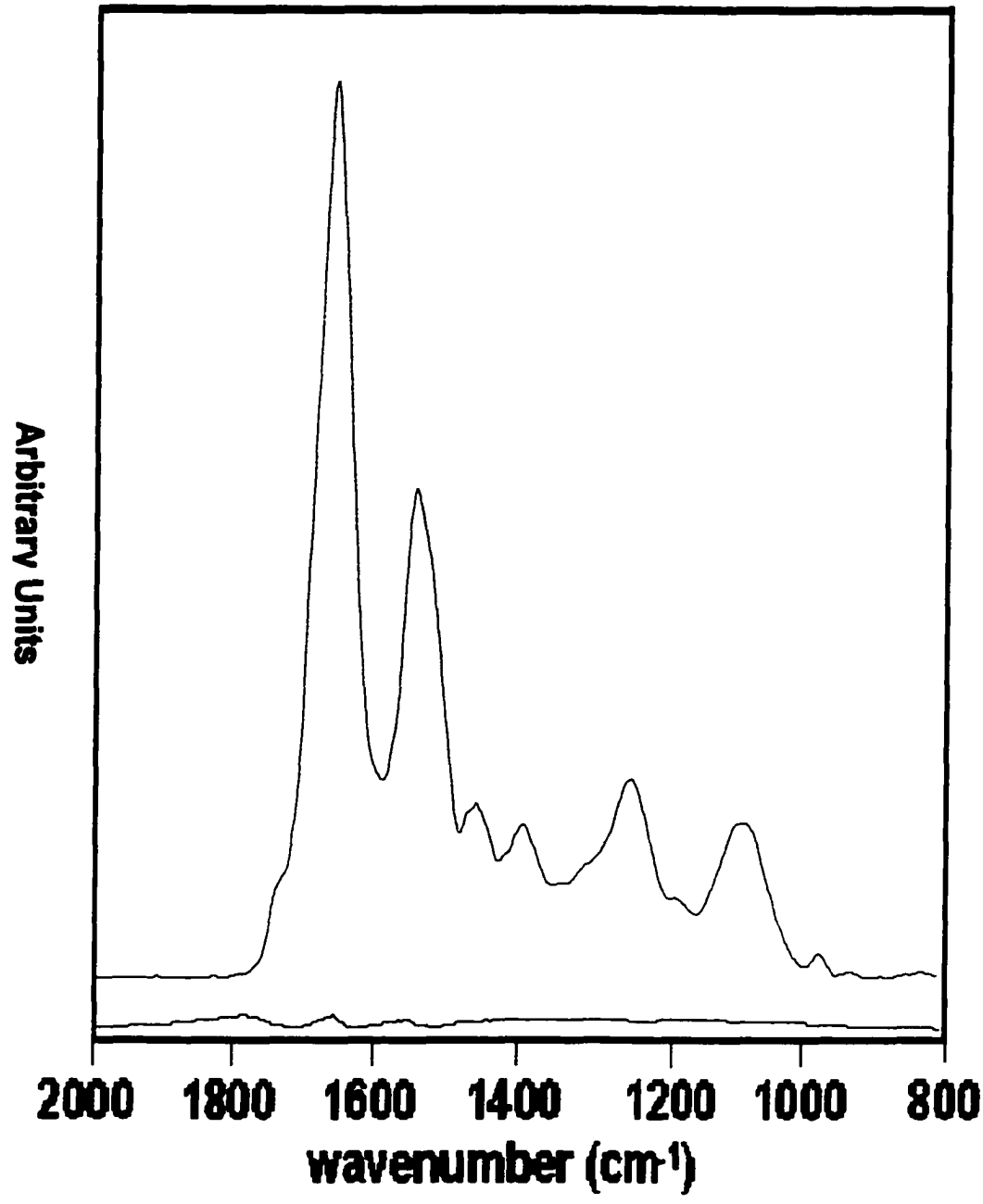

Figure 20: Averaged spectrum of dried 3Y1 cells after 48 hours of serum stimulation. Standard deviation was calculated and shown below.

2. Second Derivative Analysis of Dried 3Y1 Cells That Have Been Serum Stimulated for 48 hours: Shown in **Figure 21** is the averaged second derivative spectrum for the dried cells that have been serum stimulated for 48 hours. The same peaks observed in the 24 serum stimulation data set are present in the nucleotide region of the averaged spectrum.

The nucleotide region contains four peaks in the second derivative. The symmetric phosphate stretch peak does not change in bandshape or width relative to the 24 hour timepoint. It is between 1101 -1076 cm^{-1}in this sample. The ribose ring vibrations between 1135 – 1114 cm^{-1} and 1076 – 1043 cm^{-1} also remain similar in bandshape and width compared to the 24 hour timepoint. The peak between 1116 –1101 cm^{-1} in cells after 24 hours of serum stimulation has a similar bandwidth in the 36 hour sample between 1114 -1102 cm^{-1}after 48 hours of serum stimulation.

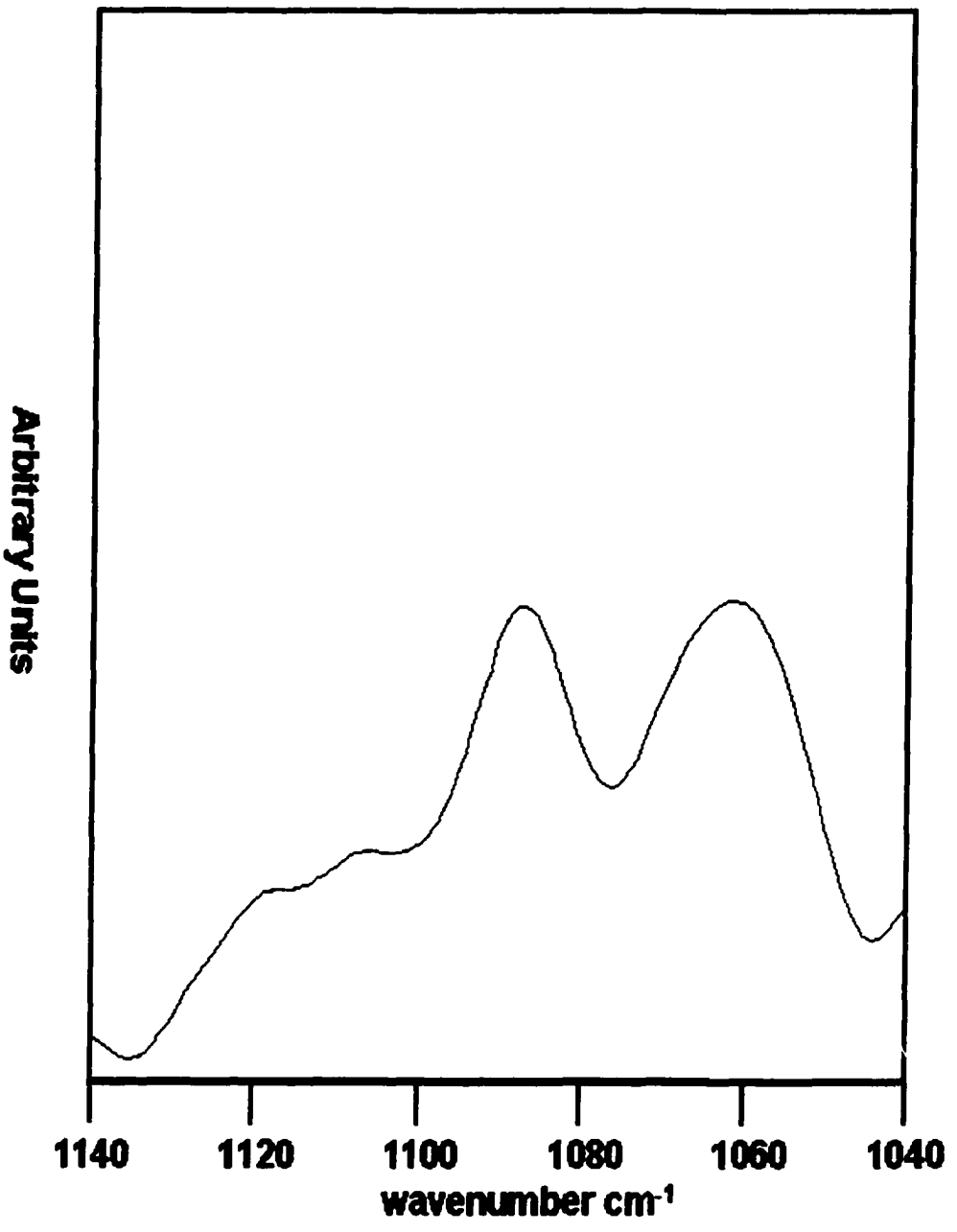

Figure 21: Averaged second derivative spectrum from dried 3Y1 cells that have been serum stimulated for 48 Hours.

3. Effect of Ethanol on the Spectra Generated From Dried 3Y1 Cells That Have Been Serum Stimulated for 48 hours: Upon washing with 100% ethanol, we see that the intensity of the symmetric and antisymmetric phosphate stretching vibrations at ca. 1080 and 1235 cm^{-1} is decreased respectively in **Figure 22**. This is due to the removal of extraneous phosphorous containing biomolecules. The effect of ethanol is identical in all treated spectra.

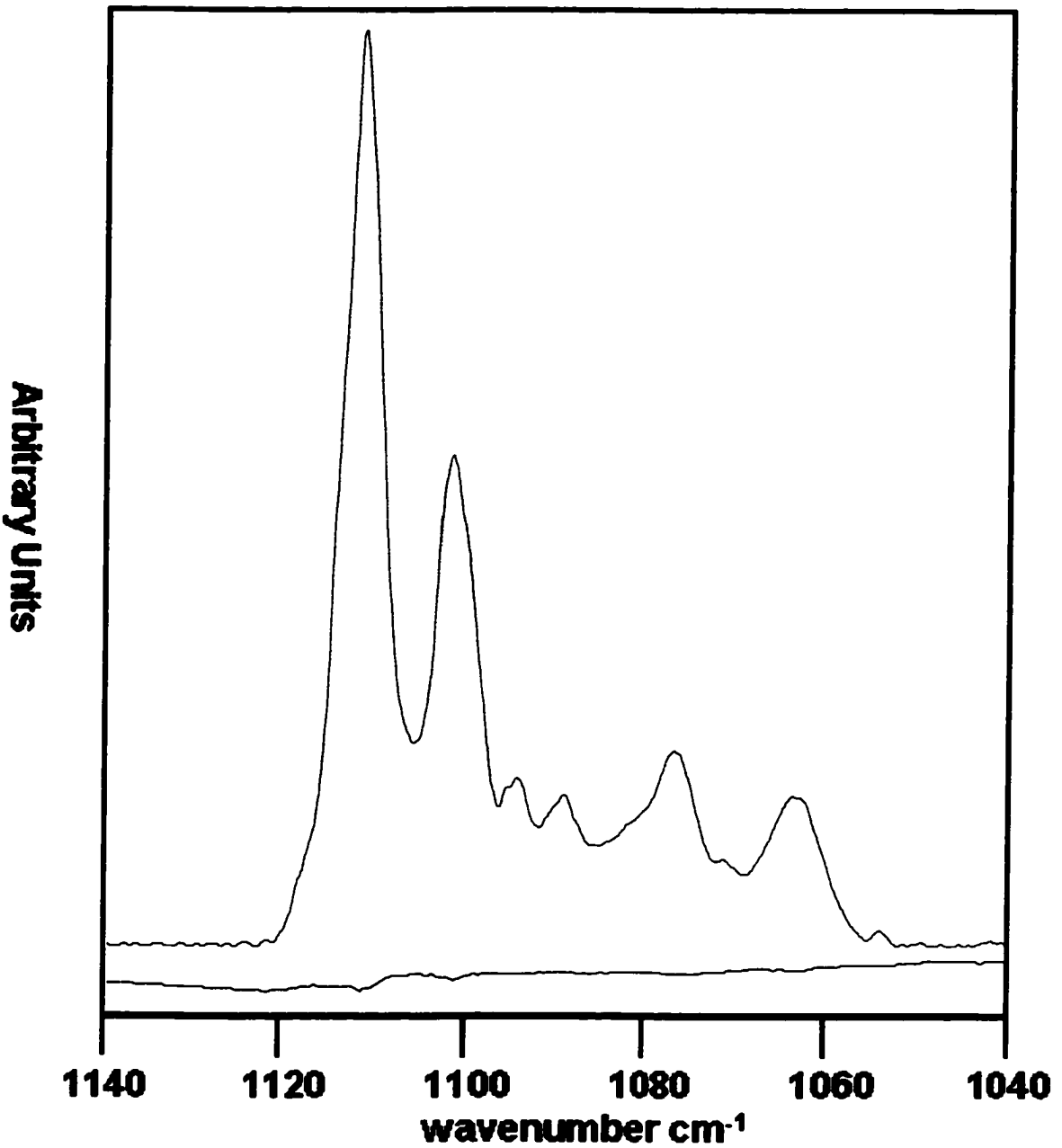

Figure 22: Spectra of ethanol treated 3Y1 cells that have been serum stimulated for 48 hours. Standard deviation was calculated and shown below.

4. Second Derivative Analysis of the Spectra From Ethanol Treated 3Y1 Cells After 48 hours of Serum Stimulation: In **Figure 23**, the high wavenumber ribose ring vibration between 1137 – 1108 cm^{-1} observed in the 24 hour time point narrowed to between 1138 – 1114 cm^{-1} after 48 hours. The low wavenumber ribose ring vibration peak between 1072 – 1045 cm^{-1} does not change relative to the first time point. The symmetric phosphate narrowed from between 1104 – 1074 cm^{-1} to 1095 – 1072 cm^{-1} after 48 hours. Also present is the peak first reported in the previous data set. It has broadened to between 1114 - 1095 cm^{-1} after 48 hours of serum stimulation. This band was not observed in the ethanol treated cells that had been serum stimulated for only 24 hours.

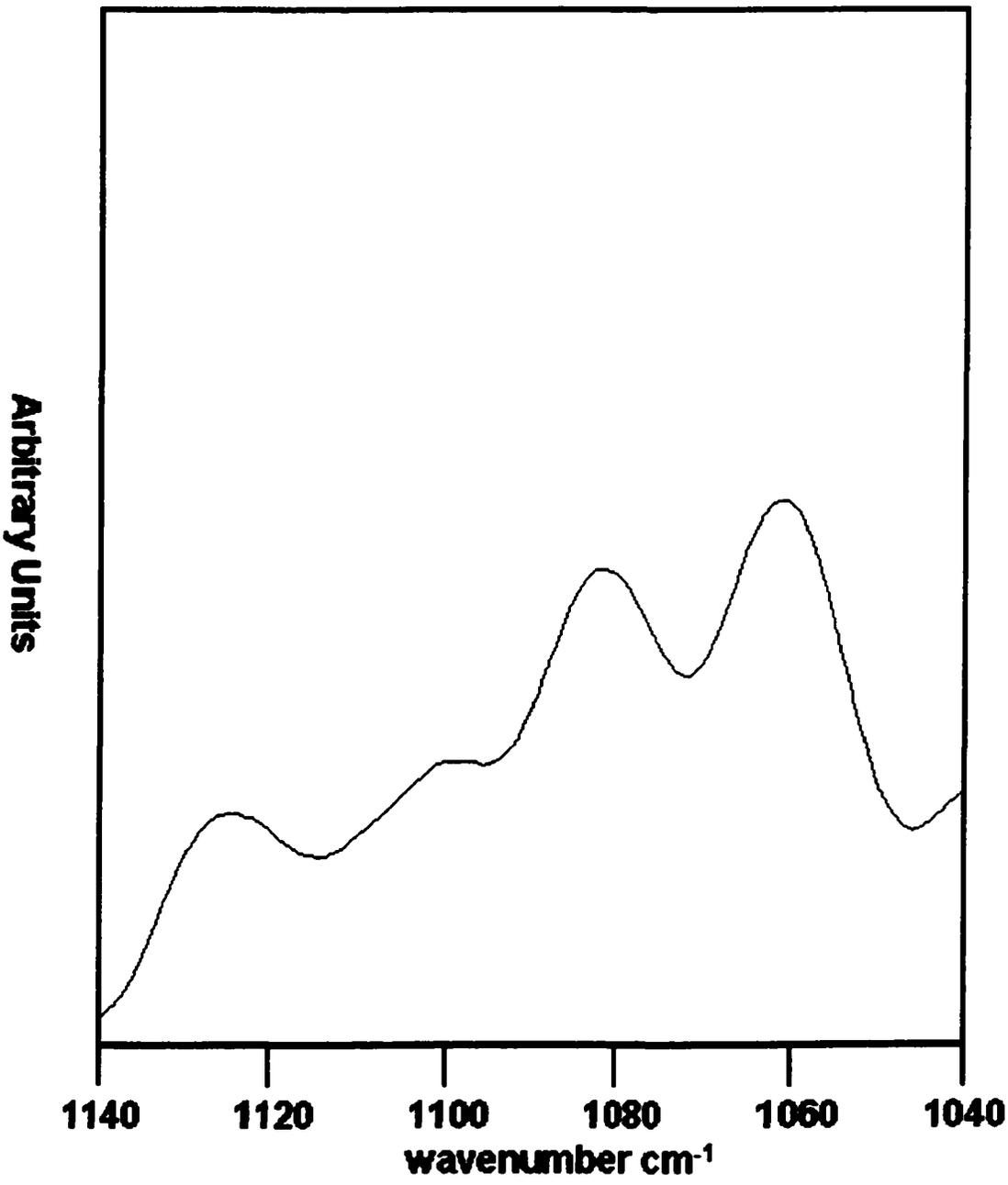

Figure 23: Averaged second derivative spectrum of ethanol treated 3Y1 cells that have been serum stimulated for 48 hours.

5. Effect of RNase Digestion on the Spectra Generated From 3Y1 Cells After 48 Hours of Serum Stimulation: There is a residue of phosphoester containing biomolecules as confirmed by the band at 1740 cm^{-1} in **Figure 24**. The nucleotide peak has lost more intensity since the Ethanol treatment as characterized by a further decrease in the symmetric and antisymmetric phosphate vibrations.

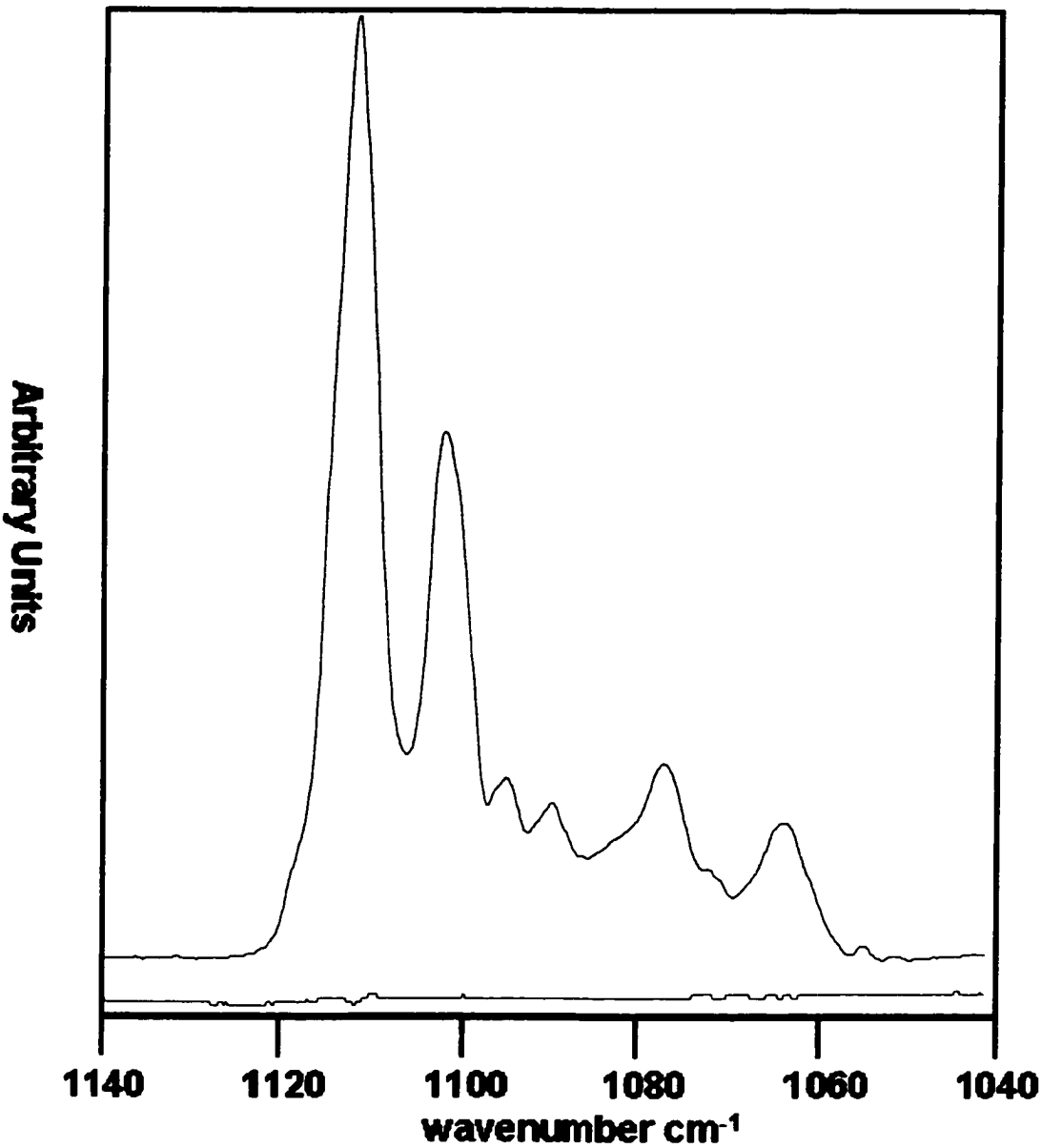

Figure 24: Spectra of RNase digested 3Y1 cells that have been serum stimulated for 48 hours. The standard deviation was calculated and is shown below.

6. Second Derivative Analysis of the Spectra From RNase Digested 3Y1 Cells After 48 Hours of Serum Stimulation: The peaks of the deoxy/ ribose ring vibrations between 1137 – 1109 cm^{-1} and 1074 – 1044 cm^{-1} in **Figure 25** do not change relative to the earlier time points. The symmetric phosphate between 1105 – 1079 cm^{-1} narrowed to between 1097-1074 cm^{-1} after 48 hours of serum stimulation. The peak observed in the ethanol treated cells between 1114 - 1095 cm^{-1}remained after **RNase** digestion. The band is observed between 1107 - 1097 cm^{-1} which narrowed after **RNase** treatment as compared to the ethanol treated sample from this time point. This may represent a partial digestion of biomolecules contributing to this peak.

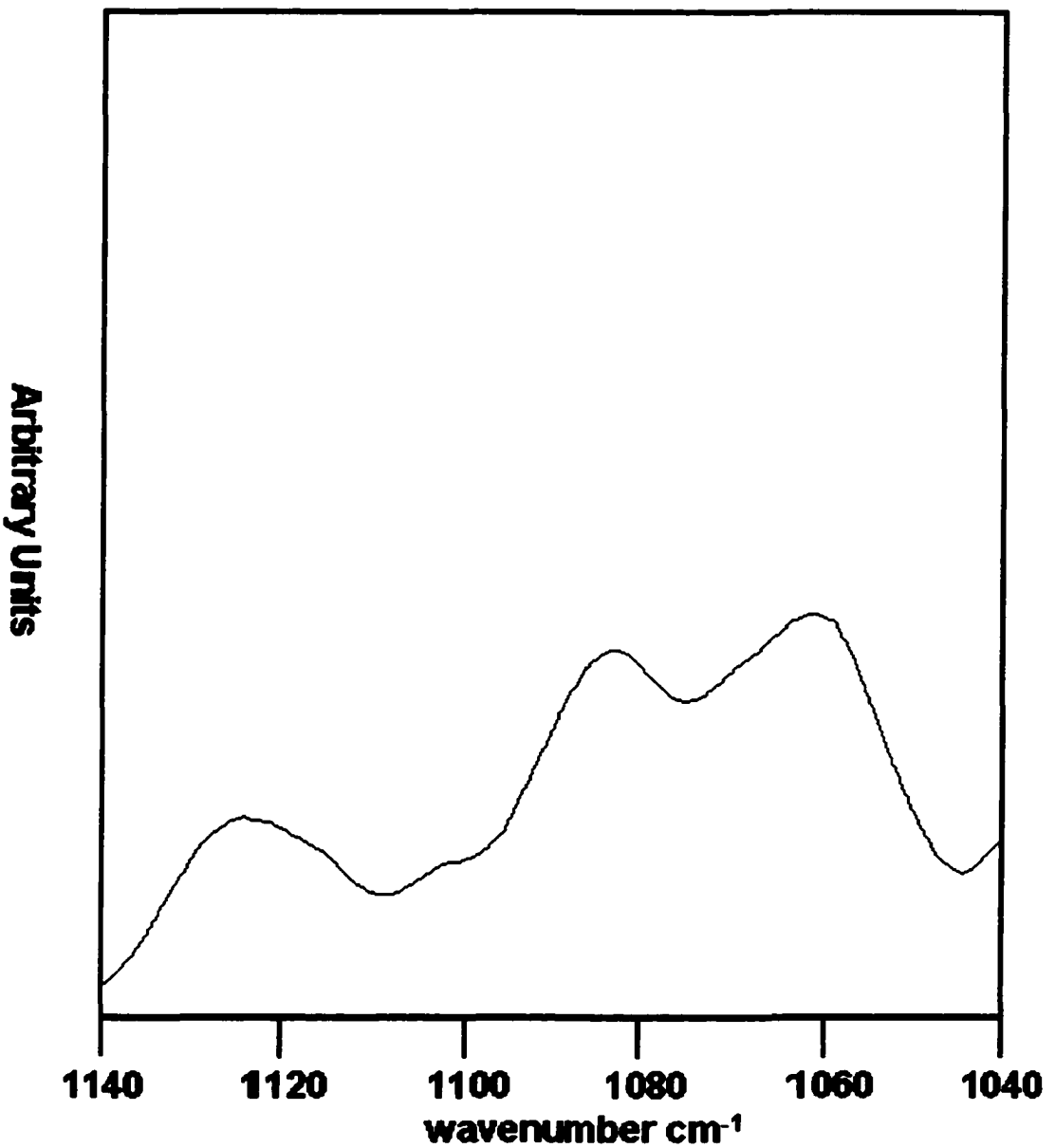

Figure 25: Averaged second derivative spectrum of RNase digested 3Y1 cells that have been serum stimulated for 48 hours.

D. Serum Stimulated 3Y1 Cells After 60 Hours: The spectra for this sample were derived from the fourth time course point of the confluence data set. The percentage of S and G2 cells in this sample decreased to less than 18.3 %.

1. Spectra Generated From Dried 3Y1 Cells After 60 Hours of Serum Stimulation: This spectrum shown in **Figure 26** represents cells that have been serum stimulated for a total of 60 hours. These cells have been dried and prepared as previously mentioned. This spectrum is in many ways almost identical to that of the serum deprived and 24 hour stimulated cells.

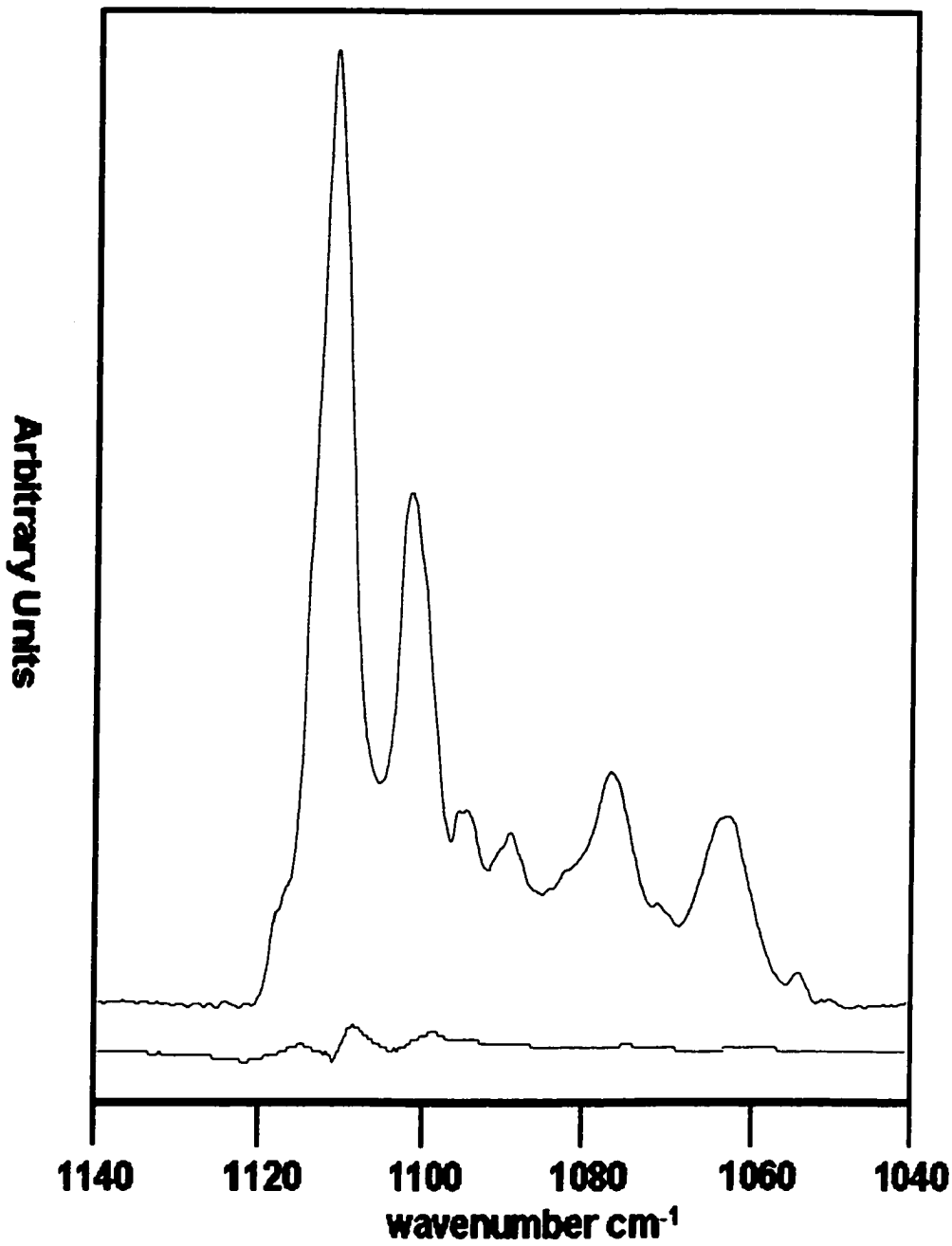

Figure 26: Averaged spectrum of dried 3Y1 cells after 60 hours of serum stimulation. Standard deviation was calculated and shown below.

2. Second Derivative Analysis of Dried 3y1 Cells That Have Been Serum Stimulated for 60 Hours: The nucleotide region contains four peaks in the second derivative in **Figure 27**. As compared to the 24 hour serum stimulated cells the changes are large. These spectra resemble the data from the serum starved cells and 72 hour serum stimulation time points. The symmetric phosphate stretch peak broadens to between 1110 – 1076 cm^{-1} relative to the 24 hour time point. This peak is between 1100 - 1074 cm^{-1} in the 24 hour sample. The high wavenumber deoxy / ribose ring vibration between 1138 – 1125 cm^{-1} peak has narrowed from between 1135 -1116 cm^{-1} at 24 hours. The low wavenumber deoxy / ribose ring vibration between 1076 – 1044 cm^{-1} peak remains similar in bandshape and width compared to the 24 hour timepoint. The peak between 1116 –1101 cm^{-1} observed after 24 hours and ranged between 1125- 1110 cm-1 at 60 hours.

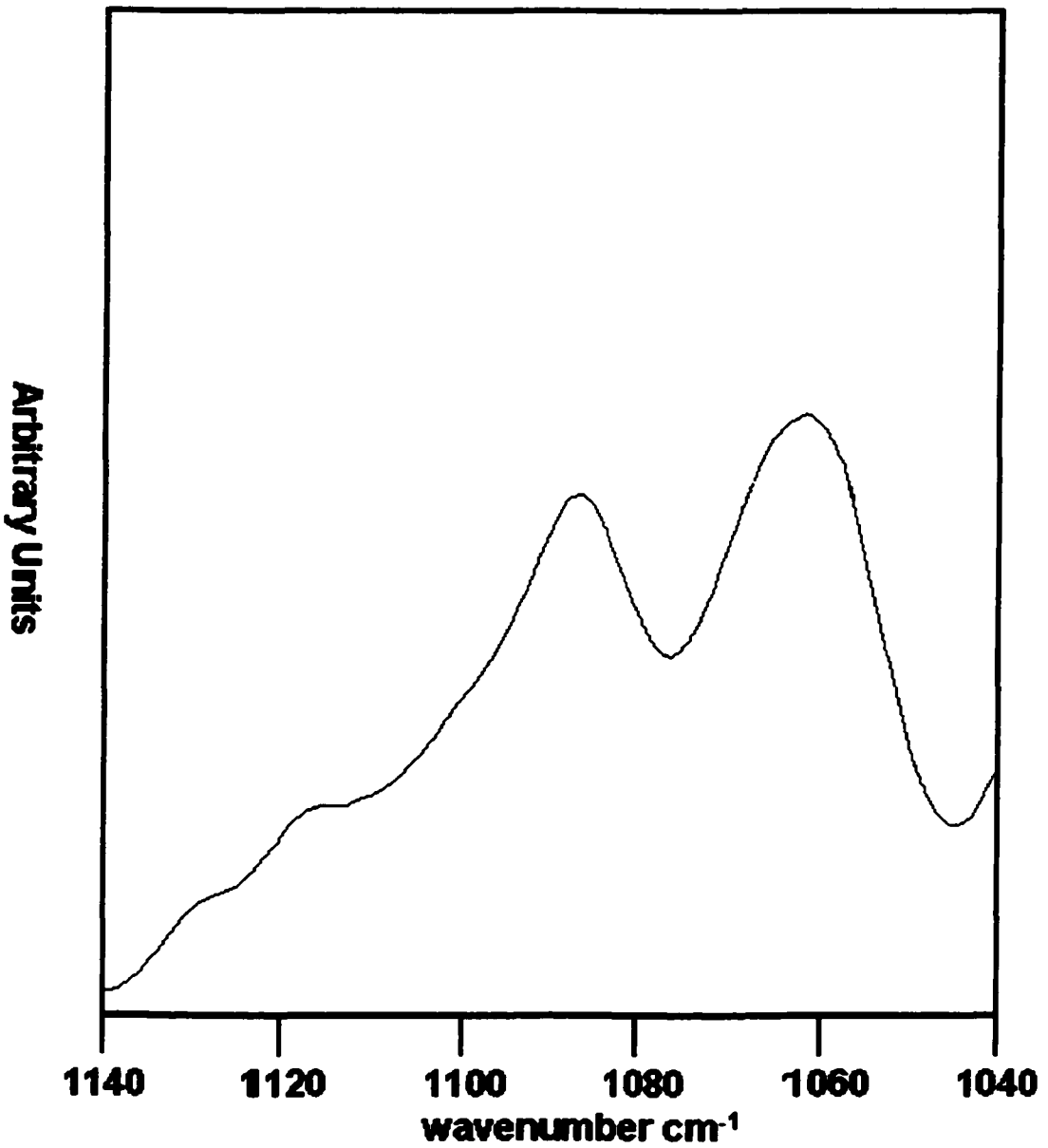

Figure 27: Averaged second derivative spectrum from dried 3Y1 cells that have been serum stimulated for 60 hours.

3. Effect of Ethanol on the Spectra Generated From 3Y1 Cells After 60 Hours of Serum Stimulation: Upon washing with 100% ethanol, we see that the intensity of the symmetric and antisymmetric phosphate stretching vibrations at ca. 1080 cm^{-1} and 1235 cm^{-1} is decreased respectively due to the removal of extraneous phosphorous containing biomolecules. The nucleotide peak is thus enriched in nucleotide content. The phosphoester vibration at 1740 cm^{-1} is nearly completely removed in **Figure 28**. The spectrum shown here is almost identical to that of the 24 hour serum stimulated that has been ethanol treated.

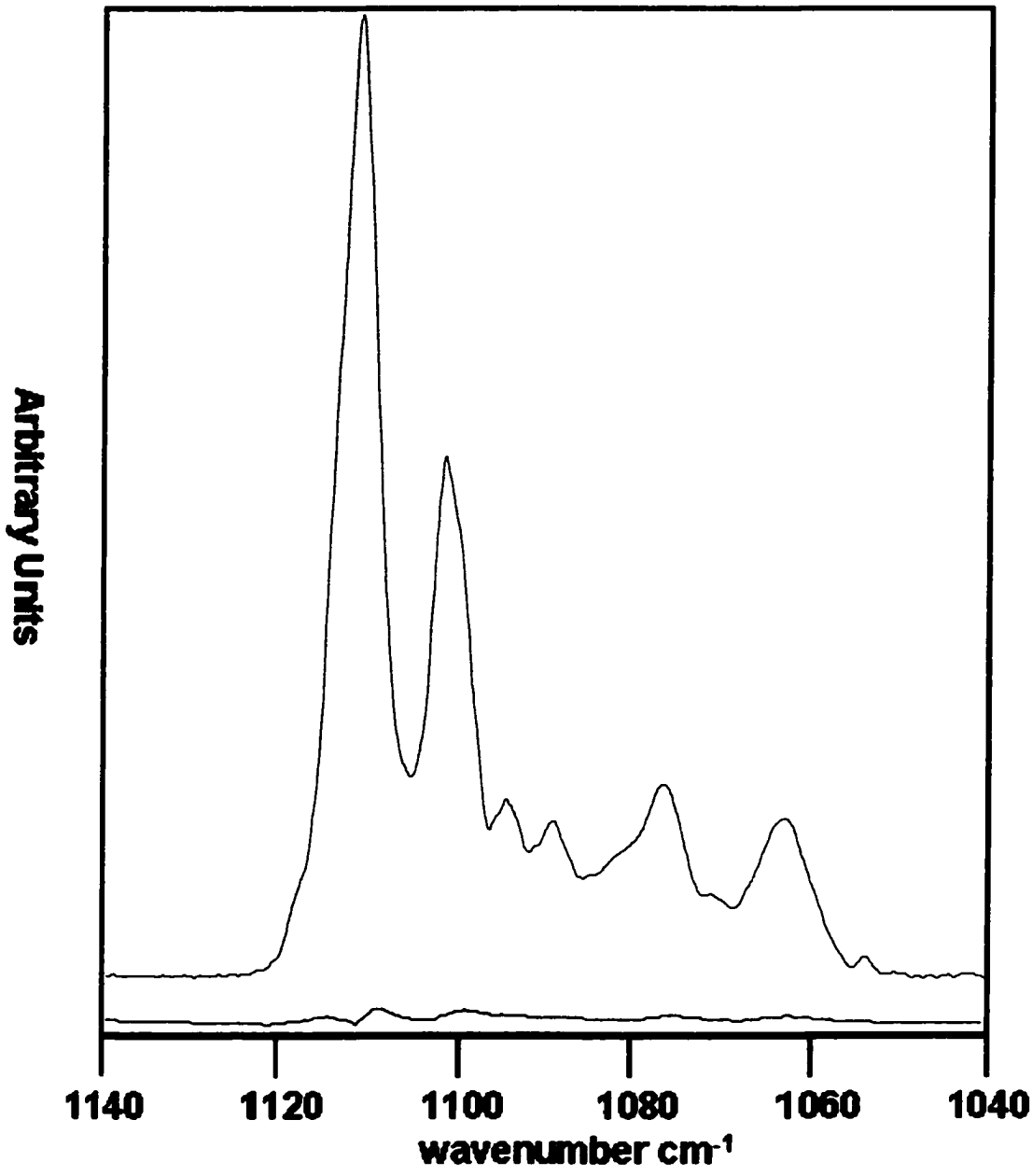

Figure 28: Spectra of ethanol treated 3Y1 cells that have been serum stimulated for 60 hours. The standard deviation was calculated and is shown below.

4. Second Derivative Analysis of the Spectra From Ethanol Treated 3Y1 Cells After 60 Hours of Serum Stimulation: The high wavenumber deoxy /ribose vibration peak between 1138 – 1108 cm^{-1} observed in the ethanol treated cells after 24 hours narrows to between 1136 – 1113 cm^{-1} after 60 hours. The low wavenumber deoxy /ribose vibration peak between 1075 – 1047 cm^{-1} does not change significantly in terms of bandshape or width. The symmetric phosphate narrows from between 1104 – 1074 cm^{-1} to 1095 – 1075 cm^{-1} at 60 hours. The averaged spectrum is shown in **Figure 29**.

The peak observed earlier in the 36 and 48 hour time points is present after 60 hours of serum stimulation. It is between 1113 –1095 cm^{-1} in this sample. This band was not observed in the ethanol treated cells that had been serum stimulated for only 24 hours.

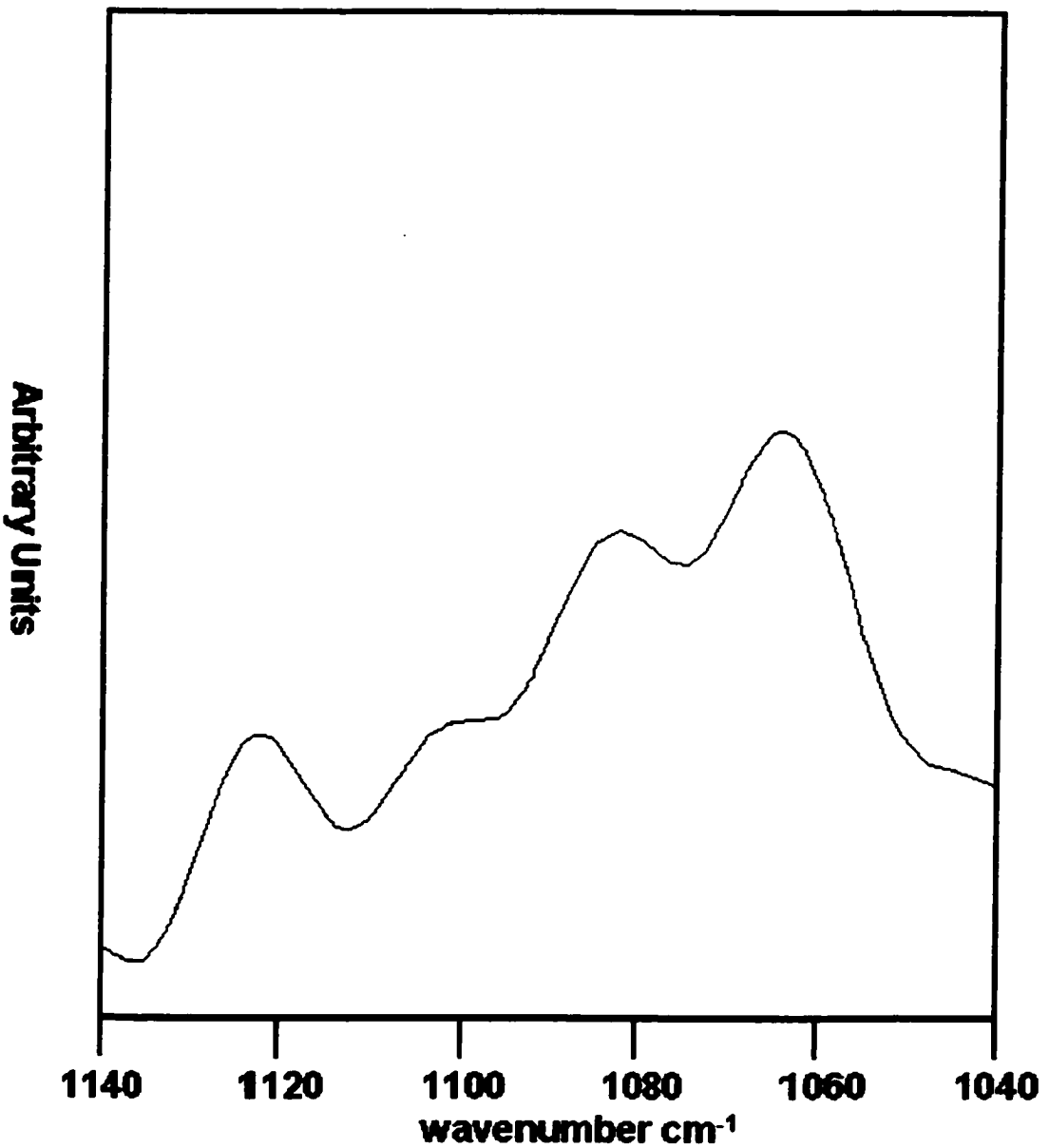

Figure 29: Averaged second derivative spectrum of ethanol treated 3Y1 cells that have been serum stimulated for 60 hours.

5. Effect of RNase Digestion on the Spectra Generated From 3Y1 Cells After 60 Hours of Serum Stimulation: There is a residue of phosphoester containing biomolecules as confirmed by the band at 1740 cm^{-1}. The nucleotide peak has lost more intensity since the Ethanol treatment as characterized by a further decrease in the symmetric and antisymmetric phosphate vibrations. The averaged spectrum of these cells is shown in **Figure 30**.

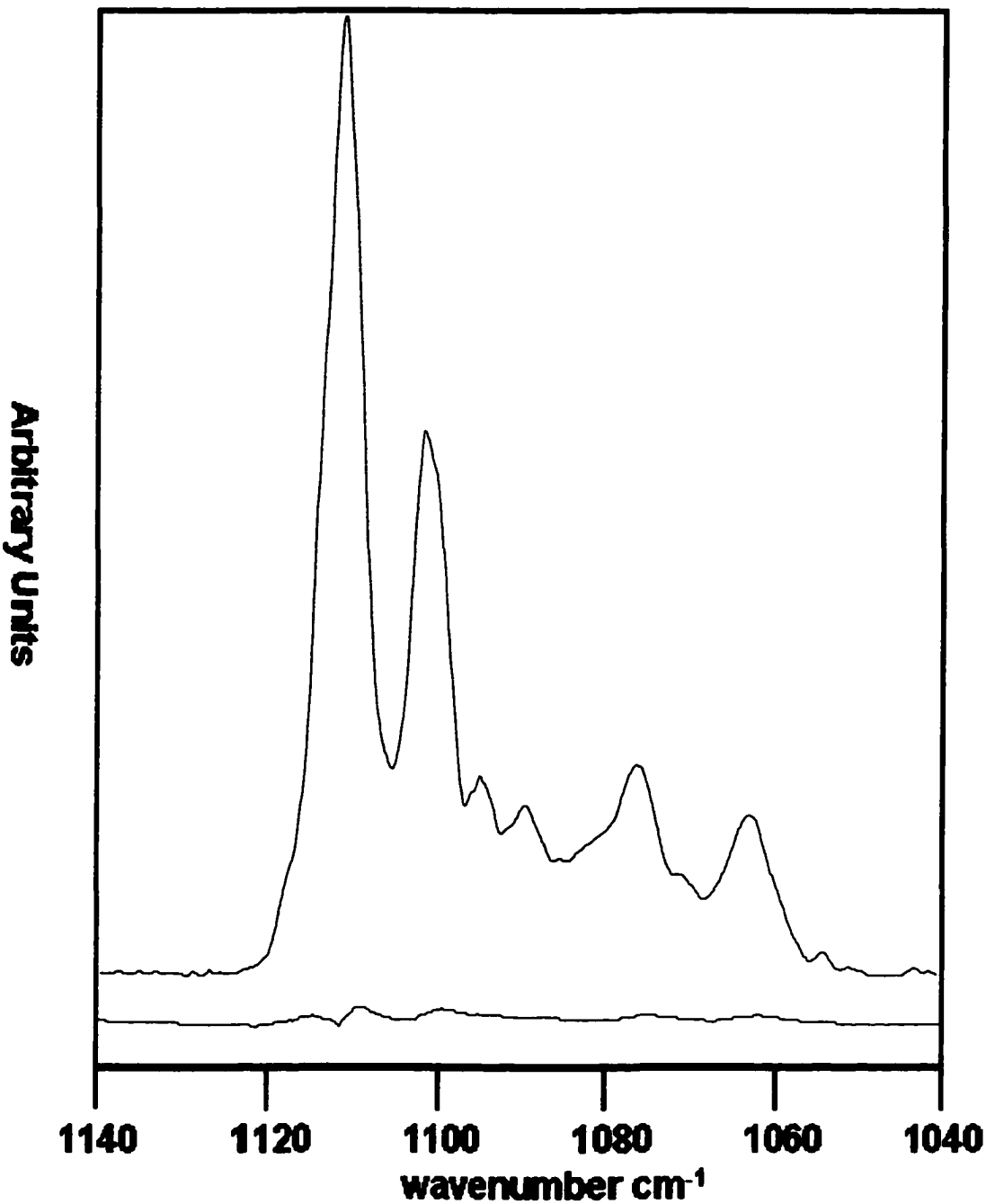

Figure 30: Spectra of RNase digested 3Y1 cells that have been serum stimulated for 60 hours. The standard deviation was calculated for this spectrum and shown below.

6. Second Derivative Analysis of the Spectra From RNase Digested 3Y1 Cells After 60 Hours of Serum Stimulation: The low wavenumber deoxy/ ribose ring vibration peak between 1071 –1043 cm^{-1} does not change in terms of bandwidth as compared to the 24 hour serum stimulated cells that had been **RNase** digested. The high wavenumber deoxy/ ribose ring vibration peak between 1137 – 1108 cm^{-1} observed after 24 hours narrows to between 1139 – 1117 cm^{-1}. The symmetric phosphate between 1108 – 1075 cm^{-1} at 24 hours narrowed to between 1100 -1071 cm^{-1} at 60 hours. The peak observed in the ethanol treated cells between 1113 - 1095 cm^{-1} remains after **RNase** digestion in this sample. The averaged second derivative spectrum for this is shown in **Figure 31**.

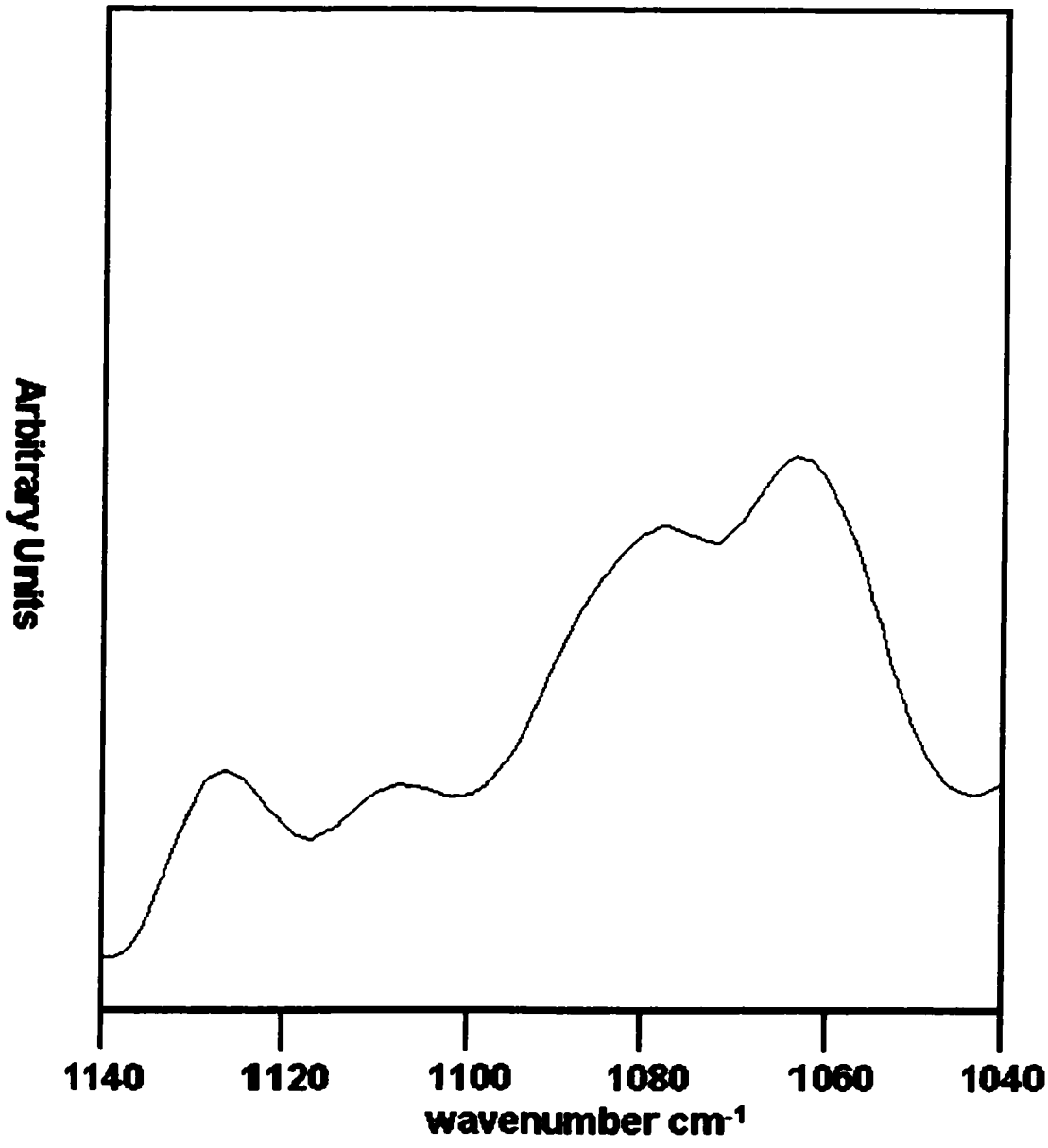

Figure 31: Averaged second derivative spectrum of RNase digested 3Y1 cells that have been serum stimulated for 60 hours.

E. Serum Stimulated 3Y1 Cells After 72 hours: The spectra for this sample were derived from the fourth time course point of the confluence data set. The percentage of **S phase** and **G2** cells in this sample decreases to 14 %.

1. Spectra Generated From Dried 3Y1 Cells After 72 Hours of Serum Stimulation: The spectrum shown in **Figure 32** represents cells that have been serum stimulated for a total of 72 hours. These cells have been dried and prepared as previously mentioned. This spectrum is in many ways almost identical to that of the serum deprived and 24 hour stimulated cells.

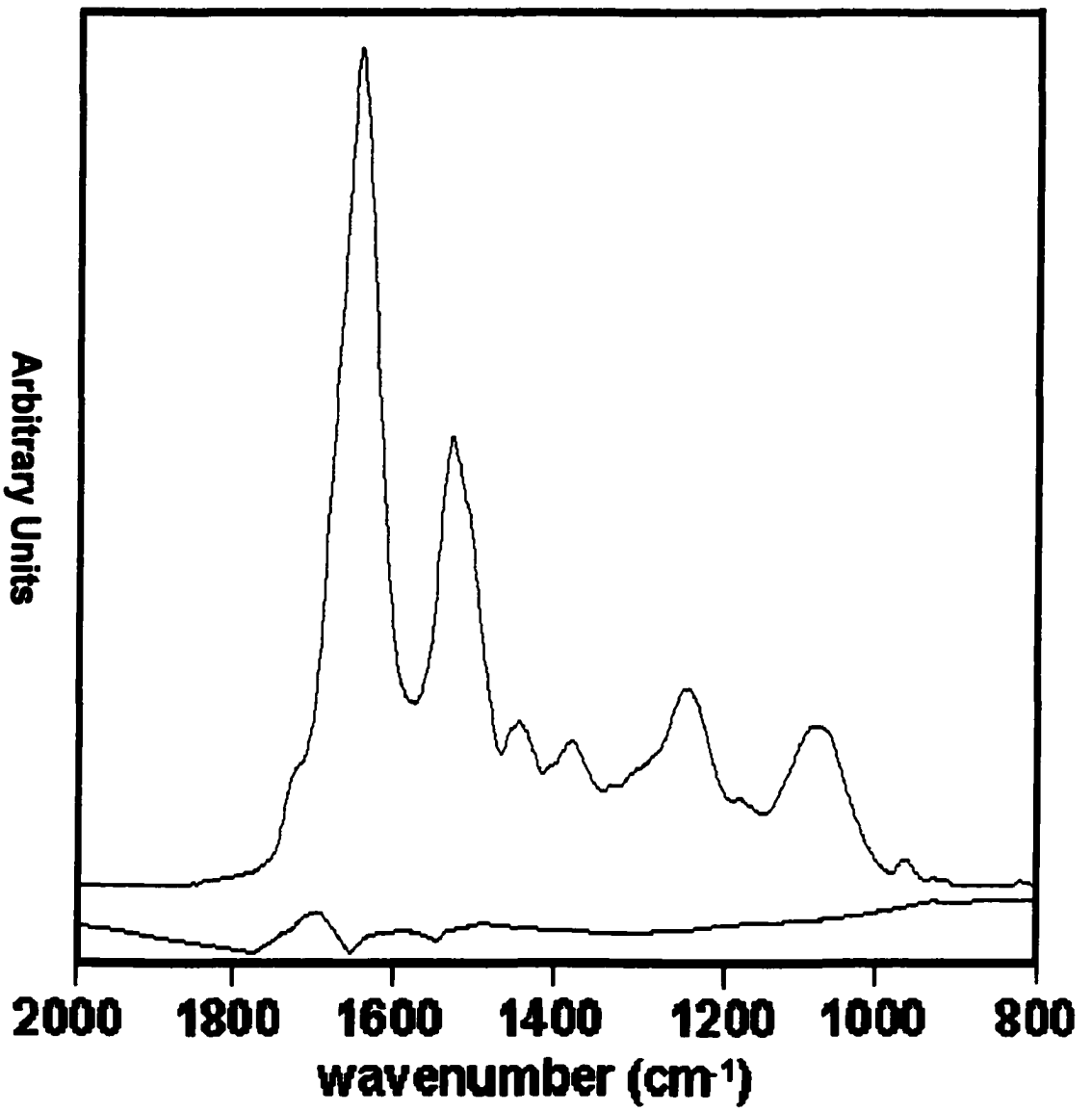

Figure 32: Averaged spectrum of dried 3Y1 cells after 72 hours of serum stimulation. Standard deviation was calculated and is shown below.

2. Second Derivative Analysis of Dried 3Y1 Cells That Have Been Serum Stimulated for 72 Hours: The nucleotide region contains four peaks in the second derivative as in **Figure 33**. As compared to the 24 hour serum stimulated cells the changes are large. These spectra resemble the data from the serum starved cells and 60 hour serum stimulation time points. The symmetric phosphate stretch peak is between 1100 – 1074 cm^{-1} and between 1135 -1116 cm^{-1} peaks are identical to the dried cells from the 24 hour time point. The low wavenumber ribose ring vibration peak between 1074 – 1042 cm^{-1} remains similar in bandshape and width compared to the 24 hour time point as well. The peak between 1116 –1100 cm^{-1} is present and shared the same bandwidth and shape as the 24 hour sample.

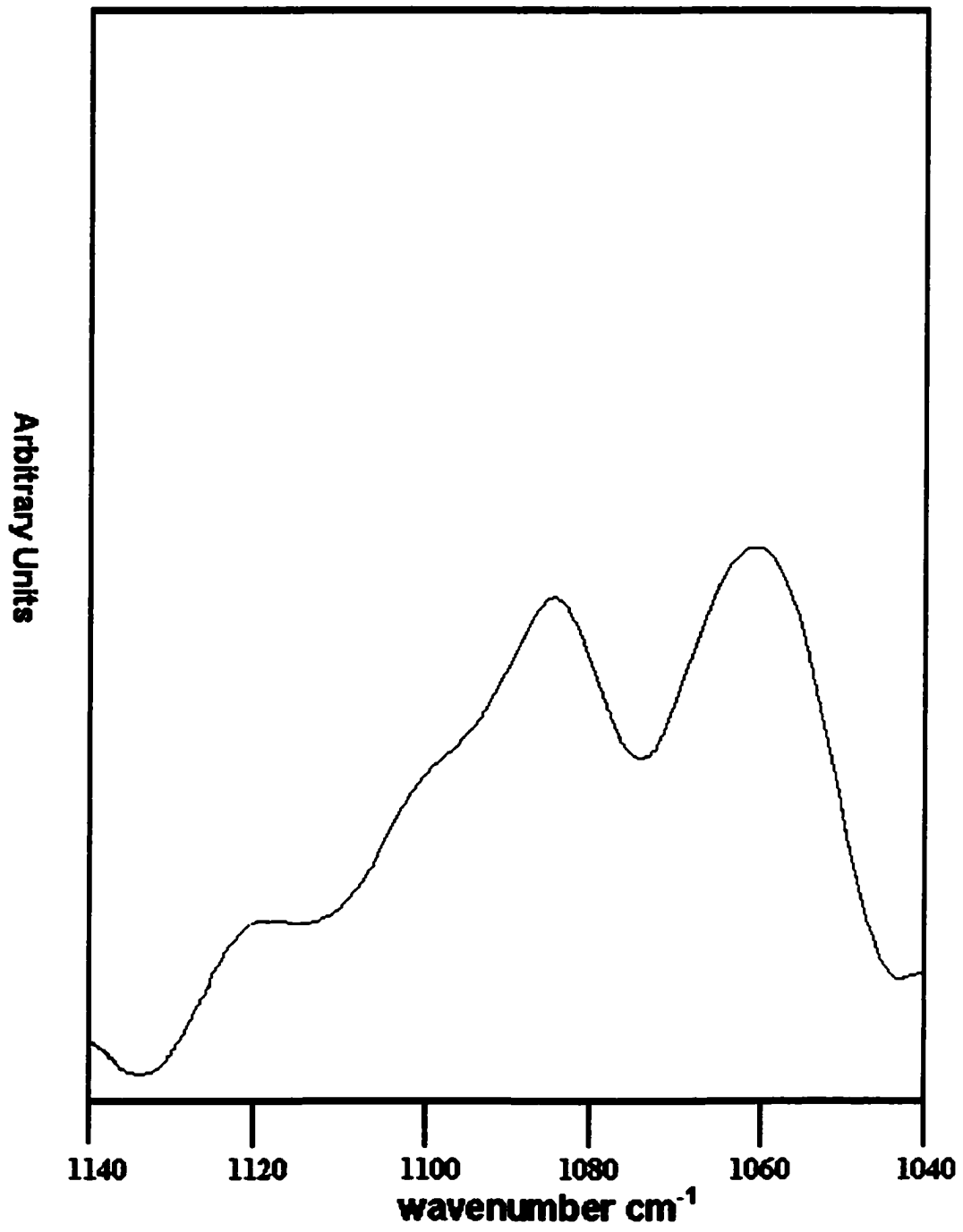

Figure 33: Averaged second derivative spectrum from dried 3Y1 cells that have been serum stimulated for 72 hours.

3. Effect of Ethanol on the Spectra Generated From 3Y1 Cells After 72 Hours of Serum Stimulation: Upon washing with 100% ethanol, we see that the intensity of the symmetric and antisymmetric phosphate stretching vibrations at ca. 1080 and 1235 cm^{-1} is decreased respectively due to the removal of extraneous phosphorous containing biomolecules. The nucleotide peak is thus enriched in nucleotide content. The phosphoester vibration at 1740 cm^{-1} is nearly completely removed in **Figure 34**. The spectrum shown here is almost identical to that of the 24 hour serum stimulated that has been ethanol treated.

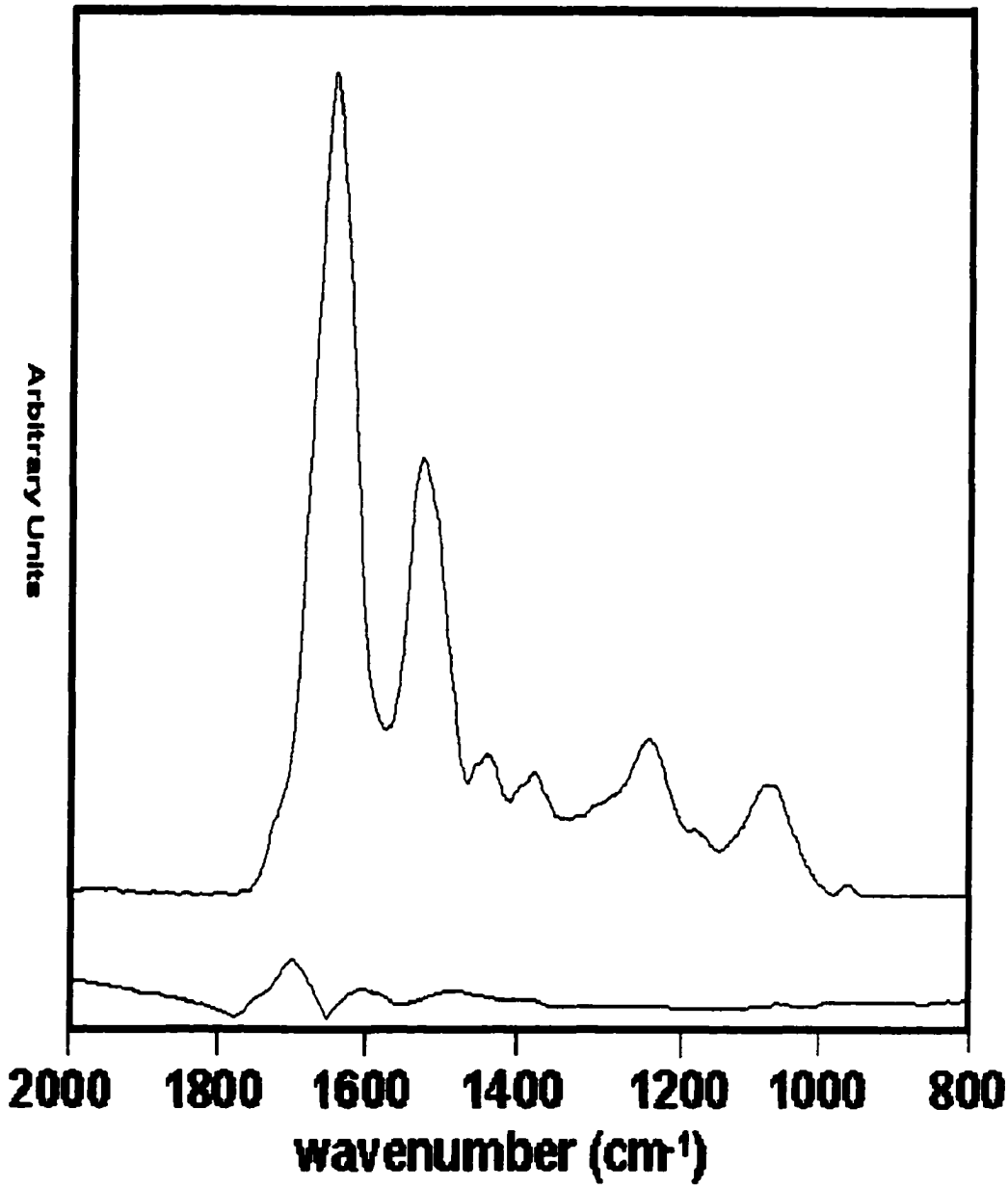

Figure 34: Spectra of ethanol treated 3Y1 cells that have been serum stimulated for 72 hours. The standard deviation was calculated and is shown below.

4. Second Derivative Analysis of the Spectra From Ethanol Treated 3Y1 Cells After 72 Hours of Serum Stimulation: The second derivative of the averaged spectrum generated from ethanol treated 3Y1 cells after 72 hours of serum stimulation is shown **Figure 35**. The high wavenumber ribose ring vibration peak between 1138 – 1108 cm^{-1} observed in the ethanol treated cells after 24 hours narrowed to between 1138 – 1114 cm^{-1}at 72 hours. The low wavenumber ribose ring vibration peak between 1076 – 1049 cm^{-1} observed in the spectrum from the 24 hour timepoint broadens slightly to between 1076 – 1044 cm-1 at 72 hours. The symmetric phosphate vibration narrows from between 1104 – 1074 cm^{-1} after 24 hours to 1096 – 1076 cm^{-1} at 72 hours.

This band between 1114 –1097 cm^{-1} in this sample was also observed after 24 hours of serum stimulation in the ethanol treated cells. This band broadens slightly upon ethanol treatment when compared to the dried cells.

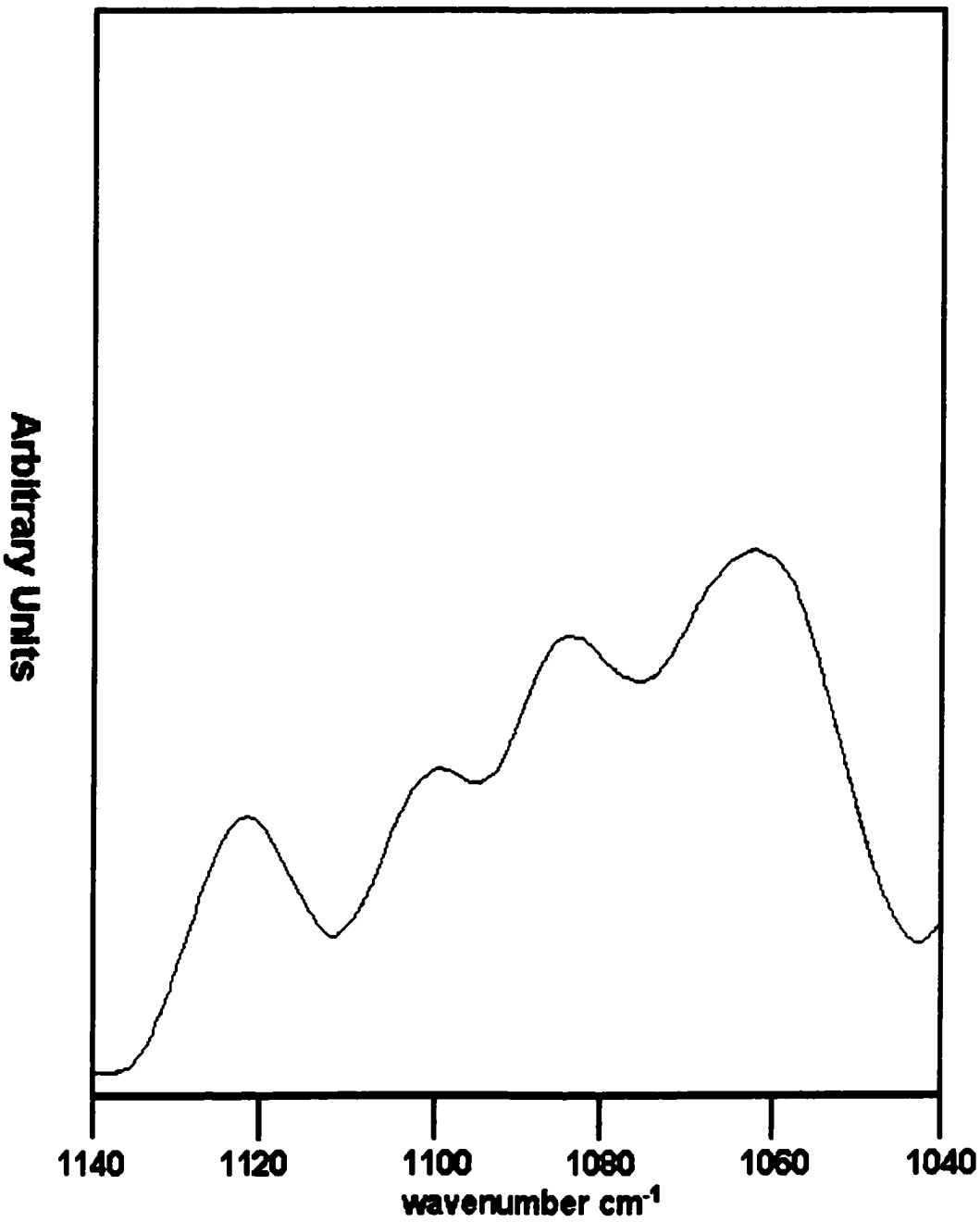

Figure 35: Second derivative analysis of the averaged spectrum generated from ethanol treated 3Y1 cells after 72 hours of serum stimulation.

5. Effect of RNase Digestion on the Spectra Generated From 3Y1 Cells After 72 Hours of Serum Stimulation: The nucleotide peak has lost more intensity since the Ethanol treatment as characterized by a further decrease in the symmetric and antisymmetric phosphate vibrations in **Figure 36**.

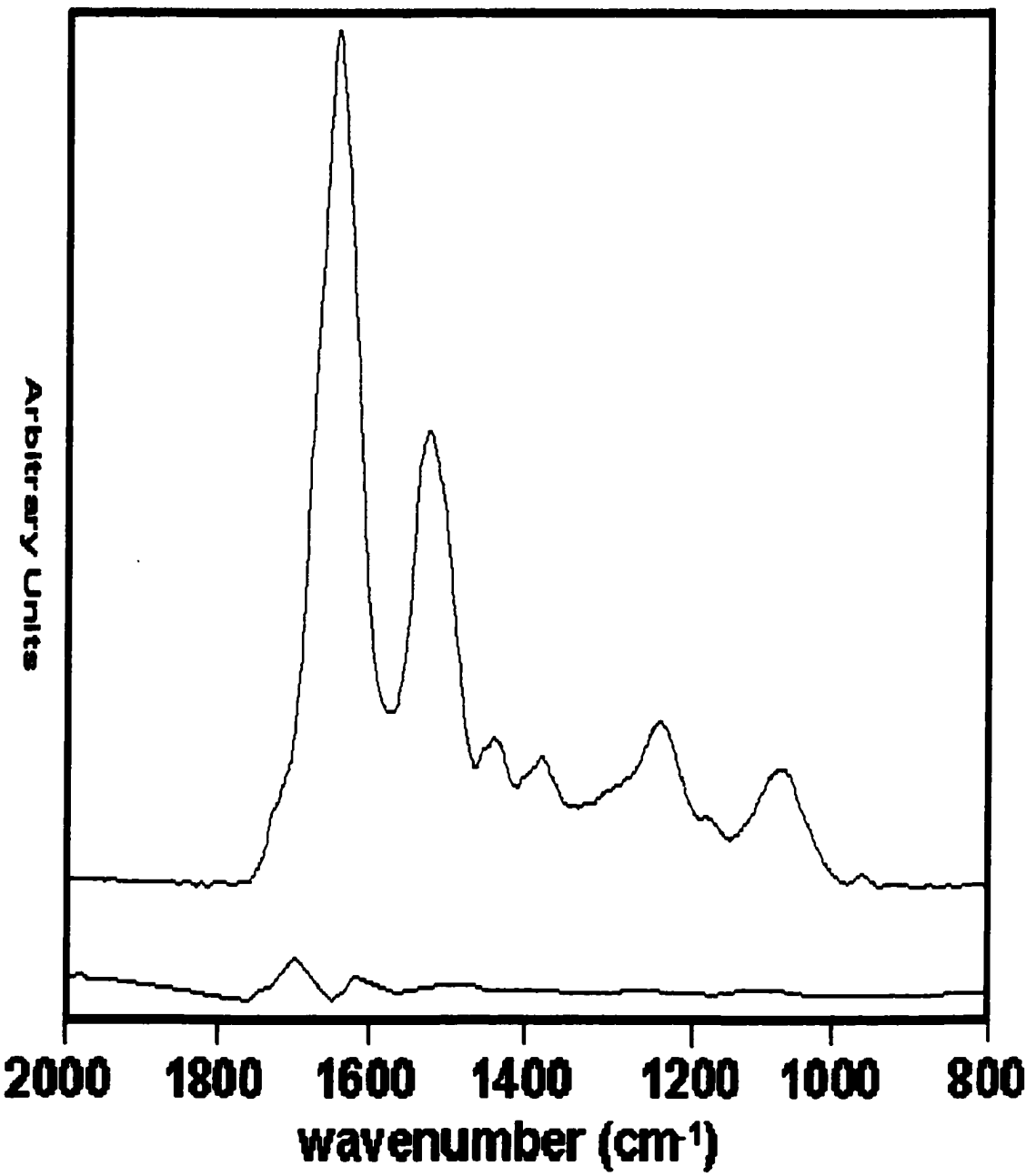

Figure 36: Spectra of RNase digested 3Y1 cells that have been serum stimulated for 72 hours. Standard deviation was calculated and is shown below.

6. Second Derivative Analysis of the Spectra from RNase Digested 3Y1 Cells After 72 hours of Serum Stimulation: The averaged second derivative spectrum of **RNase** digested **3Y1** cells is shown in **Figure 37** for this sample. The low wavenumber ribose ring vibration peak between 1075 –1042 cm^{-1} does not change in terms of bandwidth or shape as compared to the 24 hour serum stimulated cells that had been **RNase** digested. The high wavenumber ribose ring vibration between 1137 – 1108 cm^{-1} peak observed after 24 hours narrowed to between 1139 – 1113 cm^{-1} after 72 hours. The symmetric phosphate between 1108 – 1075 cm^{-1} at 24 hours narrowed to between 1096 -1075 cm^{-1} after 72 hours of serum stimulation. The peak observed in the ethanol treated cells between 1114 - 1097 cm^{-1}remains after **RNase** digestion. The peak is observed between 1113 - 1096 cm^{-1}after 72 hours in the **RNase** digested cells.

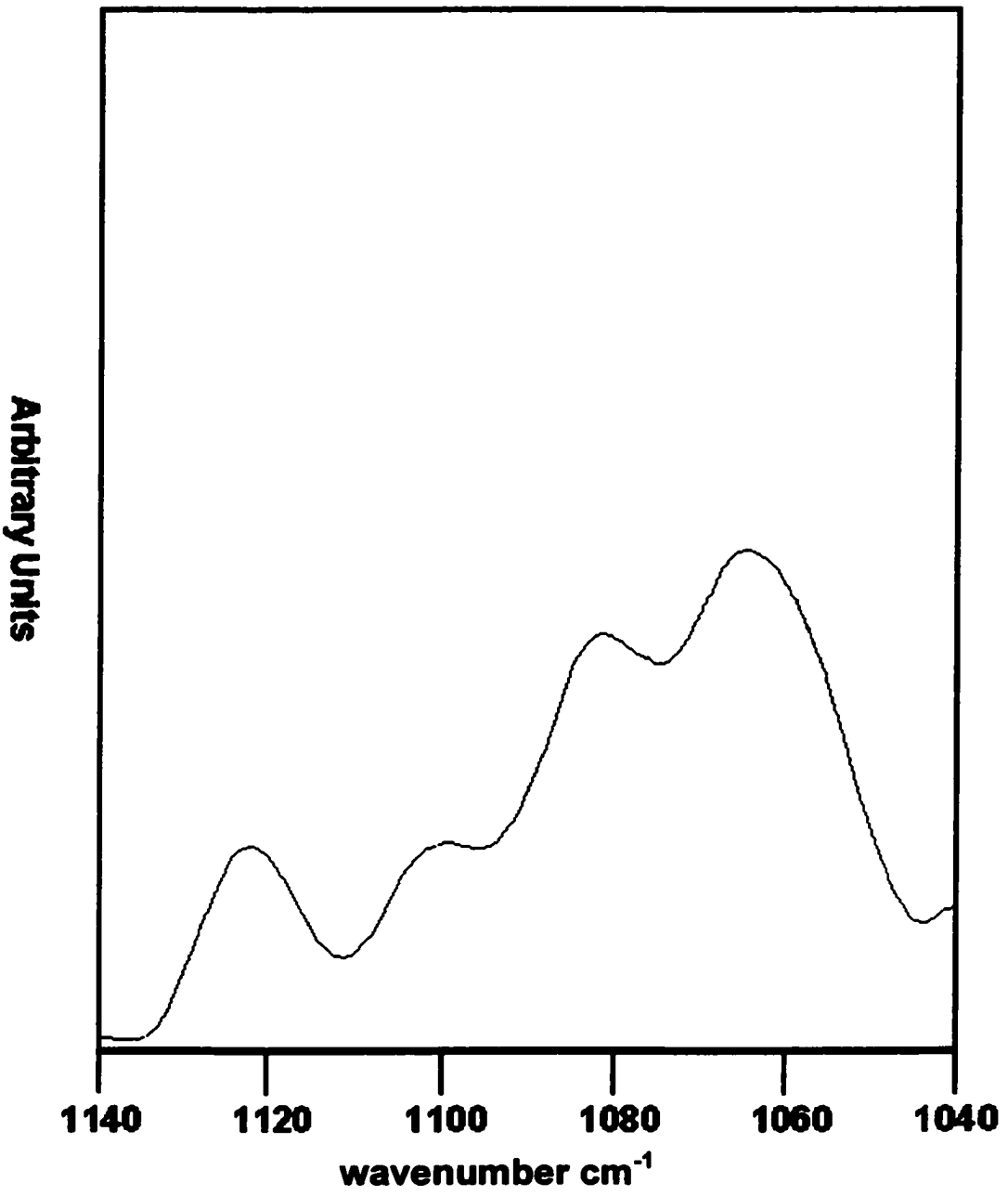

Figure 37: Averaged second derivative spectrum of RNase digested 3Y1 cells that have been serum stimulated for 72 hours.

F. Flow Cytometry Results From Serum Stimulated 3Y1 Cells:

The spectral changes observed in the serum stimulated cells have been correlated against flow cytometry. This technique is used to determine the relative number of cells in cell cycle by measuring the **DNA** content of the cells. Before any cell begins proliferating, many are poised to reproduce their **DNA** during **S phase** and await mitosis after **G2**. Entrance into **S phase** and subsequently **G2** phase proceeds only after the right conditions are achieved. Therefore determination of the number of cells within these two phases gives an indication of the population of cells that are proliferating (Nunez, 2001, Keng, 1986). Therefore any changes in the number of **G2** and **S phase** cells per sample can be used as a marker for cellular proliferation.

The technique measures the magnitude of the fluorescence from Propidium Iodide **(PI)**, a **DNA** intercalating drug. The fluorescence intensity corresponds directly to the amount of **DNA** per cell. This directly relates to the phase of the cell cycle of which any given cell will be in. Cells in **G1** will have one complete copy of **DNA** whereas cells in **G2** will have double the amount. The **S phase** cells will be somewhere in the middle depending upon how far into **S phase** a particular cell may be. As a consequence the intensity of the **PI** in **G2** cells will be double that of **G1** cells. The following data are plotted as the number of cells versus relative copies of **DNA** per cell. **Table 4** gives the mean peak heights in terms of fluorescence for **G1** and **G2** cells.

1. FLOW Cytometric Analysis of Serum Stimulated 3Y1 Cells

After 24 Hours: The data from set of cells yielded a large population of cells in either **S phase** or **G2**. Approximately 43.6% of the cells were in these phases after 24 hours of serum stimulation as in **Figure 38**. The remainder of the cells were in the **G1** phase of the cell cycle. The number of cells counted was 15000.

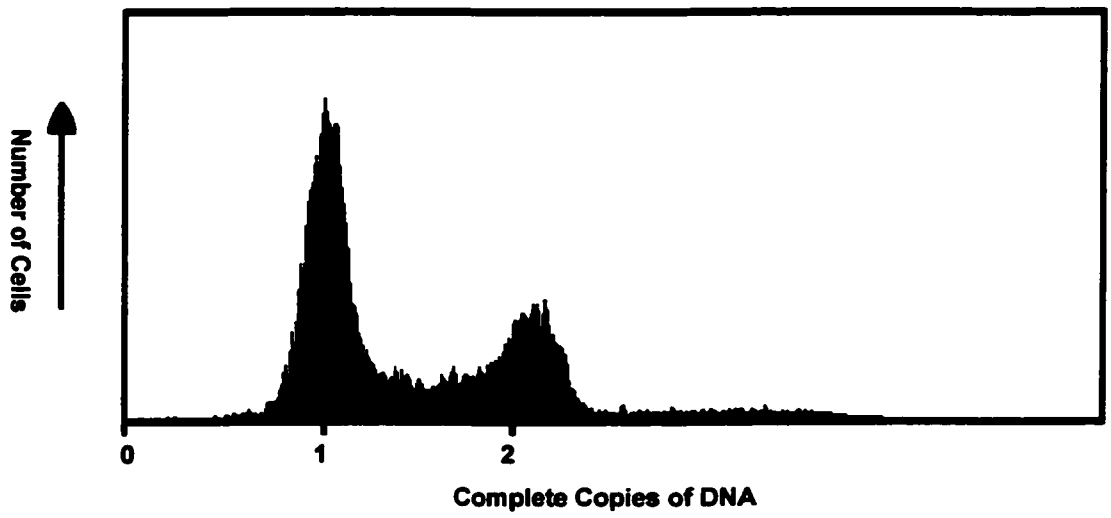

Figure 38: Flow cytometry data of serum stimulated 3Y1 cells after 24 hours.

2. FLOW Cytometric Analysis of Serum Stimulated 3Y1 Cells

After 36 Hours: The data from set of cells yielded a large population of cells in either **S phase** or **G2** as shown in **Figure 39**. The amount of cells in either phase decreased slightly from 43.6% to 32.5% after 36 hours of serum stimulation. The remainder of the cells were in the **G1** phase of the cell cycle. The number of cells counted was 15000.

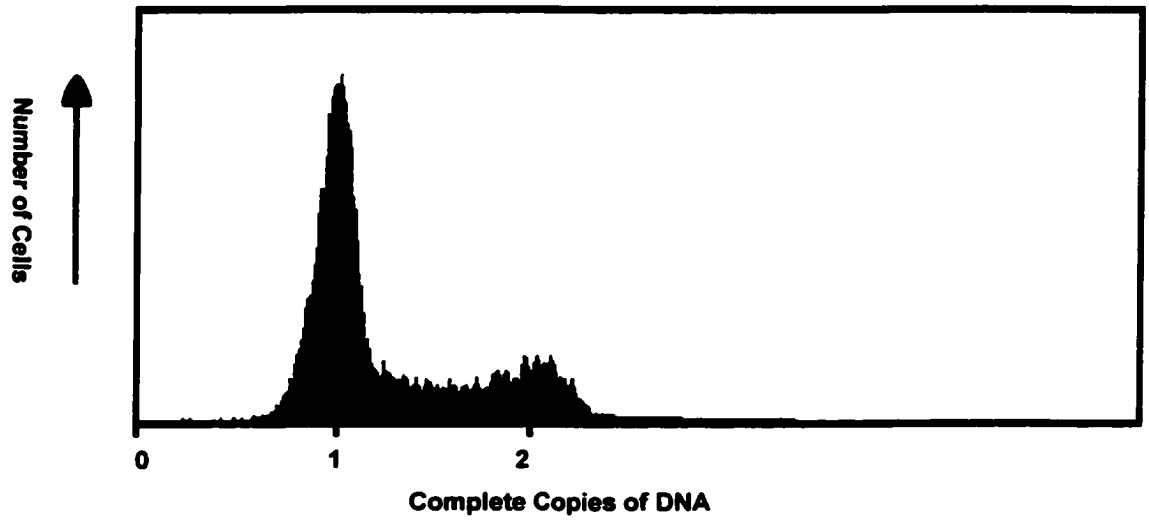

Figure 39: Flow cytometry data of serum stimulated 3Y1 cells after 36 hours.

3. FLOW Cytometric Analysis of Serum Stimulated 3Y1 Cells

After 48 Hours: The data from set of cells yielded a similar population of cells in either **S phase** or **G2** as compared to 36 hours of serum stimulation in **Figure 40**. There were 35.0% of the cells in either phase after 36 hours. The remainder of the cells were in the G1 phase of the cell cycle. The number of cells counted was 15000.

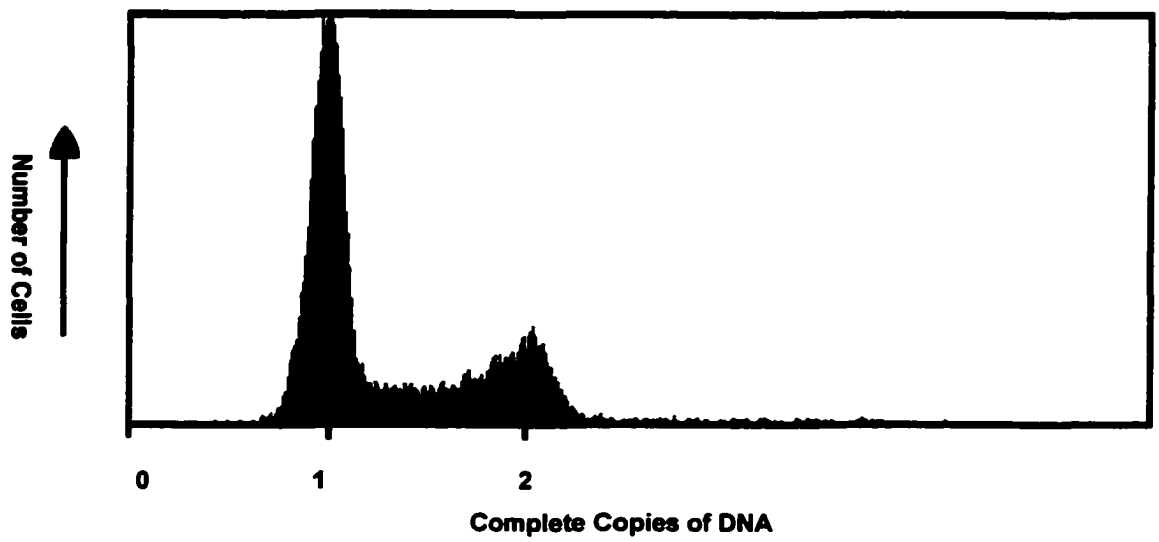

Figure 40: Flow cytometry data of serum stimulated 3Y1 cells after 48 hours.

4. FLOW Cytometric Analysis of Serum Stimulated 3Y1 Cells

After 60 Hours: This sample showed a large decrease in number cells in either **G2** or **S phase** relative to the 24-hour time point as in **Figure 41**. The amount of cells in either phase decreased from 43.6% after 24 hours to 18.3% after 60 hours of serum stimulation. The remainder of the cells were in the G1 phase of the cell cycle. The number of cells counted was 15000.

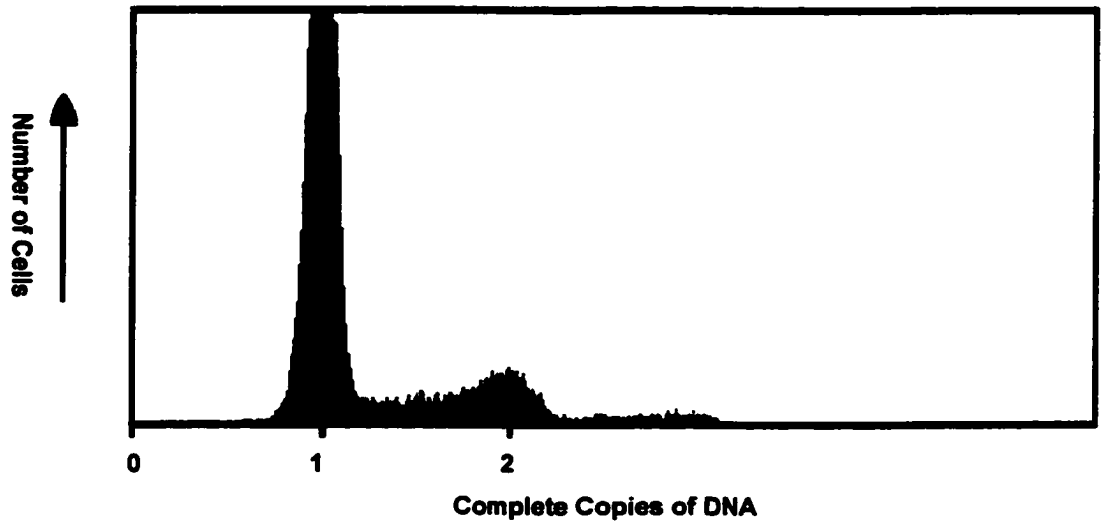

Figure 41: Flow cytometry data of serum stimulated 3Y1 cells after 60 hours.

5. FLOW Cytometric Analysis of Serum Stimulated 3Y1 Cells

After 72 Hours: This sample continued the trend of decreased cells in either **G2** and **S phase** cells relative to the 24-hour time point as shown in **Figure 42**. The amount of cells in either phase decreased from 43.6% after 24 hours to 14.3 % after 72 hours of serum stimulation. The remainder of the cells were in the G1 phase of the cell cycle. The number of cells counted was 15000.

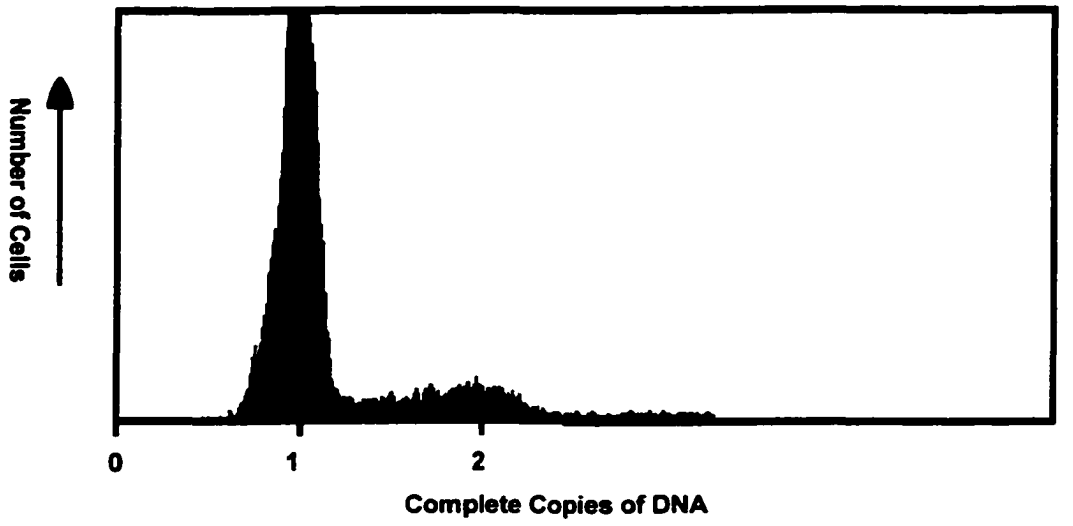

Figure 42: Flow cytometry data of serum stimulated 3Y1 cells after 72 hours.

Time (H)	% of S and G2 cells	Median Peak Height (G1)	G2
24	43.6	210	396
36	32.5	210	365
48	35.0	205	372
60	18.3	205	371
72	14.3	200	369

Table 4: Summary of the FLOW Cytometry results.

G. Serum Deprived 3Y1 Cells: The spectra for this sample were deprived of high serum containing media for a total period of 60 hours. The percentage of **G2** and **S phase** cells in this sample decreased to less than 27 % as shown in **Table 5**. This was a small decrease relative to the exponentially growing cells used as a control experiment. The spectroscopic data obtained for the serum deprived cells was similar in nature to that of the high confluence experiments.

The exponentially growing cells were prepared in a fashion that was nearly identical to the to the 24 hour time point experiment. Cells were seed at a lower concentration ($3 \cdot 10^5$ cells per plate) than for the confluence studies. Spectroscopic as well as **FLOW** cytometry data were similar for both the exponentially growing cells and the 24 hour time point. The reader is therefore referred to **Section A** of the results as the reference data for this experiment.

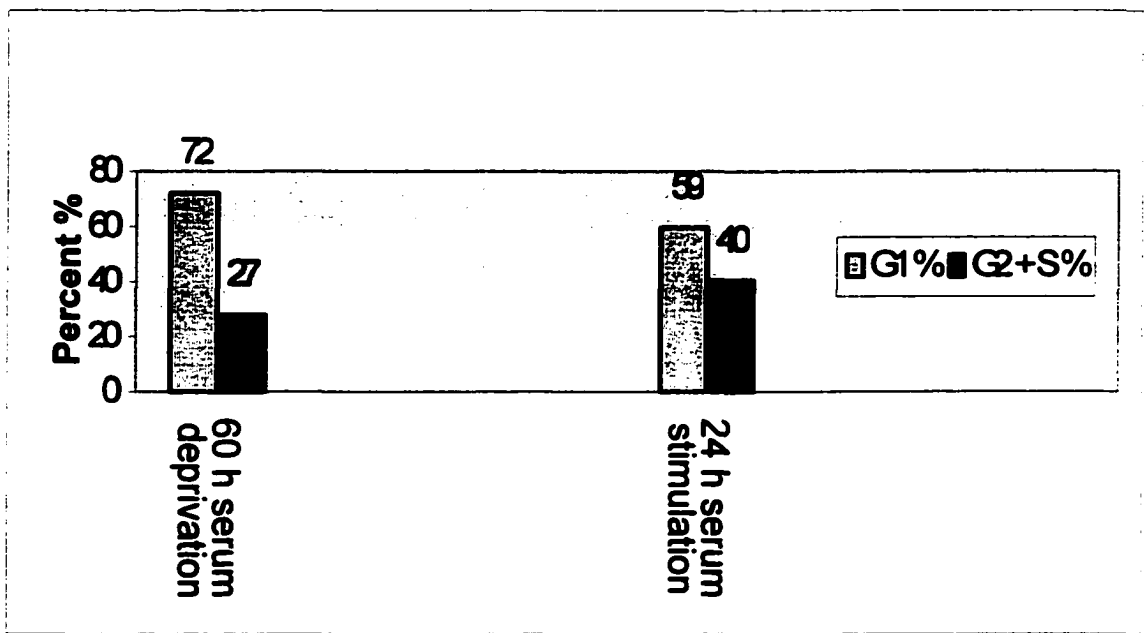

Table 5: Results from FLOW cytometry of 3Y1 cells after serum deprivation. Cells after 24 hours of serum stimulation are assumed to be exponentially growing.

1. Spectra Generated From Dried 3Y1 Cells After 60 Hours of Serum Deprivation: The spectrum in **Figure 43** represents cells that have been serum deprived for a total period of 60 hours. After 36 hours of serum deprivation, the cells were rinsed with fresh 0.5% serum containing medium.

These cells have been dried and prepared as previously mentioned. This spectrum is in many ways almost identical to that of the highly confluent and 24 hour stimulated cells. The intensity in the nucleic acid envelope is slightly less intense than the cell spectra from the 24 hour time point.

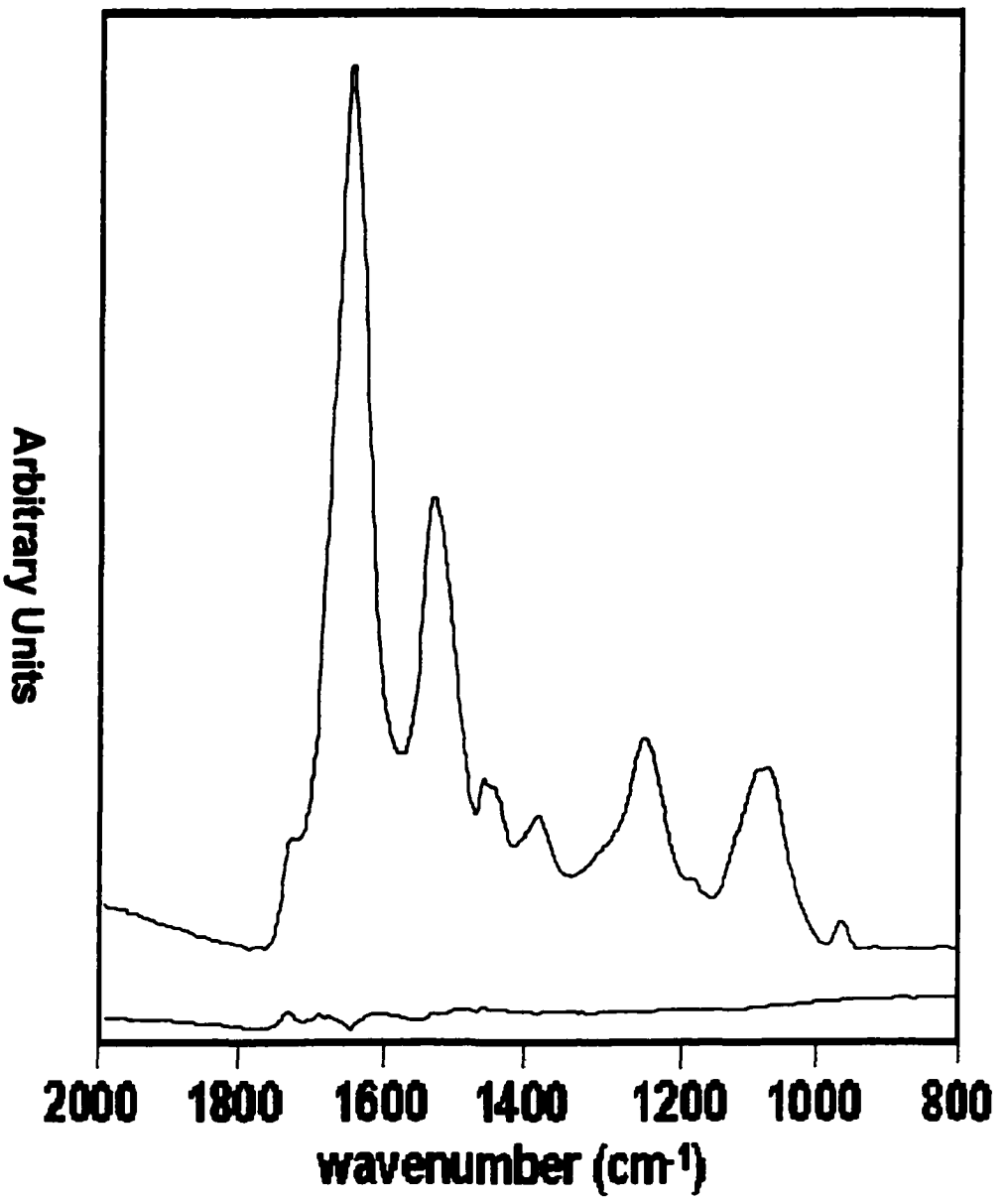

Figure 43: Composite spectrum of dried 3Y1 cells after 60 hours of serum stimulation. Standard deviation for the spectrum was calculated and is shown below.

2. Second Derivative Analysis of the Composite Spectrum From Serum Deprived Dried 3Y1 Cells: The nucleotide region contains four envelopes in the second derivative as in **Figure 44**. As compared to the 24 hour serum stimulated cells the changes are large. These spectra resemble the data from the 60 and 72 hour serum stimulation time points. The symmetric phosphate stretch envelope in this sample between 1094 – 1073 cm^{-1} narrows in bandwidth relative to the 24 hour timepoint. This band is between 1100 - 1074 cm^{-1} in the 24 hour sample. The 1137 – 1113 cm^{-1} and 1074 – 1043 cm^{-1} envelopes remain similar in bandshape and width compared to the 24 hour timepoint. The envelope between 1116 –1101 cm^{-1} is absent.

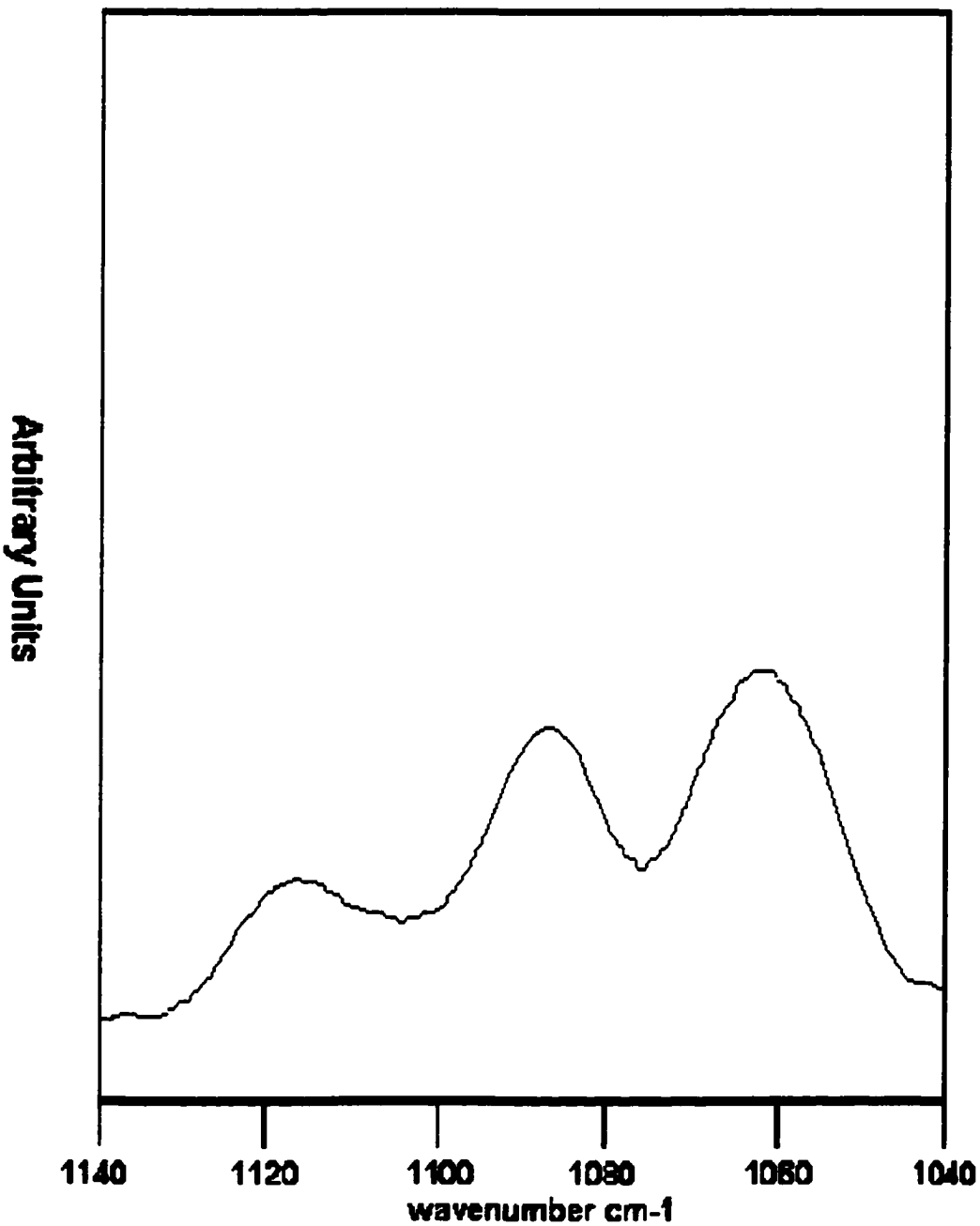

Figure 44: Second derivative spectrum from dried serum deprived 3Y1 cells.

3. Spectra Generated From Ethanol Treated RNase Digested 3Y1 Cells After 60 Hours of Serum Deprivation: There is a residue of phosphoester containing biomolecules as confirmed by the band at 1740 cm^{-1} as seen in **Figure 45**. The nucleotide envelope has lost more intensity since the ethanol treatment as characterized by a further decrease in the symmetric and antisymmetric phosphate vibrations.

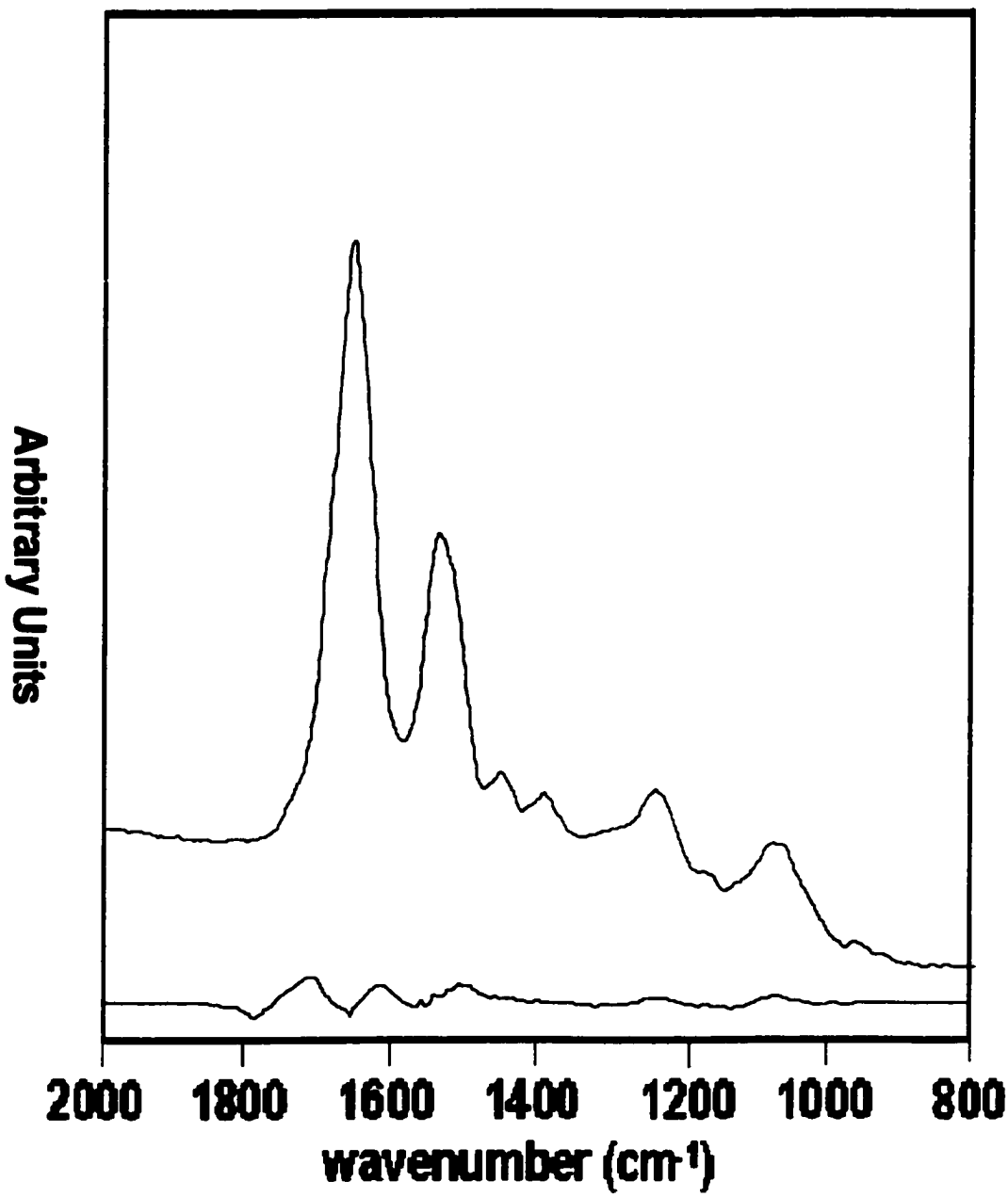

Figure 45: Spectra of ethanol treated/ RNase digested 3Y1 cells that have been serum stimulated for 72 hours. Standard deviation was calculated and is shown below the spectrum.

4. Second Derivative Analysis of the Composite Spectrum of Ethanol Treated / RNase Digested 3Y1 Cells: The high wavenumber ribose ring vibration was observed between 1140 – 1116 cm^{-1} in this sample as shown in **Figure 45**. This envelope narrowed slightly relative to the control (1140 – 1108 cm^{-1} for exponentially growing cells at 24 hours). The low wavenumber ribose ring vibration narrowed as well from 1077 – 1045 cm^{-1} at 24 hours of growth to 1070 –1045 cm^{-1} in the arrested cells. The symmetric phosphate narrows and shifts in the arrested cells rorm 1108 – 1077 cm^{-1} to 1070 – 1044 cm^{-1} relative to the exponentially growing cells. The novel peak is present from 1097 – 1070 cm^{-1}.

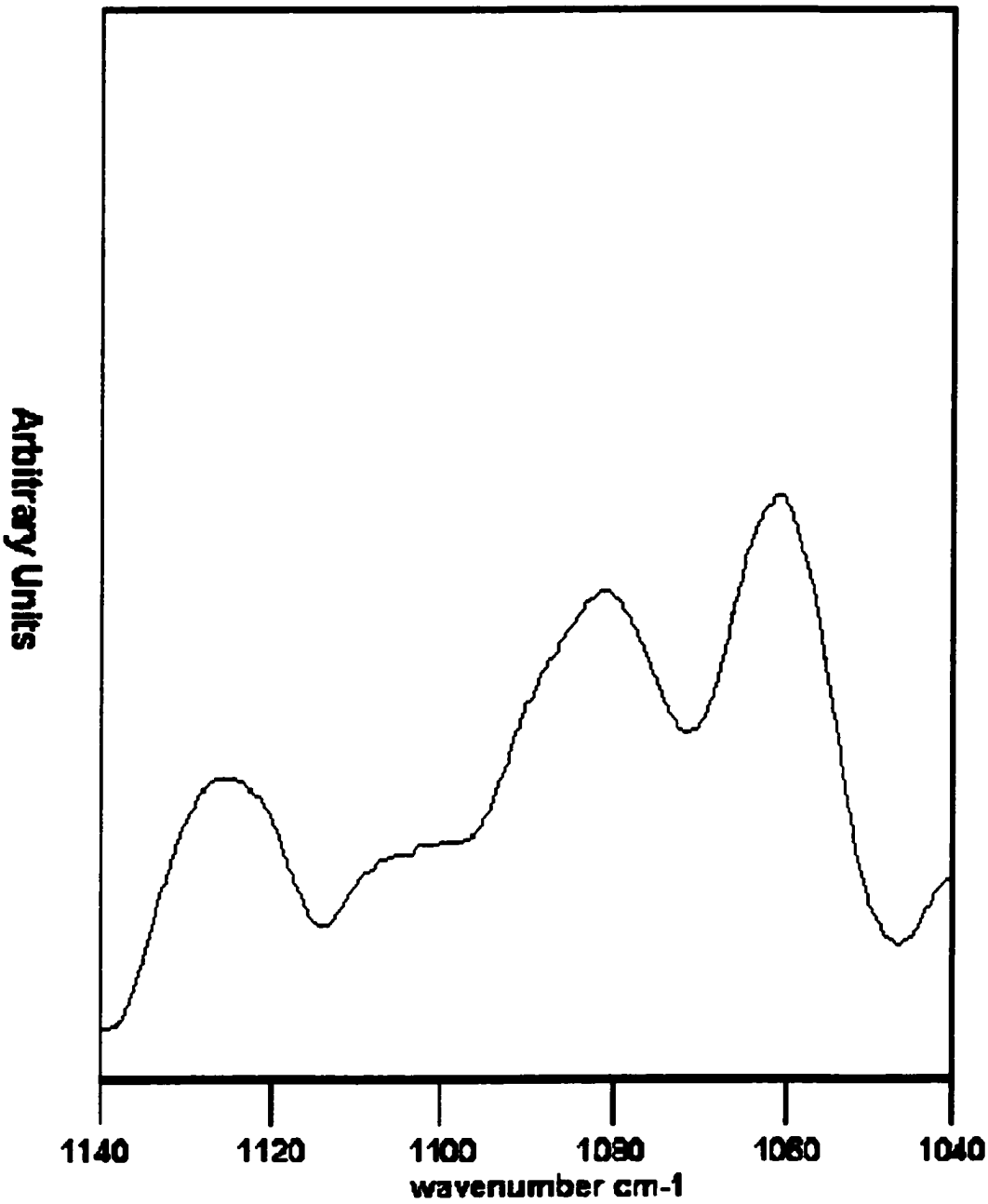

Figure 45: Second derivative spectrum from ethanol treated RNase digested serum deprived 3Y1 cells.

H. DNase Digestion of 3Y1 Cells: DNA contained within the 3Y1 cells was removed enzymatically by digestion with Deoxyribonuclease (DNase) after the previously discussed treatments. The resulting spectra should composed of mostly protein. Exponentially growing, highly confluent and serum deprived cells were compared after the removal of DNA. Sections A, E and F respectively in the results section represent these samples.

1. Spectra of DNase Digested Cells: The spectra shown in **Figure** represents cells that have been **DNase** digested. Shown in **Figure 46** are composite spectra from exponentially growing, highly confluent and serum deprived cells.

The intensity of the nucleic acid region in all samples has been greatly reduced after digestion by **DNase**. Interestingly, the spectral features for this region are slightly different for the exponentially growing cells versus the other two experiments. This suggests that the samples at this stage can be differentiated based on the cellular components that remain after the **DNase** digestion which should be mainly protein.

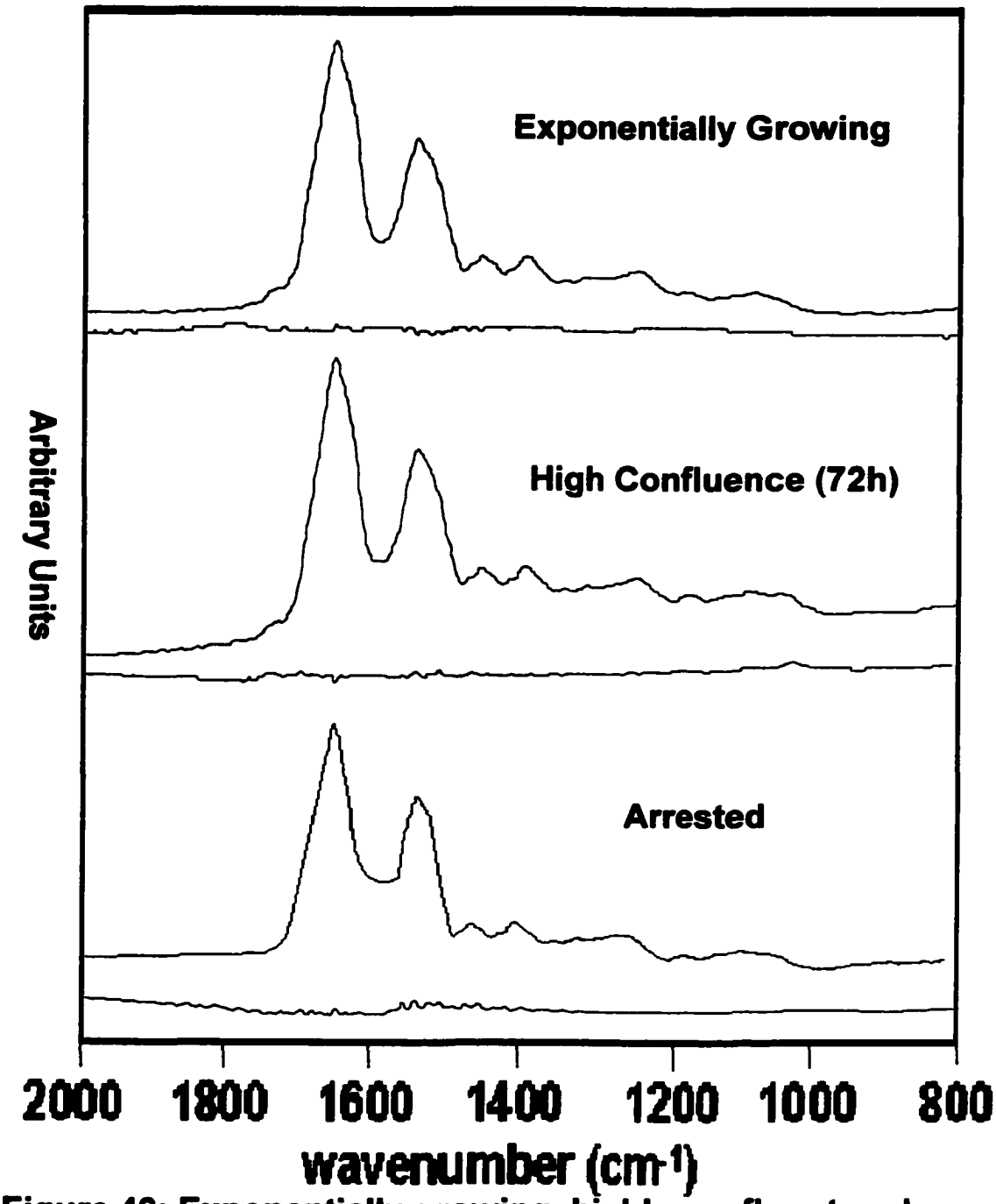

Figure 46: Exponentially growing, highly confluent and arrested 3Y1 cells after DNase digestion. Standard deviations were calculated and are shown below each spectrum.

2. Second Derivative Spectra of DNase Digested Cells: The second derivative spectra shown in **Figure 47** represents cells that have been **DNase** digested.

Spectral features in the nucleic acid region between 1140 – 1040 cm^{-1} differentiate all three types of spectra. The exponentially are quite different form the high confluence or serum deprived cells. These two spectra are nearly identical. The spectrum obtained from the high confluence cells contains two extra peaks between 1140 – 1120 cm^{-1} and 1115 –1110 cm^{-1} relative to the arrested cells. The differences shown here are presumably due to alterations in cellular metabolism of proteins associated with cell cycle progression.

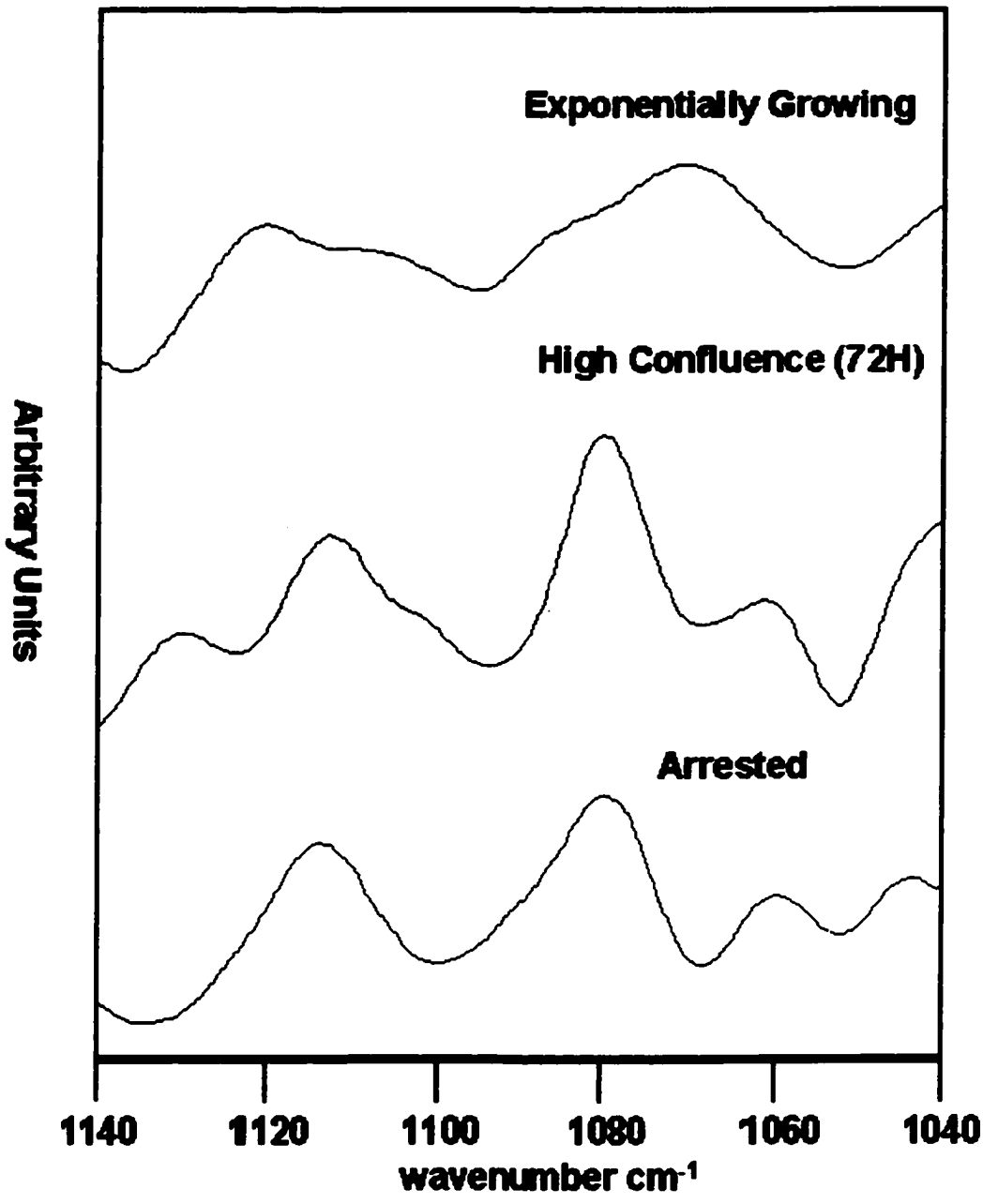

Figure 47: Second derivative spectra of 3Y1 cells after DNase digestion.

VI. Discussion:

A. Technical Aspects of Sample Preparation: The potential for detecting small biological changes within cells and tissues using IR spectroscopic methods is quite large. The sensitivity of IR microspectroscopy to changes within the environment of growing 3Y1 cells has been well characterized throughout this work. In this research, we want to set forth the spectral changes observed when eukaryotic cells are subject to a number of different growth conditions. The first of these efforts was to establish whether or not growth inhibition induced by serum deprivation or confluence could be observed spectroscopically. To this end, it is necessary to design methods towards harnessing the power of this technique.

1. Cell Culture: There are several subtle issues that need to be considered in terms of the preparation of eukaryotic cell samples for IR spectroscopic measurements. Many of these parameters are quite obvious to the cell biologist. However, these parameters are critical as IR spectroscopy is potentially subject to artifacts from cell culture preparations.

It is important to know the source and history of the cells that one will be working with. Issues such as the number of times the cells have been passed are extremely critical. Eukaryotic cells in general may only be passed a finite number of times as they will eventually become senescent. It is best to work with cells that have not been passed often and that are from the same passage number.

There is also a possibility that the cells may be able to differentiate or transform into other types of cells. This ability is quite common and the cell types used for future studies should be well characterized in terms of the conditions necessary to avoid or enhance this behavior.

Third, the lot of serum and type are critical to the maintenance of biological responses from sample to sample. Serum is rich in the protein factors that control biological responses within cells. As different lots will be taken from different animals these molecules will vary in concentration. It is necessary to normalize the responses of cells to the growth environment. Therefore each set of experiments needs to use the same lot of serum.

2. Sample Preparation of Dried 3Y1 Cells: The growth environment of cells is an extremely rich matrix of minerals, proteins, vitamins and other biomolecules that are found both in serum and the medium necessary for growth. As the cells are dispersed within culture dishes that contain both serum and medium, it necessary to remove both so that artifacts attributable to them are removed.

To this end, we have chosen to rinse the adherent cells free of serum and medium by washing them with saline while still attached to the culture dish. The cells are then freed with trypsin and the trypsin is rinsed away with saline containing doubly distilled water. To remove the salt, the cells are washed and dried quickly with just doubly distilled water. The cells once attached are rinsed again and dried. This ultimately yields cells that free of contamination from serum, medium or salt.

3. Ethanol Treatment of 3Y1 Cells: Ethanol has been shown to drastically alter the spectral features of 3Y1 rat liver fibroblast cells via removal of most phospholipids from cellular membranes. This has been demonstrated as the nearly complete loss of ester peak at 1740 cm-1. We therefore believe that the choices of solvents used to either fix or prepare samples for future IR measurements should be closely studied before usage in the literature.

The solubilities of Phosphatidylcholine, Cardiolipin, Sphingomyelin and Cerebrosides are high in ethanol. Other phospholipids such as Phospatidylserine, Ethanolamine and Inositol are poorly soluble. **(Avanti POLAR Lipids Catalog, 2001)**. In both Erythrocyte and Liver Plasma membranes, the most common phospholipid constituents are Phosphatidylcholine and Sphingomyelin. These two lipids alone comprise 35 – 43% of the total lipid extracted from these membranes **(Alberts et al., 1994)** as compare with Phosphatidylethanolamine and serine which compose only 11 – 25%.

The removal of these phosphate containing compounds leads to a nucleotide envelope that is now enriched in terms of nucleotides as the extraneous phosphorous containing compounds are at least partially removed. The spectral difference between the salt free and ethanol treated cells is attributed to the removal of phospholipids, other small biomolecules and possibly that of water.

4. RNase Digestion of 3Y1 Cells: One aim considered here focuses upon changes in the level of proliferation of 3Y1 cells due to serum deprivation or high confluence. Both the levels of **RNA** and **DNA** synthesis are influenced by these changes. **RNA** synthesis is a marker of changes in levels of gene transcription and is not as sensitive to the level of proliferation as **DNA** synthesis or conformational changes could be. In order to test whether or not the changes in the spectra were due to **DNA,** the **RNA** was removed by **RNase** digestion. There are still several groups of biomolecules that can potentially interfere even after these treatments and digestions. Phosphorylated proteins and sugars can complicate the region of the spectrum between 1140 – 1040 cm^{-1}, which is rich in nucleotide vibrations. It is also important to note here that this digestion was more or less incomplete in all samples. This is a consequence of not knowing how much nuclear **RNA** had been digested or how much **RNA** bound by proteins had been protected. It is however fair to say that most of the RNA had been removed by digestion and that the level of removal is consistent from sample to sample.

B. Interpretation of Spectroscopic Changes:

1. Use of Second Derivative Analysis: Spectroscopic measurements of cells are quite sensitive to a variety of factors such as solvents and or chemical treatment of samples. The spectral differences between dried cells, ethanol treated cells and **RNase** digested cells are quite obvious. However, all of the spectra from the dried cells closely resemble each other regardless of the length of serum exposure. The spectra from the ethanol treated and **RNase** digested cells are also similar in this respect. The changes sought between different lengths of serum stimulation therefore must be quite small. It is necessary to use a technique with the sensitivity capable of detecting these minute changes.

Second derivative spectral analysis, could detect these small spectral differences between any two spectra. Second derivative spectra are obtained by numeric differentiation of the spectral intensity (ν) with respect to the wavenumber:

$$\frac{d^2 I(\nu)}{d\nu^2} \qquad (6.1)$$

In the differentiation process, information on absolute band intensities and band shapes are lost; however, the 2nd derivative spectrum provides accurate information on the position and number of component

bands under a broad spectral envelope. Thus, the subsequent interpretation of spectral changes will be presented for 2^{nd} derivative spectra.

To simplify this process, the nucleotide envelope between 1140 – 1040 cm^{-1} was analyzed for consistent pattern of changes associated with increased confluence due to serum stimulation. The data were acquired for cells that had been dried, ethanol treated and **RNase/ DNase** digested. This served to provide a multilayer approach to dissect the spectral changes. The overall goal here was to understand these changes in terms of the biochemistry of the cell which was controlled by the conditions discussed earlier. Removing biomolecules somewhat selectively was the approach used to accomplish this.

2. Second Derivative Analysis of Dried 3Y1 Cells at Different Timepoints: The results here show an overall picture of the changes in the nucleotide envelope of the dried cells after 24, 36, 48, 60 and 72 hours of serum stimulation. The high and low wavenumber ribose ring vibrations and the symmetric phosphate envelopes did not change in bandshape or width throughout any of the timepoints. The behavior of the envelope between ca. 1120 – 1100 cm^{-1} is similar. It was present and did not change in any of the samples. The many biomolecules absorbing in this region apparently complicate any observation of changes within this region.

3. Second Derivative Analysis of Ethanol Treated 3Y1 Cells at Different Timepoints: The results here show an overall picture of the changes in the nucleotide envelope of the dried cells after 24, 36, 48, 60 and 72 hours of serum stimulation. The symmetric phosphate envelope narrowed in all samples after 24 hours from 1104 – 1074 cm^{-1} to finally between 1096 –1076 cm^{-1} after 72 hours. The high wavenumber ribose ring vibration envelope narrowed from 1138 –1108 cm^{-1} at 24 hours to 1138 –1114 cm^{-1} after 72 hours. The low wavenumber ribose ring vibration underwent a slight broadening from 1076 – 1049 cm^{-1} after 24 hours to 1076 – 1044 cm^{-1}. The band between 1116 –1101 cm^{-1} is present in the dried cells at 24 hours but not after ethanol treatment. It is however present in all other samples and does not vary with respect to time. The ethanol treatment apparently removes phospholipid molecules. This allows for the detection of small changes due primarily to features associated with nucleotides.

4. Second Derivative Analysis of RNase Digested 3Y1 Cells at Different Timepoints: The results here show an overall picture of the changes in the nucleotide envelope of the dried cells after 24, 36, 48, 60 and 72 hours of serum stimulation. The symmetric phosphate envelope narrowed in all samples after 24 hours from 1108 – 1075 cm^{-1} to finally between 1096 –1075 cm^{-1}after 72 hours. The high wavenumber ribose ring vibration envelope narrowed from 1138 –1108 cm^{-1} at 24 hours to 1139 –1113 cm^{-1} after 72 hours. The low wavenumber ribose ring vibration underwent a slight broadening from 1075 – 1045 cm^{-1} after 24 hours to 1075 – 1042 cm^{-1}. These results were similar to those observed in the ethanol treated cells.

The band between 1116 –1101 cm^{-1} is present in the dried cells after 24 and 36 hours of serum stimulation but not after **RNase** treatment. The 48 hour, 60 and 72 hour samples all contain this envelope. This envelope broadens from 1107 – 1097 cm^{-1} at 48 hours to between 1113 – 1096 cm^{-1} at 72 hours. The data is summarized in **Table 6**.

5. Second Derivative Analysis of Serum Deprived 3Y1 Cells:

Serum deprivation of **3Y1** cells for 60 hours led to decrease in the level of proliferation in the culture as assayed by FLOW cytometry. The percentage of **G2** and **S Phase** cells fell from 40% in the control to 27% after removal of the growth factors for 60 hours. The spectral changes in the second derivative were very similar to those found in cells that were highly confluent.

In the dried cells, the symmetric phosphate stretch envelope in this sample between 1094 – 1073 cm^{-1} narrows in bandwidth relative to the 24 hour timepoint. This band is between 1100 - 1074 cm^{-1} in the 24 hour sample. The 1137 – 1113 cm^{-1} and 1074 – 1043 cm^{-1} envelopes remain similar in bandshape and width compared to the 24 hour timepoint. The envelope between 1116 –1101 cm^{-1} was absent.

In the **RNase** digested cells, the high wavenumber ribose ring vibration was observed between 1140 – 1116 cm^{-1} in this sample. This envelope narrowed slightly relative to the control (1140 – 1108 cm^{-1} for exponentially growing cells at 24 hours). The low wavenumber ribose ring vibration narrowed as well from 1077 –1045 cm^{-1} at 24 hours of growth to 1070 –1045 cm^{-1} in the arrested cells. The symmetric phosphate narrows and shifts in the arrested cells from 1108 – 1077 cm^{-1} to 1070 – 1044 cm^{-1} relative to the exponentially growing cells. The novel peak is present from 1097 – 1070 cm^{-1}. This data is also summarized in **Table 6**.

Experiment	%G2 + S	Ribose Ring Vibration (cm-1)	Novel Envelope (cm-1)	Symmetric Phosphate (cm-1)
24 hour time point	44	1137 - 1108		1108 - 1075
72 hour time point	14	1139 - 1113	1113 - 1096	1096 - 1075
Exponential	40	1140 - 1108		1108 - 1077
Arrested	28	1140 - 1116	1097 - 1070	1070 - 1044

Table 6: Summary of results for RNAse digested 3Y1 cells.

6. DNase Digestion of 3Y1 Cells: The resulting spectra should composed of nearly all protein. Exponentially growing, highly confluent and serum deprived cells were compared after the removal of **DNA**.

The intensity of the nucleic acid region in the intensity spectra of all samples has been greatly reduced after **DNase** digestion. The spectral features for this region are different for exponentially growing cells versus serum deprived or confluent cells. This suggests the samples can be differentiated based on the remaining cellular components after **DNase** digestion. The metabolism of proteins changes in cells that are non-proliferative versus proliferative cells and could be detected using **IR-MSP**.

The spectral features observed in the second derivative in the nucleic acid region between 1140 – 1040 cm-1 further differentiate all three types of spectra. The exponentially growing cells are quite different from the high confluence or serum deprived cells.

The non- proliferative cells are nearly identical as observed in the intensity spectra. The spectrum obtained from the high confluence cells contains two extra peaks between 1140 – 1120 cm-1 and 1115 –1110 cm-1 relative to the arrested cells. The differences from the exponentially growing cells shown here are presumably due to alterations in cellular metabolism of proteins associated with cell cycle progression. The difference between the confluent cells and serum deprived cells may be compounded by the stress of high cell density and alterations in the cytoskeleton of the cells to compensate for this stress.

C. Correlation of Spectroscopic Results with FLOW Cytometry Data: The spectral changes have been correlated against flow cytometry. This technique is used to determine the relative number of cells in cell cycle by measuring the **DNA** content of the cells. When cells are proliferating, they reproduce their **DNA** during **S phase** and await mitosis in **G2**. Therefore determination of the number of cells within these two phases gives an indication of the population of cells that have doubled their **DNA** content **(Nunez, 2001, Keng, 1986)**.

The flow cytometry data for the confluence experiments revealed a strong correlation between the level of proliferation and confluence. There is a slight decrease the number of cells of in the **G2** phase, from 34 to 27%, in the first 48 -hour growth phase, and a more significant decrease to 11% at 72 hours. At this point, the cells are very densely packed onto the surface of the tissue culture plate and restricted from growing by space constraints as only a monolayer of cells is permitted. We believe that these two facts – the formation of a monolayer of cells, as well as the low percentage of cells in the **S/G2** phase, are indicative that the cell population had achieved confluence.

The serum deprived cells also showed a decrease in the percentage of **S/G2** phases of the cell cycle. The decrease in proliferation from the exponentially growing cells was not as dramatic as found with the confluent cells, falling only to 27% from 40% in the control.

The low proportion of cells transiting **S phase** may be due to the fact that the length of this period is approximately 6 - 8 hours for mammalian cells **(Lewin, 1994)**. It is possible that this time scale prevents noticeable changes as the transition to growth is very gradual (approximately 1/3 of the entire cell cycle). Okuda et al. show that the number of cells passing through **S phase** changes very gradually under the conditions used herein for **3Y1** cells. This fits nicely with the observation of the small changes in the standard deviation observed in the standard deviations of the intensity spectra presented herein.

VII. Conclusion: The spectral changes reported between proliferative and non- proliferative cells are small, but reproducible. Indeed, the standard deviation for any intensity spectrum presented here is less than 5%. All intensity spectra look remarkably similar. In fact, it is hard to discern any spectral characteristic that differ between the 24 and 72 or hour time points or the serum deprived cells.

The small magnitude of the spectral changes makes analysis via 2nd derivative spectra an attractive method of analysis, since the derivatives are more sensitive to the appearance of small spectral contributions than the original spectra. An analogous observation was reported in the classification of prokaryotic cells, for which the spectral differences are even smaller than the ones reported here **(Helm, et al., 1991).**

The ethanol treatment and **RNase** digestions do alter the spectral characteristics gathered from the cells. The ethanol treatment eliminated phospholipids in each sample. This was a possible cause for the non-specific spectral changes in dried cells. The phospholipids were shown have to confounded the results that differentiated proliferative versus non-proliferative cells. The removal of phospholipids was indicated by the reduction in the 1740 cm^{-1} shoulder.

By treating cells with **RNase**, nucleic acids were removed that may hide the spectral changes due to either growth or growth arrest that may

be attributed to **DNA**. The digestion of **RNA** leads to a reduction in intensity between 1150 – 950 cm^{-1}, which is the nucleic acid envelope.

Elimination of effects to the **RNA** and phospholipids suggests that the observed spectral changes are due to changes in **DNA**. This is because the spectral changes associated with high confluence or serum deprivation do not disappear after phospholipids and **RNA** were removed. After removal of **RNA** and phospholipids, the spectral changes are much more pronounced in the 1140 –1040 cm^{-1} region. The second derivative spectra of the **RNase** treated cells for each time point are shown in **Figure 48**.

The **DNase** digestion experiments indicate that the protein cytoskeleton may also play a role in the spectroscopic differentiation of proliferative versus non-proliferative cells. Alterations in protein metabolism should be expected as it is dependent upon cell cycle progression. Removal of **DNA** suggests that some of the observed spectral changes are due to proteins to some extent. This is because there are spectral changes between the exponentially growing, high confluence and serum deprived cells.

Many growth factor associated pathways use phosphorylation of proteins as a means to signal the initiation, and regulation of cell growth **(Winkles, 1998, Frederickson et al., 1992, Goldring et al., 1991)**. It is conceivable that the spectral differences are partly due to this phenomenon. However, there are several arguments that suggest that the

spectral changes are significantly due to the changes in conformation or detectability of **DNA**. These arguments may be summarized as follows.

First, given the enormous concentration of proteins (ca. 60 % by weight), the phosphorylated proteins would have to be an enormously abundant, since the spectral results suggest an overall change in the 1108 cm^{-1} peak of about 1%.

Secondly, we have shown (unpublished results) that phosphorylation of peptides and proteins is indicated by the appearance of a strong C-O-P vibration at about 914 cm^{-1}, and a "phosphate" stretching band at 1077 cm^{-1}, which is significantly lower than the frequency of the spectral change observed here. In addition, a change in the amide I / II region was observed, presumably due to protein conformational changes accompanying phosphorylation. Since there is no good agreement between the shoulder observed at 1108 cm^{-1} for the confluent cells, and the bands of the phosphorylated protein, we believe that phosphorylation of proteins is an unlikely cause for the spectral changes in the phosphate region. A similar argument can be made for differently modified proteins (e.g., glycosylated proteins), which are not expected to occur in cells at concentrations detectable by IR-MSP.

Lastly, **DNA** is the most likely cellular component responsible for the spectral changes. It is known that **DNA** undergoes large conformational changes during replication. The **DNA** must be denatured, replicated and the strands re-annealed during **S phase**. In addition, the

number of "origins of replication" is not known for mammalian cells and is estimated to be quite high **(Jackson et al., 1998)**. This would also contribute to our observations. Detection of the cell cycle phase via flow cytometry (fluorescence activated cell sorting) is based on the quantitative differences in the amount of **DNA** in the cell. Furthermore, we and others have shown that **DNA**, in vitro, undergoes small spectral change when the typical canonical double stranded structure is perturbed. Such conformational changes can be induced by variations of the hydration of the **DNA**, and can be further enhanced by salt effects.

It is very promising that this small difference between the samples can be detected spectroscopically. These observations reported here suggest that an assay for detecting cell growth by spectroscopic means may be developed.

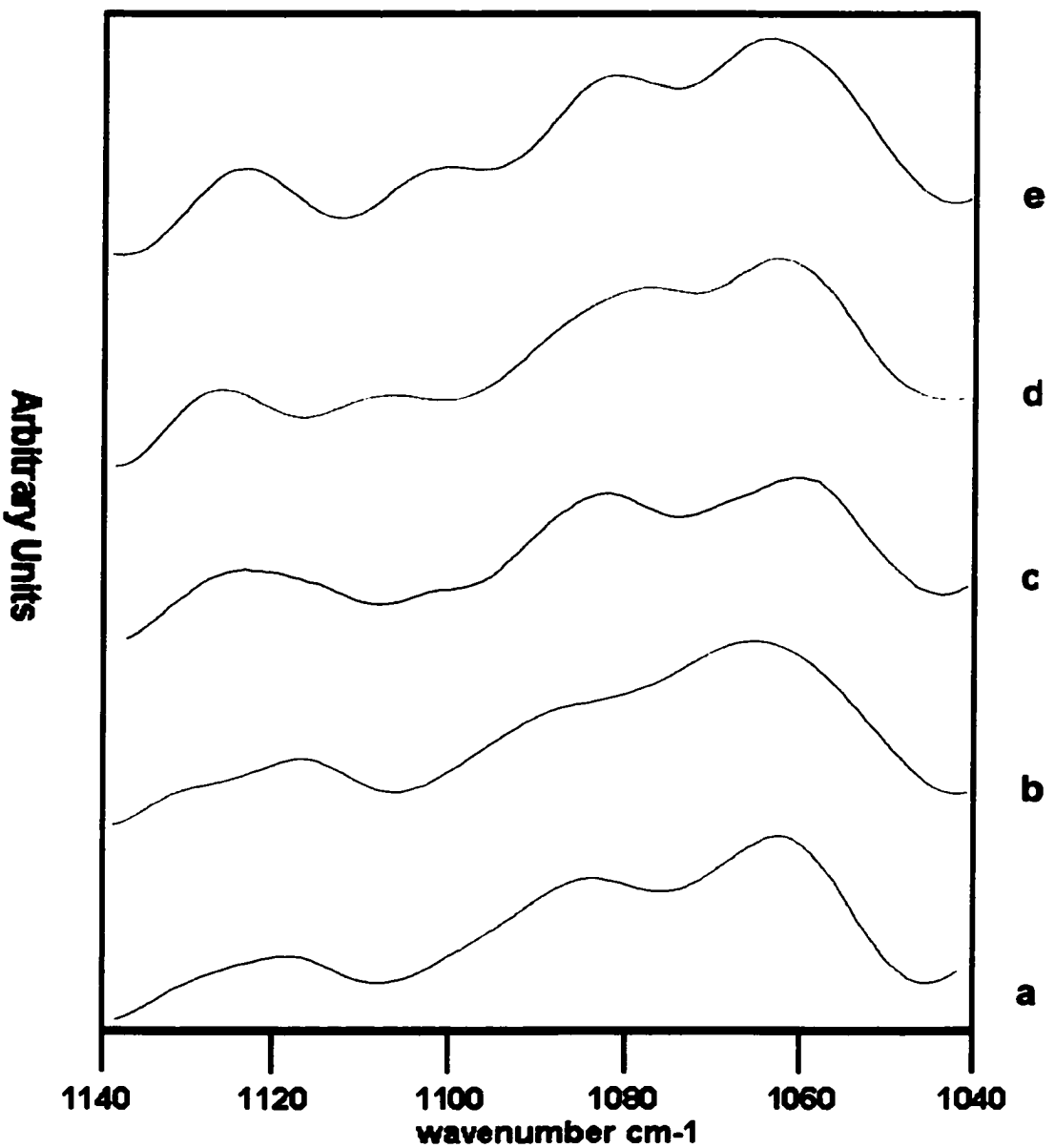

Figure 48: Second derivative spectra of RNase treated cells after 24 (a), 36(b), 48 (c), 60 (d) and 72 (e) hours of serum stimulation.

References cited:

Alberts, B., Bray, D., Lewis, J., Raff, M., Roberts K., Watson, J., "Molecular Biology of the Cell," Third Edition, Garland Publishing, New York, pg. 482 (1994)

Alberts, B., Bray, D., Lewis, J., Raff, M., Roberts K., Watson, J., "Molecular Biology of the Cell," Third Edition, Garland Publishing, New York, pgs. 896 - 897 (1994)

Anggard, E., Lancet, **343**, pgs. 1199 – 1206 (1994).

Avanti Polar Lipids Catalogue, 2001

Baba, M., Hirai, S., Kawakami, S., Kishida, T., Sakai, N., Kaneko, S., Yao, M., Shuin, T., Kubota, Y., Hosaka, M., Ohno, S., Tumor supressor protein VHL is induced at high cell density and mediates contact inhibition of cell growth. Oncogene, **20**, pgs. 2727 - 36. (2001)

Benedetti, E., Palatresi, M.P., Vergamini, P., Papineschi, F., Spremolla, G., "New possibilities of research in chronic lymphatic leukemia by means of Fourier transform-infrared spectroscopy—II", Leuk Res. **9(8)**, pgs. 1001-1008 (1985)

Benedetti, E., E. Bramanti, F. Papineschi, I. Rossi, and E. Benedetti, "Determination of the relative amount of nucleic acids and proteins in leukemic and normal lymphocytes by means of Fourier transform infrared microspectroscopy," Applied Spectroscopy, **51**, pgs. 792-797 (1997).

Benedetti, E., Bramanti, F., Papineschi, F., Vergamini, P., Benedetti, E., "An Approach to the study of promitive thrombocytemia (PT) megakaryocytes by means of Fourier transform infrared microspectroscopy (FT-IR-M)", Cell. Mol. Biol., **44(1)**, pgs. 129-140 (1998)

Boydston-White, S., Gopen, T., Houser, S., Bargonetti, J. and Diem, M., "Infrared Spectroscopy of Human Tissue: V. Infrared spectroscopic studies of Myoeloid Leukemia (ML-1) cells at different phases of the cell cycle", Biospectroscopy, **5**, pgs. 219-227 (1999)

Broderson, R., "Independent Binding of Ligands to Human Serum Albumin", J. Biol. Chem., **252 (14)**, pgs. 5067-5072 (1977)

Chiriboga, L.; Xie, P.; Yee, H.; Zarou, D.; Zakim, D. Diem, M., Infrared spectroscopy of human tissue. IV. Detection of dysplastic and neoplastic changes of human cervical tissue via infrared microscopy, *Cell. Mol. Biol.*, **44(1)**, pgs. 219-229 (1998)

Chiriboga, L., Yee, H., Diem, M., Infrared Spectroscopy of Human Cells and Tissue. VI. A Comparative Study of Histopathology and Infrared Microspectroscopy of Normal, Cirrhotic and Cancerous Liver Tissue, Appl.Spectrosc., **54(1)**, pages 1-8 (2000)

Chiriboga, L., Yee, H.,Diem, M., Infrared Spectroscopy of Human Cells and Tissue. VII. FT-IR Microspectroscopy of DNase and RNase Treated Normal, Cirrhotic and Neoplastic Liver Tissue, *Appl.Spectrosc.*, **54(4)**, pgs. 480-485 (2000)

Cohen, S., Proc. Natl. Acad. Sci., **85**, pgs. 324 (1960)

Dbaibo,G. S., El-Assaad, W., Krikorian, A., Liu, B., Diab, K., Idriss, N. Z., El-Sabban, M., Driscoll, T. A., Perry, D. K., Hannun, Y. A., "Ceramide generation by two distinct pathways in tumor necrosis factor alpha-induced cell death", FEBS Lett., **503 (1)**, pgs. 7-12 (2001)

Diem, M., " Modern Vibrational Spectroscopy, " John Wiley & Sons, New York, pg. 29 (1993)

Diem, M., Lasch, P., Pacifico, A., "Spatially resolved IR microspectroscopy of single cells" Biospectroscopy, (In press)

Evans, T., Rosenthal, E., Youngblom, J., Distel D., and Hunt, T., Cell, **33**, pgs. 389 –396 (1983)

Frederickson, R. M., Sonenberg, N., "Signal transduction and regulation of translation initiation", Semin Cell Biol, **3(2)**, pgs. 107-115, (1992)

Goldring, M.B. Goldring, S.R., "Cytokines and Growth Control", Crit. Rev. Eukaryot. Gene Expr., **1(4)**, pgs. 301-26, (1991)

Helm, D., Labischinski H., G. Schallen, D.Naumann, "Classification and identification of bacteria by FT-IR spectroscopy", J. Gen. Microbiol., **137**, pgs. 69-79 (1991)

Jackson, D.A., Pombo A., "Replicon clusters are stable units of chromosome structure: Evidence that nuclear organization contributes to the efficient activation and propagation of S phase in Human Cells", J. Cell Biol., **140**, pgs. 1285-1295 (1998)

Jamin, N., Dumas, P., Moncuit, J., Fridman, J.L., Teillaud, G.L., Carr, G.P., Williams, G.P., "Chemical Imaging f nucleic acids, proteins and lipids of a single living cell. Application of sychrotron infrared microspectrometry in cell bioology", Cell. Mol. Biol., **44(1)**, pgs. 9-14 (1998)

Keng, P. C., "Use of flow cytometry in the measurement of cell mitotic cycle", Int. J. Cell Cloning, **4(5)**, pgs. 295-311 (1986)

Lasch P., Naumann, D., "FT – IR microspectroscopic imaging of human carcinoma thin sections based on pattern recognition techniques", Cell. Mol. Bio., **44(1)**, pgs. 189-202 (1998)

Lasch, P., Boese, M., Pacifico, A., Diem, M., " FT- IR Spectroscopic Investigations of Single Cells on the Subcellular Level" Vibrational Spectroscopy, In Press, (2001)

Leonhardt, H., Histologie, Zytologie und Mikroanatomie des Menschen, Thieme Verlag, Stuttgart New York, (1981)

Lewin, B., Genes V, Oxford University Press, Oxford, 1994, pg. 350

Mantsch, H. H., Liu, K., Schultz, C.P., Johnston, J. B., Lee, K., "Comparison of Infrared Spectra of CLL Cells with their Ex Vivo Sensitivity to Chlorambucil and Cladribine", Leukemia Research, **21**, pgs. 1125-1133 (1997)

Mantsch, H. H., Mohammad, R. M., Liu, K., Schultz, C.P., Katato, K., Almatchy, V. P., Wall, N., Vaterasian, M., Al-Katib, A. M., "Sequential Treatment of Human Chronic Lymphocytic Leukemia with Bryostatin 1 followed by 2 Chlorodeoxyadenosine: Preclinical Studies", Clinical Cancer Research, **4**, pgs. 445-453, (1998)

Mc Intosh, J. R., Mc Donald, K., Scientific American, **261 (4)**, pgs. 48 –56 (1989)

Nunez, R., "DNA measurement and cell cycle analysis by flow cytometry", Curr. Issues Mol. Bio. , **3(3)**, pgs. 67-70 (2001).

Okuda, A., Kimura, G., "Kinetic analysis of entry into S phase in resting rat 3Y1 cells stimulated by serum. Effects of serum concentration and temperature" Exp Cell Res 1983 Apr 15; **145(1)**, pgs. 155-65

Quack, M., Clarin, A., Binderup, E., Bjorkling, F., Hansen, C. M., Carlberg C., J. Cellular Biochemistry, **71**, pgs. 340 –350 (1998)

Rigas, B., Wong, P.T.T., "Human Colon Adenocarcinoma Cells Display IR Spectroscopic Features of Malignant Colon Tissues", Cancer Res., **52**, pgs. 84 –88 (1992)

Sawin, K. E., Scholey, J. M., Trends in Cell Biology, 1, pgs. 122-129 (1991).

Voet D., Voet, J., "Biochemistry," Second Edition, John Wiley & Sons, New York, pgs. 251 – 276 (1995)

Winkles, J. A., "Serum and polypeptide growth factor-inducible gene expression in mouse fibroblasts" Prog. Nucleic Acid Res. Mol. Bio., 58, pgs. 41– 78 (1998)

Wong, P.T.T. , R.K.Wong, T.A.Caputo, T.A.Godwin and B.Rigas, "IR Spectroscopy of Exfoliated Human Cervical Cells; Evidence of Extensive Structural Changes During Carcinogenesis", *Proc.Natl.Acad.Sci.,USA*, 88, pgs. 10988-10992 (1991)

Wood, B. R., Tait, B., Mc Naughton, D., "Fourier Transform Infrared Spectroscopy as a Method for Monitoring the Molecular Dynamics of Lymphocyte Activation", Applied Spectroscopy, 54(3), pgs. 353 –359 (2000)